CORRELATION OF STRUCTURE AND FUNCTION OF THE ACETYLCHOLINE RECEPTOR FROM *TORPEDO CALIFORNICA*

Thesis

by

Hsiao-Ping Hsu Moore

In Partial Fulfillment of the Requirements

for the Degree of

Doctor of Philosophy

California Institute of Technology

Pasadena, California

1980

(Submitted May 13, 1980)

To my parents and Kevin

ACKNOWLEDGMENTS

I wish to thank my advisor, Professor Michael A. Raftery, for his guidance, support, patience, and interest in this work. I also express my appreciation to Professor Norman Davidson for his encouragement, friendship, and professional and personal interest, and also for being an inexhaustible supply of raisins. Professor Tun-Bin Lo of National Taiwan University was instrumental in my coming to Caltech, for which I am grateful.

I very much appreciate the collaboration of Professor Paul R. Hartig on the work described in Chapters Two and Three and on preliminary studies which led to the work described in Chapter Four. I learned a great deal from him. Dr. Susan M. J. Dunn and Dr. Steven G. Blanchard were very helpful in teaching me the use of the stopped-flow instrument and computer, and provided numerous helpful, insightful discussions. I thank Dr. Dunn also for her critical reading of this thesis. Mr. John Racs is a very congenial and pleasant coworker, and provided the multitude of receptor preparations used in these studies. I thank Ms. Valerie Purvis for typing the original manuscripts and preparing the figures. The members of the Raftery group have provided an enjoyable and stimulating environment in which to work. I also thank Ms. Vere Snell for her skillful typing of this thesis.

Most importantly, I want to thank my husband, Kevin W. Moore, for his love, constant encouragement, and moral support during these four years. My parents, T. W. Hsu and C. H. Liu sacrificed a great deal so that I could come here to study. Finally, my brother and sister-in-law, Shi-ping and Jin-chen Hsu, have helped in so many ways with friendship

and concern to make this place feel like 'home'.

Chapter I

Abstract

The interaction of a cholinergic depolarizing agent, bromoacetylcholine, with acetylcholine receptor enriched membrane fragments and Triton-solubilized, purified AcChR from T. californica has been studied. The reagent bound to membrane-bound AcChR reversibly with an apparent dissociation constant of 16 ± 1 nM at equilibrium. This 600 - fold higher affinity for the receptor than found from physiological studies ($K_{activation} \simeq 10$ μM, Karlin (1973) Fed. Proc. 32, 1847-1853) can be attributed to a ligand induced affinity change of the membrane-bound receptor upon preincubation with bromoacetylcholine. At equilibrium [^{3}H] bromoacetylcholine bound to half the number of α-bungarotoxin sites present in the preparation without apparent positive cooperativity and this binding was competitively inhibited by acetylcholine.

In the presence of dithiothreitol [^{3}H]-bromoacetylcholine irreversibly alkylated both membrane-bound and solubilized, purified acetylcholine receptor, with a stoichiometry identical to that for reversible binding. The labeling was inhibited by acetylcholine and α-bungarotoxin. SDS-polyacrylamide gel electrophoresis of the labeled acetylcholine receptor showed that only the 40,000 dalton subunit contained the label. From these results it is concluded that the 40,000 dalton subunit represents a major component of the agonist binding site of the receptor.

Chapter II

Abstract

The vesicular properties of the Torpedo membrane preparations have been investigated with a view towards understanding and improving the methods for in vitro ion flux studies. Crude acetylcholine receptor preparations isolated from Torpedo electroplaques under conditions isotonic to Torpedo plasma contain a large number of sealed vesicles capable of entrapping radioactive solutes and maintaining a transmembrane potential. Osmotic shock of these vesicles causes transient pores to form in the membrane which allow cations, anions and neutral species of molecular weights up to 8000 daltons to readily pass through. Resealing of the pores occurs spontaneously within five seconds after osmotic shock at both 4°C and 25°C. This spontaneous resealing of vesicles allows purification of sealed membrane vesicles that are greatly enriched in acetylcholine receptor by osmotic shock and sucrose density gradient centrifugation. The resulting vesicles acquire low osmolarity medium in their interior and behave as fully inflated vesicles only when suspended in medium of low osmolarity. The transient pores formed during osmotic shock can also be used to load impermeant solutes into the vesicle interior. For the purified receptor-vesicles which are more resistant to osmotic shock due to the low interior osmolarity, 'freeze-thaw' cycles provide an alternative method for this purpose. With this information on the vesicular properties of the Torpedo membrane preparations it will be easier to design preparative methods for biochemical studies utilizing the vesicle nature of the receptor membranes.

Chapter III

Abstract

Closed membrane vesicles derived from the innervated face of T. californica electroplaque responded to the cholinergic agonist carbamylcholine by a rapid efflux of vesicle-entrapped $^{22}Na^{+}$. The response is considerably faster than previously reported for this in vitro assay system and displays many of the pharmacological properties characteristic of the in vivo response. Rapid efflux is stimulated by the quaternary ammonium ligands acetylcholine, carbamylcholine, bromoacetylcholine and S-acetylthiocholine and is inhibited by α-bungarotoxin and histrionicotoxin. Preincubation of the vesicles with carbamylcholine causes desensitization of the receptors and hence blocks the flux response. Removal of a substantial fraction of the 43,000-dalton, 90,000-dalton and other polypeptide components from the membrane preparation by base extraction does not significantly alter the pharmacological characteristics of carbamylcholine induced $^{22}Na^{+}$ efflux. Quantitative analysis of the flux amplitude, the only quantity measurable by the filtration assay method, produced by membrane preparations in which variable fractions of the receptors are inactivated by α-bungarotoxin, reveals that a large excess of receptor-associated channels is present on the vesicle surface above the level needed to produce a full $^{22}Na^{+}$ flux response. The dependence of flux response on the degree of toxin inactivation is identical for both base-treated and untreated membranes. Therefore, the 43,000-dalton and 90,000-dalton polypeptides removed by base extraction do not appear essential for acetylcholine receptor-mediated ion translocation.

Chapter IV

Abstract

Direct determination of the kinetics of carbamylcholine mediated cation transport across the membrane of acetylcholine receptor containing vesicles has been achieved on the physiologically relevant time scale of a few milliseconds. The stopped-flow spectroscopic approach utilizes thallium (I) as the cation transported into sealed vesicles containing a water soluble fluorophore. Upon entry of thallium (I) fluorescence quenching occurs by a heavy atom effect. Rapid thallium translocation into the vesicles is mediated by cholinergic agonists and the effect is blocked by antagonists, neurotoxins and by desensitization. The kinetics of thallium transport are used to demonstrate that the four polypeptides of 40,000, 50,000, 60,000 and 65,000 daltons are the only protein components necessary for cation translocation. The kinetics of thallium (I) transport at saturating agonist concentrations are also used to calculate the apparent ion transport number for a single receptor per unit time. The minimal value obtained is close to that for a single activated channel determined *in vivo*. This demonstrates that the physiological receptor has been isolated in intact form.

Chapter V

Abstract

The acetylcholine receptor from T. californica, in membrane-bound form, can undergo conversion from a state(s) of low affinity to one(s) of high affinity for carbamylcholine upon pretreatment with this ligand. Reduction of the membrane preparations by dithiothreitol followed by alkylation with iodoacetamide or N-ethylmaleimide prevents the conversion. Treatment with p-chloromercuribenzoate similarly blocks the conversion to high affinity state(s) by the cholinergic ligand, while other reagents such as iodoacetic acid or iodoacetamide do not. Unmodified receptor in the high-affinity form(s) induced by carbamylcholine can revert to a form(s) of low affinity upon removal of the ligand. However, treatment with p-chloromercuribenzoate prior to such removal prevents the system from reverting to low affinity after removal of carbamylcholine. These results suggest that sulfhydryl as well as disulfide bonds may be important in the interconversion of affinity states of the receptor. Two possible simple models which involve both cysteine and cystine residues in interconversion of the affinity states of the receptor are discussed.

TABLE OF CONTENTS

Chapter II

Osmotic properties of membrane vesicles from T. californica: Preparation of AcChR-enriched membrane vesicles suitable for in vitro ion flux studies

Chapter III

Rapid cation translocation in Torpedo membrane vesicles: I. Acetylcholine receptor mediated $^{22}Na^{+}$ efflux and correlation of polypeptide composition with functional events

Chapter IV

Rapid cation translocation in Torpedo membrane vesicles: II. Spectroscopic studies on a time scale of physiological relevance

ABBREVIATIONS

AcCh:	acetylcholine
AcChE:	acetylcholinesterase
AcChR:	acetylcholine receptor
α-BuTx:	α-bungarotoxin
ANTS:	8-amino-1,3,6-naphthalenetrisulfonate
BrAcCh:	Bromoacetylcholine
Carb:	carbamylcholine
CBB:	Coomassie Brilliant Blue
DAPA:	1,10-bis(3-azidopyridinio)decane perchlorate
DEAE:	diethylaminoethyl
Deca:	decamethonium
$diSC_3$-(5):	3,3'-dipropylthiadicarbocyanine iodide
DNPP:	diethylnitrophenylphosphate
d-Tc:	d-tubocurarine
DTNB:	5,5'-dithio-bis(2-nitrobenzoic acid)
DTT:	dithiothreitol
EDTA:	ethylenediaminetetraacetic acid
Hepes:	N-2-hydroxyethylpiperazine-N'-2-ethanesulfonic acid
HTX:	histrionicotoxin
MBTA:	4-(N-maleimido)-benzyltrimethylammonium iodide
NEM:	N-ethylmaleimide
PCMB:	p-chloromercuribenzoate

PMSF:	phenylmethanesulfonylfluoride
POPOP:	1,4-bis[2-methyl(5-phenyloxazolyl)]benzene
PPO:	2,5-diphenyloxazole
SDS:	sodiumdodecylsulfate
Tris:	tris(hydroxymethyl)methylamine

INTRODUCTION

The Chemical Synapse:

The first direct evidence supporting the concept of chemical synaptic transmission between cells was provided by Otto Loewi in 1921 who demonstrated that electrical stimulation of the vagus nerve of a frog heart caused the release of a chemical substance which was capable of influencing the beat rate of a second unstimulated heart present in the incubation medium. This transmitter molecule was later identified by Loewi and his colleagues to be acetylcholine (AcCh). Since then AcCh has been identified as the neurotransmitter at the neuromuscular junctions of skeletal muscles and at many synapses of invertebrates and vertebrates. The advent of the voltage clamp technique (Takeuchi and Takeuchi, 1960), the iontophoretic method for the application of AcCh to localized regions of the membrane (Nastuk, 1953) and improved electric recording techniques on isolated nerve-muscle preparations have greatly facilitated subsequent investigations on the transmitter-mediated synaptic transmission.

The basic mechanisms underlying chemical synaptic transmission are now clear. An impulse arriving at the presynaptic nerve terminal of a neuromuscular junction triggers an influx of calcium ions across the nerve membrane (Katz and Mideli, 1971). This causes secretion of the transmitter AcCh, present in discrete packets called synaptic vesicles (Fatt and Katz, 1952), from the nerve terminal. The released transmitter molecules then diffuse across the synaptic cleft to the postsynaptic membrane. Interaction of the transmitters with the receptor molecules

in the subsynaptic membrane then triggers the opening of ion transport channels which allow both K^+ and Na^+ ions to pass through (Fatt and Katz, 1951). The flow of these ions results in a postsynaptic potential (or end-plate potential) which depolarizes the normal resting membrane (Göpfert and Schaefer, 1938). The AcCh molecules are quickly hydrolyzed by the enzyme acetylcholinesterase into acetate and choline. The growth phase of the end-plate current lasts 0.5-1 msec and decays in an exponential manner with a half-life of a few milliseconds (Magleby and Stevens, 1972).

The Pharmacology and Physiology of the Nicotinic Acetylcholine Receptor:

A number of structural analogues of AcCh are known to affect the end-plate potential of neuromuscular junctions by interacting with the postsynaptic nicotinic acetylcholine receptor (AcChR). Some, such as carbamylcholine, nicotine, or pheynltrimethylammonium, cause a depolarizing synaptic potential in a manner similar to AcCh, while others (such as d-tubocurarine, flaxedil or hexamethonium) block the AcCh response by decreasing its apparent affinity to the receptors without affecting the maximal response. The former are called agonists and the latter competitive antagonists. Noncompetitive blocking agents which reversibly decrease the permeability response without affecting the affinity of agonists to the receptors are also known. These include local anesthetics such as procaine, lidocaine (Seeman, 1972) and histrionicotoxin from the Columbian frog Dendrobates histrionicus (Albuquerque et al, 1973). α-Bungarotoxin (α-BuTx) from the venom of

Bungarus multicinctus irreversibly blocks the end-plate potential by specifically binding to the AcChR (Lee, 1972). Other toxins which have been reported to act at the end-plates include ceruleotoxin from the venom of Bungarus caeruleu (Bon and Changeux, 1975) and α-mambatoxin from the venom of Dendroaspis viridis (Patrick et al, 1980). In addition to the pharmacological specificity of AcChR for the various drugs, the receptor is also known to exhibit the phenomenon of desensitization (Katz and Thesleff, 1957); the response to agonists decreases after prolonged exposure of the receptors to AcCh.

Insights into the elementary events associated with a single activated channel came from the elegant work of Katz and Miledi (1970, 1972) who analyzed the electrical noise produced by a steady dose of AcCh. The fluctuations around the mean depolarization reflect the opening and closing of individual ion channels as a result of collision of AcCh molecules with the receptors. It was found from such noise analysis that the single channel conductance at the end-plate is approximately 20 pmho (Stevens, 1975) and each channel on the average stays open for 1-3 msec when activated. The relaxation experiments conducted by Sheridan and Lester (1977) provide another way to study the rates at which channels open and close. By introducing a large perturbation from the equilibrium state (such as a voltage jump) and observing the rate at which the system relaxes to a new equilibrium, information about the rate of transition between open and closed channels was obtained. It was found that in Electrophorus electroplaques (see below) the postsynaptic channels open with a rate constant

of 10^7 to $2x10^8$ $M^{-1}s^{-1}$ and close with a voltage-dependent rate constant of 10^2 to $3x10^3$ s^{-1} as the receptors bind or dissociates the agonist molecules.

Studies of the dependence of postsynaptic conductance on the agonist concentration revealed a nonlinear relationship in the dose-response curve (Katz and Thesleff, 1957; Jenkinson and Terrar, 1974; Dreyer and Pepper, 1975). The sigmoidal nature of the concentration-conductance curve can be adequately explained by assuming that two agonist molecules are required to efficiently activate a channel (Adams, 1975; Sheridan and Lester, 1977; Dionne et al, 1978). The binding of the two agonists may or may not be cooperative.

Biochemical Isolation of the AcChR:

To study the molecular structure of the AcChR and its associated channel and to correlate such structures with the physiological function, it is necessary to isolate and purify the receptor macromolecules and study their functional organization at the biochemical level. Subcellular fractionation of the AcChR has been greatly facilitated by the discoveries of an abundant source and a specific molecular marker for the receptor. First, alphabungarotoxin (α-BuTx) in the venom of the banded krait Bungarus multicinctus was found to irreversibly block neuromuscular transmission by binding to the AcChR in a highly specific way (Lee and Chang, 1966; Lee et al, 1967). This observation and the finding that the toxin is readily radiolabelled without affecting its function make α-BuTx an ideal marker for identifying the AcChR. Secondly, the electric organs of Electrophorus, a fresh water

teleost, and Torpedo, a sea water elasmobranch, are exceptionally rich in nicotinic cholinergic synapses and hence provide abundant sources for the subsynaptic membranes (Bennett, 1961). The electric organs consist of parallel columns of large, flat cells called electroplaques (dimensions: 10 mmx1mmx0.3mm in Electrophorus and 5mmx5mmx0.02mm in Torpedo) which develop in the embryo from the same type of tissue that gives rise to muscle. One face of the electroplaques receives a great number of nerve terminals that form nicotinic cholinergic synapses. Intracellular recordings carried out on single isolated electroplaques from both Electrophorus and Torpedo (although the latter to a much lesser extent because of the fragility of the cells) showed that the electroplaque synapses are functionally very similar to those of muscle (Bennett et al, 1961). In Electrophorus electroplaques, only about 1-2% of the total surface of the plasma membrane of the innervated face receives synapses while as much as 50% of the area of the membrane is subsynaptic in Torpedo electroplaques. Thus the Torpedo electric organs provide a richer source of AcChR.

Membrane fragments highly enriched in AcChR have been isolated from homogenates of the electroplaque of various species by differential centrifugation and purification on sucrose density gradients. These membrane-bound receptors can be solubilized with detergents such as Triton X-100 and purified by affinity chromatography to yield the highly purified, solubilized AcChR (Narcine entemedor: Schmidt and Raftery, 1972; Torpedo californica: Schmidt and Raftery, 1973; Weill et al, 1974; Torpedo marmorata: Karlsson et al, 1972; Eldefrawi and

Eldefrawi, 1973; Gordon et al, 1974; Electrophorus electricus: Olsen et al, 1972; Biesecker, 1973; Karlin and Cowburn, 1973; Klett et al, 1973; Chang, 1974; Torpedo nobiliana: Ong and Brady, 1974). Both types of preparations are useful for in vitro characterization of AcChR.

Molecular Weight and Subunit Structure of AcChR:

The purified AcChR has been characterized as an oligomeric glycoprotein. Sucrose gradient sedimentation shows that the solubilized AcChR are present as two molecular species of 9S and 13S (Raftery et al, 1972). Upon denaturation, both forms dissociate into four polypeptides of M.W. 40,000, 50,000, 60,000, and 65,000 daltons. Evidence has been obtained which indicates that the 13S species is a dimeric form of the 9S protein through a disulfide linkage between two 65,000-dalton polypeptides (Suarez-Isla and Huchs, 1977; Chang and Boch, 1977; Hamilton et al, 1977; Witzemann and Raftery, 1978a). The four polypeptides of M.W. 40,000, 50,000, 60,000 and 65,000 are present in a ratio of 2:1:1:1 (Lindstrom et al, 1979; Strader et al, 1980a).

The molecular weight of the receptor from Torpedo has been estimated by several methods. Because of complications arising from bound detergent and differences in the methods used, values ranging from 190,000 (Gibson et al, 1976) to 450,000 daltons (Heilbronn, 1975) have been assigned for the 9S protein. Recently, improved methods for molecular weight determination were employed and somewhat more consistent values

were obtained (Martinez-Carrion et al, 1975; Edelstein et al, 1975; Reynolds and Karlin, 1978; Hucho et al, 1978). At present the most reasonable estimate of the molecular weight for the monomeric receptor is in the range of 250,000-270,000 daltons.

Although the general pattern of polypeptides with approximate molecular weights of 40,000, 50,000, 60,000 and 65,000 daltons has been reported for purified AcChR preparations from several laboratories (Raftery et al, 1974a; Weill et al, 1974; McNamee et al, 1975), considerable variability in the subunit pattern and the stoichiometry of the polypeptide components still exists. For instance, Sobel et al (1978) reported an AcChR preparation from T. Marmorata which contained only two major polypeptide components of 40,000 and 43,000 daltons. Based on this result, they suggested that the polypeptides of 50,000, 60,000 and 65,000 daltons may simply be contaminants which copurify with the AcChR and that loss of an essential component of 43,000 daltons may have occurred during the solubilization and purification procedures. This issue will be further discussed in Chapter 3.

Since calcium-activated proteases have been shown to be present in the preparations (Moore and Raftery, unpublished data), the possibility that the four polypeptides of 40,000, 50,000, 60,000, 65,000 daltons are proteolytic degradation products from a single polypeptide precursor has been examined. Antibodies against each of the four polypeptides were prepared and shown not to crossreact with any of the other three subunits (Claudio and Raftery, 1977). In addition, no similarity was found between peptide maps of the four subunits

(Lindstrom et al, 1979). These results suggest that the four polypeptides are different proteins and that they do not represent degradation products of the same protein. Recently, the N-terminal amino acid sequence has been determined for the 40,000-dalton polypeptide (Devillers-Thiery et al, 1979; Hunkapiller et al, 1979) as well as for the other three subunits (Raftery et al, 1980). The results showed striking sequence homology among the four polypeptides. The 40,000, 50,000, 60,000 and 65,000-dalton polypeptides are therefore structurally similar, but not identical, entities.

The receptor protein is phosphorylated in vivo. Evidence for the presence of O-phosphoserine residues in the purified protein has been reported (Vandlen et al, 1979).

Organization of AcChR in the Membrane:

Negative staining of the AcChR-enriched membranes isolated from Torpedo electroplaques revealed closed vesicular structures (averaged diameter $\sim$6000 Å on electron micrographs (Strader et al, 1979). A large fraction of these vesicles showed densely packed cylindrical rosette structures 60-80 Å in diameter in the membrane (Cartaud et al, 1973; Nickel and Potter, 1973; Raftery et al, 1974b). The density of these hexagonal arrays was estimated to be $\sim 10^4$ particles per μm^2 (Nickel and Potter, 1973). Similar structures have been observed for isolated purified AcChR from Electrophorus electricus (Meunier et al, 1974). These rosette structures have subsequently been identified as AcChR molecules by immunospecific labeling of negatively stained membrane fragments with antibodies to AcChR (Klymkowsky and Stroud, 1979).

X-ray diffraction studies of the AcChR-enriched membranes have shown that the receptor spans the membrane, exposing 55 Å on one side and 15 Å on the other side of the bilayer (Ross et al, 1977).

The topology of AcChR in the membrane has been investigated by chemical (Witzemann and Raftery, 1978b), enzymatic (Hartig and Raftery, 1977) and immunospecific (Tarrab-Hazdai et al, 1978; Strader et al, 1979) labelling. It was shown that the receptor spans the membrane with all four subunits considerably exposed on the extracellular side of the membrane. The 50,000, 60,000 and 65,000-dalton polypeptides were susceptible to tryptic digestion from the cytoplasmic side of the membrane, suggesting that they span the membrane bilayer while the 40,000 dalton subunit showed a much lesser exposure (Strader and Raftery, 1980b).

Cross-linking experiments have provided evidence for the close association of AcChR polypeptide components in the membrane-bound state (Witzemann and Raftery, 1979). An Azido-derivative of [^{125}I-] α-BuTx was prepared and used to photolabel the subunit with which it interacts and the adjacent subunits. In addition to the 40,000 dalton polypeptide which is known to contain the α-BuTx site (Hucho et al, 1976), the toxin derivative was found to be crosslinked to the 65,000 dalton subunit, indicating that this subunit may be in close proximity to the 40,000-dalton polypeptide in the membranes.

Ligand-Binding Studies:

Binding of cholinergic ligands to the purified AcChR preparations has been studied in a number of ways. Binding of radioactive ligands

can be measured by equilibrium dialysis or centrifugation (Eldefrawi et al, 1971; Moody et al, 1973; Chang, 1974; Meunier et al, 1974; Raftery et al, 1974a). An alternative method involves the use of fluorescent cholinergic analogues (Cohen and Changeux, 1973; Martinez-Carrion and Raftery, 1973; Raftery et al, 1974a). The binding properties of cholinergic ligands can be characterized by the way in which they inhibit the binding of a fluorescent analogue. A third method exploits the binding of radiolabelled α-BuTx to AcChR, which is relatively slow compared to the diffusion-controlled binding of cholinergic ligands. In this case, inhibition of the initial rate of formation of the AcChR-toxin complex by cholinergic ligands is studied (Moody et al, 1973; Schmidt and Raftery, 1973; Fulpius et al, 1974; Meunier et al, 1974; Weber and Changeux, 1974a,b).

Data obtained for the binding characteristics of cholinergic ligands by the above methods are quite diverse. Values ranging from 1 to 2 have been reported for the ratio of α-BuTx sites to quaternary ligand binding sites (Moody et al, 1973; Meunier et al, 1974; Weill et al, 1974). Furthermore, the apparent binding affinities of these ligands for the various states of the purified AcChR are bewilderingly complex. Although a homogeneous population of high-affinity ligand binding sites ($K_D \sim 10$ nM for AcCh) is generally observed for membrane-bound AcChR at equilibrium, multiple states of affinity often result after solubilization of the AcChR with various detergents (Franklin and Potter, 1972; Cohen et al, 1974; Raftery et al, 1975; O'Brien and Gibson, 1975). Dissociation constants ranging from 10^{-9}M to 10^{-6}M have

been reported for the binding of AcCh to Triton X-100 or Na-cholate solubilized, purified AcChR.

Comparison of the dissociation constants obtained from such *in vitro* binding studies and those measured *in vivo* with electroplaque by electrophysiological recordings reveals great discrepancies between their values. AcChR-enriched membrane fragments bind AcCh at equilibrium with an affinity that is 2-3 orders of magnitude higher than that required to elicit the *in vivo* physiological response (Moreau and Changeux, 1976).

Conformational Transitions of AcChR:

Insight into the above question has come from the observation that preincubation of electroplaque with certain agonists causes an increase in AcChR affinity for antagonists (Rang and Ritter, 1970a,b). Weber *et al* (1975) and Lee *et al* (1977) reported that exposure of receptor-enriched membrane fragments from *Torpedo* electroplaques to certain agonists causes a slow, reversible change of the receptor protein to a high affinity form, as manifested by a decrease in the initial toxin binding rate with time in the presence of these agonists. This phenomenon is thought to be related to the *in vivo* desensitization described by Katz and Thesleff (1957) as they occur on similar time scales. The data were fitted to a two-state model which assumed that the receptor exists in two states of differing ligand affinities (Rang and Ritter, 1970a,b). The discrepancy between the dissociation constants determined by the dose-response curve of electroplaque and by direct equilibrium binding

studies with membrane fragment suspensions can thus be attributed to the ligand-induced desensitization process.

Recently, the two-state model has been quantitatively tested with membrane fragments by toxin-binding techniques (Quast et al, 1978). Analysis of rate and equilibrium constants determined for the agonist carbamylcholine indicated several internal inconsistencies in the model. Thus the two state model, though it provides a qualitative picture of AcChR function, has been found to be too simple to account quantitatively for all experimental observations.

Other techniques which are faster than the toxin binding method have been developed to study the conformational transitions of the AcChR. These include stopped-flow measurements with the use of both intrinsic (Bonner et al, 1976) and extrinsic fluorescent probes. Grunhagen et al (1977), using the extrinsic fluorescence probe quinacrine, observed a rapid increase in fluorescence upon ligand binding followed by a slow decay. They attributed the fast transition to the opening of the ion channel and the slow one to desensitization. The method suffers from the drawback that quinacrine itself acts as a local anesthetic and perturbs the system under study. The fast increase in fluorescence is also too slow to correspond to opening of ion channels in intact cells.

Two independent approaches, one with the non-covalent probe ethidium (Quast et al, 1979) and the other with the covalent probe 5-iodoacetamidosalicylic acid (Dunn et al, 1980), have recently been described in studies of the interaction of cholinergic ligands

with AcChR-enriched membranes. The data obtained from both methods bear striking similarities and can be fitted to a common mechanism involving sequential binding of ligands. This mechanism is different from the model recently proposed by Heidmann and Changeux (1979) to account for the kinetics of binding of a fluorescent agonist Dansyl-C_6-choline to membrane-bound AcChR from Torpedo marmorata.

Although a consistent mechanism for ligand-receptor interactions has not as yet been obtained by the various investigators, it is clear that the AcChR undergoes a series of conformational transitions upon interacting with ligands. Correlation of these conformational states of the receptor with its physiological function will be necessary to provide a detailed mechanism for the receptor function.

Affinity-Labelling of AcChR:

Identification of the polypeptide component(s) which contain the cholinergic ligand binding site(s) has been made possible by the finding that a readily reducible disulfide bond resides in the vicinity of a cholinergic ligand binding site (Karlin, 1969). Alkylation of the reduced sulphydryl group with an antagonist, 4-(N-maleimido)-benzyltrimethylammonium iodide (MBTA), has been carried out with receptors isolated from both electroplaques and denervated rat skeletal muscle. The reagent labels a single subunit in the electroplaque receptor but labels two different subunits in the denervated rat skeletal muscle receptor (Karlin and Cowburn, 1973; Froehner et al, 1977). Chapter 1 details the interaction AcChR from Torpedo californica with an alkylating agonist, bromoacetylcholine (BrAcCh). These

investigations strongly suggest that in Torpedo the AcCh binding site(s) reside on the 40,000-dalton polypeptide of the receptor protein complex.

Interactions with Specific Toxins and Local Anesthetics:

Local anesthetics and a number of toxins such as histrionicotoxin (HTx) or ceruleotoxin represent a class of compounds which blocks neuromuscular transmission at site(s) distinct from the AcCh recognition site on the AcChR. Electrophysiological studies on the actions of these compounds suggest that they may act by binding to the open-channel form of AcChR, thereby reducing the conductance (Ruff, 1976; Neher and Sakmann, 1976; Steinbach, 1977; Albuquerque et al, 1973). This class of compounds therefore serves as a potential probe for the component(s) associated with the ion translocation.

Interactions of AcChR-enriched membrane fragments with local anesthetics have been studied by radioactive local anesthetics (Krodel et al, 1979), by inhibition of α-BuTx binding (Weber and Changeux, 1974; Blanchard et al, 1979), and by extrinsic fluorescence probe (Cohen et al, 1974; Schimerlik and Raftery, 1976; Grunhagan and Changeux, 1976). Several local anesthetics have been shown to increase the rate of the agonist-induced affinity change of AcChR (Blanchard et al, 1979). Using ^{14}C-meproadifen, Krodel et al (1979) have reported that a specific, saturable binding component is present in the receptor-rich membrane preparation from T. Marmorata. Identification of the site(s) of interaction of local anesthetics has been

approached by photoaffinity labelling techniques. The local anesthetic analog procaine amide azide was shown to preferably label a component of 43,000-dalton molecular weight (Blanchard and Raftery, 1979).

[^{3}H]H_{12}-HTx has been shown to bind to the AcChR enriched membranes from Torpedo californica in a ratio of one [^{3}H] H_{12}-HTX bound per four [^{125}I]-α-BuTx sites, with a dissociation constant of 0.3-0.5 μM (Elliott and Raftery,1977). The toxin does not significantly affect the rates of agonist-induced interconversion of affinity states of the receptor. The kinetics of binding of HTX to the receptor-enriched membrane fragments have been studied by means of the fluorescence probe, ethidium bromide (Schimerlik et al, 1979). The data are consistent with a mechanism in which a rapid preequilibrium exists between receptor and toxin, followed by a slow conformational change.

Ceruleotoxin has been isolated from the venom of Bungarus caeruleu (Bon and Changeux, 1975; Lee et al, 1976; Moody and Raftery, 1978). Its use as a potential probe for ion-channel associated components, however, has been questioned since the toxin has considerable phospholipase activity and may act by other processes such as converting the receptor into a desensitized state.

In Vitro Measurements of Ion Translocation:

Studies of AcChR-mediated membrane permeability changes have been carried out with receptor-enriched membrane preparations and with solubilized, purified AcChR after reconstitution into lipid vesicles. Using a filtration technique and the radionuclide tracer $^{22}Na^+$, Kasai and Changeux (1971) first showed that the membrane vesicles

from Electrophorus responded to cholinergic agonists by releasing vesicle entrapped $^{22}Na^{+}$. The time course ($t_{1/2} \sim 7$ min), however, is very much slower than the transient conductance change (a few milliseconds) observed in vivo. This method has subsequently been employed to study membrane permeability changes in AcChR-enriched membrane preparations from organs of other species and in reconstituted systems (Popot et al, 1976; Hess et al, 1976; Andreasen and McNamee, 1977; Schiebler and Hucho, 1978; Epstein and Racker, 1978; Wu and Raftery, 1979). The slowness of the filtration method and the enormous variabilities in the time course of the flux response, however, severely limit a quantitative correlation of the in vitro and in vivo responses. AcChR-mediated ion translocation has therefore been characterized to a much lesser extent in vitro than has ligand binding, and the physiological function of AcChR in biochemical preparations was assayed only at a qualitative level.

The work presented in this thesis describes studies on the correlation of the structure with functional events of AcChR in vitro. In view of the lack of reliable methods to measure the receptor function for such studies, a large part of this thesis has been devoted to the development of quantitative methods for measurement of AcChR-mediated permeability changes in the purified membrane preparations. Three postsynaptic events are apparently associated with AcChR, namely, the initial recognition of the neurotransmitter AcCh, the subsequent membrane permeability changes, and then the onset of pharmacological desensitization. The chapters are thus arranged in

this sequence. Chapter 1 describes the interactions of the membrane-bound and purified, solubilized AcChR with the affinity agonist, bromoacetylcholine, and the localization of the agonist binding site. Chapters 2-4 detail recent developments on the studies of ion translocation measurements and their use to define the polypeptide components necessary for AcChR function. Finally, the effects of sulfhydryl reagents on the pharmacological desensitization process is described in Chapter 5. Most of the work presented has already appeared in print (Miller et al, 1978; Moore et al, 1979a,b; Moore and Raftery, 1979a,b; Hartig et al, 1980; Moore and Raftery, 1980).

REFERENCES

1. P. R. Adams (1975) Pflügers Arch. 360, 145
2. E. X. Albuquerque, E. A. Barnard, T. H. Chiu, A. J. Lapa, J. O. Dolly, S. E. Jausson, J. Daly, B. Witkop (1973) Proc. Natl. Acad. Sci. 70, 949.
3. T. J. Andreasen and M. G. McNamee (1977) Biochem. Biophys. Res. Commun. 79, 958.
4. M. V. L. Bennett, M. Wurzel and H. Grundfest (1961) J. Gen. Physiol. 44, 757.
5. G. Biesecker (1973) Biochemistry 12, 4403.
6. S. G. Blanchard and M. A. Raftery (1979) Proc. Natl. Acad. Sci. 76, 81.
7. S. G. Blanchard, J. Elliott and M. A. Raftery (1979) Biochemistry 18, 5880.
8. C. Bon and J.-P. Changeux (1975) FEBS Letters 59, 212.
9. R. Bonner, F. J. Barrantes and T. M. Jovin (1976) Nature 263, 429.
10. J. Cartaud, E. L. Benedetti, J. B. Cohen, J. C. Meunier and J.-P. Changeux (1973) FEBS Letters 33, 109.
11. H. W. Chang (1974) Proc. Natl. Acad. Sci. USA 71, 2113.
12. H. W. Chang and E. Bock (1977) Biochemistry 16, 4513.
13. T. Claudio and M. A. Raftery (1977), Arch. Biochem. Biophys. 181, 484.
14. J. B. Cohen and J.-P. Changeux (1973) Biochemistry 12, 4855.

15. J. B. Cohen, M. Weber and J.-P. Changeux (1974) Mol. Pharmacol. 10, 904.

16. A. Devillers-Thiery, J.-P. Changeux, P. Parsutaud and A. D. Strosberg (1979) FEBS Letters 104, 99.

17. V. E. Dionne, J. H. Steinbach and C. F. Stevens (1978) J. Physiol. 281, 421.

18. F. Dreyer and K. Pepper (1975) Nature 253, 641.

19. S. M. J. Dunn, S. G. Blanchard and M. A. Raftery (1980) Biochemistry submitted.

20. S. J. Edelstein, W. B. Beyer, A. T. Eldefrawi, and M. E. Eldefrawi (1975) J. Biol. Chem. 250, 6101.

21. M. E. Eldefrawi, A. G. Britten and A. T. Eldefrawi (1971) Science 173, 338.

22. M. E. Eldefrawi and A. T. Eldefrawi (1973) Arch. Biochem. Biophys. 159, 362.

23. J. Ellott and M. Raftery (1977) Biochem. Biophys. Res. Commun. 77, 1347.

24. M. Epstein and E. Racker (1978) J. Biol. Chem. 253, 6660.

25. P. Fatt and B. Katz (1951) J. Physiol.115, 320.

26. P. Fatt and B. Katz (1952) J. Physiol.117, 109.

27. G. I. Franklin and L. T. Potter (1972) FEBS Letters 28, 101.

28. S. C. Froehner, A. Karlin and Z. W. Hall (1977) Proc. Natl. Head. Sci. 74, 4685.

29. B. W. Fulpius, R. P. Klett and E. Reich (1974) in Neurochemistry of Cholinergic Receptors (E. de Robertis and J. Schacht, eds.) Raven Press, N.Y. pp. 19-29.

30. R. E. Gibson, R. D. O'Brien, S. J. Edelstein and W. R. Thompson (1976) Biochemistry 15, 2377.

31. H. Göpfert and H. Schaefer (1938) Pflügers Arch. 239, 597.

32. A. Gordon, G. Bandini and F. Hucho (1974) FEBS Letters, 47, 204.

33. H. H. Grünhagen and J.-P. Changeux (1976) J. Mol. Biol. 106, 497.

34. H. H. Grünhagen, W. Iwatsubo and J.-P. Changeux (1977) Eur. J. Biochem. 80, 225.

35. S. L. Hamilton, M. McLaughlin and A. Karlin (1977) Biochem. Biophys. Res. Commun. 79, 692.

36. P. R. Hartig and M. A. Raftery (1977) Biochem. Biophys. Res. Commun. 78, 16.

37. P. R. Hartig, H.-P. Moore, and M. A. Raftery (1980) Arch. Biochem. Biophys. submitted.

38. G. P. Hess, J. P. Andrews and G. E. Struve (1976), Biochem. Biophys. Res. Commun. 69, 830.

39. T. Heidmann and J.-P. Changeux (1979) Eur. J. Biochem. 94, 255.

40. E. Heilbronn (1975) in Cholinergic Mechanisms, pp. 343-364, Raven Press, New York.

41. F. Hucho, P. Layer, H. R. Kiefer and G. Bandini (1976) Proc. Natl. Acad. Sci. 73, 2624.

42. F. Hucho, G. Bandini and B. A. Suarez-Isla (1978) Eur. J. Biochem. 83, 335.

43. M. W. Hunkapiller, C. D. Strader, L. Hood and M. A. Raftery (1979) Biochem. Biophys. Res. Commun. 91 164.

44. D. H. Jenkinson and D. A. Terrar (1974) Brit. J. Pharmacol. 47, 363.

45. A. Karlin (1969) J. Gen. Physiol. 54, 2455.

46. A. Karlin and D. Cowburn (1973) Proc. Natl. Acad. Sci. 70, 3636.

47. E. Karlsson, E. Heilbronn and L. Widlund (1972) FEBS Letters 28, 107.

48. M. Kasai and I.-P. Changeux (1971) J. Mem. Biol. 6, 1.

49. B. Katz and L. Thesleff (1957) J. Physiol. 138, 63.

50. B. Katz and R. Miledi (1970) Nature 226, 962.

51. B. Katz and R. Miledi (1971) J. Physiol. 216, 503.

52. B. Katz and R. Miledi (1972) J. Physiol. 224, 665.

53. R. P. Klett, B. W. Fulpius, D. Cooper, M. Smith, E. Reich and L. D. Possari (1973), J. Biol. Chem. 248, 6841.

54. M. W. Klymkowsky and R. M. Stroud (1979) J. Mol. Biol. 128, 319.

55. E. K. Krodel, R. A. Beckman and J. B. Cohen (1979) Mol. Pharmacol. 15, 294.

56. C. Y. Lee and C. C. Chang (1966) Mem. Inst. Butantan. Symp. Int. 33, 555.

57. C. Y. Lee, F. F. Tseng and T. H. Chiu (1967) Nature 215, 1177.

58. C. Y. Lee (1972) Ann. Rev. Pharmacol. 12, 265.

59. C. Y. Lee, Y. M. Chen and D. Mebs (1976) Toxicon 14, 451.

60. T. Lee, V. Witzemann, M. Schinerlik and M. A. Raftery (1977) Arch. Biochem. Biophys. 183, 57.

61. J. Lindstrom, J. Merlie and G. Yogeeswaran (1979) Biochemistry 18, 4465.

62. O. Loewi (1921) Pflügers Arch. 189, 239.

63. K. L. Magleby and C. F. Stevens (1972) J. Physiol. 223, 151.

64. M. Martinez-Carrion and M. A. Raftery (1973), Biochem. Biophys. Res. Commun. 55, 1156.

65. M. Martinez-Carrion, V. Sator and M. A. Raftery (1975) Biochem. Biophys. Res. Commun. 65, 129.

66. M. G. McNamee, C. L. Weill and A. Karlin (1975), Ann. N. Y. Acad. Sci. 264, 175.

67. J.-C. Meunier, R. Sealock, R. Olsen and J.-P. Changeux (1974), Eur. J. Biochem. 45, 371.

68. D. L. Miller, H.-P. Moore, P. R. Hartig, and M. A. Raftery (1978) Biochem. Biophys. Res. Commun. 85, 632.

69. T. Moody, J. Schmidt and M. A. Raftery (1973) Biochem. Biophys. Res. Commun. 53, 761.

70. T. Moody and M. A. Raftery (1978) Arch. Biochem. Biophys. 189, 115.

71. H.-P. Moore, P. R. Hartig, W. C.-S. Wu and M. A. Raftery (1979a) Biochem. Biophys. Res. Commun. 88, 735.

72. H.-P. H. Moore, P. R. Hartig, and M. A. Raftery (1979b), Proc. Natl. Acad. Sci. 76, 6265.

73. H.-P. H. Moore and M. A. Raftery (1979) Biochemistry 18, 1862.

74. H.-P. H. Moore and M. A. Raftery (1979b) Biochemistry 18, 1907.

75. H. -P. H. Moore and M. A. Raftery (1980) Proc. Natl. Acad. Sci. submitted.

76. M. Moreau and J.-P. Changeux (1976) J. Mol. Biol. 106, 457.

77. W. L. Nastuk (1953) Fed. Proc. 12, 102.

78. E. Neher and B. Sakmann (1976) Nature 260, 779.

79. E. Nickel and L. T. Potter (1973) Brain Res. 57, 508.

80. R. D. O'Brien and R. E. Gibson (1975) Arch. Biochem. Biophys. 169, 458.

81. R. Olsen, J. C. Meunier and J. P. Changeux (1972) FEBS Letters 28, 96.

82. D. E. Ong and R. N. Brady (1974) Biochemistry 13, 2822.

83. J. Patrick, W. B. Stallcup, M. Zavenelli and P. Ravdin (1980) J. Biol. Chem. 255, 526.

84. J.-L. Popot, H. Sugiyama and J.-P. Changeux (1976), J. Mol. Biol. 106, 469.

85. U. Quast, M. Schimerlik, T. Lee, V. Witzemann, S. Blanchard and M. A. Raftery (1978) Biochemistry 17, 2405.

86. U. Quast, M. I. Schimerlik, and M. A. Raftery (1979) Biochemistry 18, 1891.

87. M. A. Raftery, J. Schmidt, and D. G. Clark (1972) Arch. Biochem. Biophys. 152, 882.

88. M. A. Raftery, R. Vandlen, D. Michaelson, J. Bode, T. Moody, Y. Chao, K. Reed, R. J. Deutsch and J. Duguid (1974a), J. Supramol. Struct. 2, 582.

89. M. A. Raftery, J. Bode, R. Vandlen, Y. Chao, J. Deutsch, J. R. Duguid, K. Reed, and T. Moody (1974b) in Biochemistry of Sensory Functions, Springer-Verlag, N. Y., pp. 541-564.

90. M. A. Raftery, J. Bode, R. Vandlen, D. Michaelson, J. Deutsch, T. Moody, M. J. Ross and R. M. Stroud (1975) in Protein-Ligand Interactions (H. Sund. and G. Blauer, eds.) W. de Gruyter, Berlin and N.Y., pp. 328-352.

91. M. A. Raftery, M. W. Hunkapiller, C. D. Strader and L. E. Hood (1980) Science, submitted.

92. H. P. Rang and J. M. Ritter (1970a) Mol. Pharmacol. 6, 357.

93. H. P. Rang and J. M. Ritter (1970b) Mol. Pharmacol. 6, 383.

94. J. A. Reynolds and A. Karlin (1978) Biochemistry 17, 2035.

95. M. J. Ross, M. W. Klymkowsky, D. A. Agard and R. M. Stroud (1977) J. Mol. Biol. 116, 635.

96. R. L. Ruff (1976) Biophys. J. 16, 433.

97. W. Schiebler and R. Hucho (1978) Eur. J. Biochem. 85, 55.

98. M. I. Schimerlik, U. Quast and M. A. Raftery (1979) Biochemistry 18, 1902.

99. J. Schmidt and M. A. Raftery (1972) Biochem. Biophys. Res. Commun. 49, 572.

100. J. Schmidt and M. A. Raftery (1973) Biochemistry 12, 852.

101. J. Schmidt and M. A. Raftery (1974) J. Neurochem. 23, 617.

102. P. Seeman (1972) Pharmacol. Rev. 24, 583.

103. R. E. Sheridan and H. A. Lester (1977) J. Gen. Physiol. 70, 187.

104. A. Sobel, T. Heidmann, J. Hofler and J.-P. Changeux (1978) Proc. Natl. Acad. Sci. USA 75, 510.

105. J. H. Steinbach (1977) Biophys. J. 18, 357.

106. C. F. Stevens (1975) Fed. Proc. 34, 1364.

107. C. D. Strader, J.-P. Revel and M. A. Raftery (1979) J. Cell. Biol. 83, 499.

108. C. D. Strader, M. W. Hunkapiller, L. E. Hood and M. A. Raftery (1980a) Biochem. Biophys. Res. Commun. submitted.

109. C. D. Strader and M. A. Raftery (1980b) Proc. Natl. Acad. Sci., submitted.

110. B. A. Suarez-Isla and F. Hucho (1977) FEBS Letters 75, 65.

111. A. Takeuchi and N. Takeuchi (1960) J. Physiol. 154, 52.

112. R. Tarrah-Hazdai, B. Geiger, S. Fuchs and A. Amsterdam (1978) Proc. Natl. Acad. Sci. 75, 2497.

113. R. L. Vandlen, W. C.-S. Wu, J. C. Eisenach and M. A. Raftery (1979) Biochemistry 10, 1845.

114. M. Weber and J.-P. Changeux (1974a) Mol. Pharmacol. 10, 1.

115. M. Weber and J.-P. Changeux (1974b) Mol. Pharmacol. 10, 15.

116. M. Weber, T. David-Pfeuty and J. P. Changeux (1975) Proc. Natl. Head. Sci. 72, 3443.

117. C. L. Weill, M. G. McNamee and A. Karlin (1974) Biochem. Biophys. Res. Commun. 61, 997.

118. V. Witzemann and M. A. Raftery (1978a) Biochem. Biophys. Res. Commun. 81, 1025.

119. V. Witzemann and M. A. Raftery (1978b) Biochemistry 17, 3598.

120. V. Witzemann, D. Muchmore and M. A. Raftery (1979) Biochemistry 18, 1511.

121. W.C.S. Wu and M. A. Raftery (1979) Biochem. Biophys. Res. Commun. 89, 26.

CHAPTER ONE

The reversible and irreversible interactions of an alkylating agonist, bromoacetylcholine, with *T. californica* acetylcholine receptor in membrane-bound and purified states.

INTRODUCTION

The acetylcholine receptor has been purified from the electric organs of T. californica in either membrane-bound or detergent solubilized state (Duguid and Raftery, 1973; Schmidt and Raftery, 1973a). In both cases, multiple polypeptide constituents are present in the preparations. Localization of the component(s) which contains the cholinergic ligand binding site can be approached by affinity labeling technique.

The AcChR of the electroplaque of Electrophorus electricus contains a readily reducible disulfide bond believed to reside in the vicinity of a cholinergic ligand binding site (Karlin, 1969). Reduction of this bond by dithiothreitol (DTT) altered the physiological response of the receptor to cholinergic ligands, and the effect could be reversed by reoxidation with 5,5'-dithio-bis(2-nitrobenzoic acid) (DTNB). Similar results were found with the AcChR at the frog neuromuscular junction (Ben-Haim et al, 1973). The reduced single-cell AcChR preparation of Electrophorus electroplaques could be alkylated by various active-site directing reagents; some of these resulted in irreversibly activated receptors and others in irreversibly inhibited receptors (Silman and Karlin, 1969; Kalderon and Silman, 1971; Bartels-Bernal et al, 1976). One of such antagonists, 4-(N-maleimido)-benzyltrimethylammonium iodide (MBTA), has been studied extensively as an affinity label for the subcellular characterization of AcChR. The reagent was found to bind to a single subunit of approximately 40,000

daltons in both Electrophorus and Torpedo receptors (Karlin and Cowburn, 1973; Weill et al, 1974). Moreover, both fish receptors bound twice as much α-neurotoxin as they did MBTA. With denervated rat skeletal muscle, however, [^{3}H] MBTA labeled two different subunits of the reduced AcChR and the amount of specific labeling per toxin site was also different from that for the fish receptors (Froehner et al, 1977).

Since the blocking effects exerted by reversible cholinergic antagonists on synaptic transmission are not always strictly competitive (Colquhoun et al, 1979), affinity reagents which act as depolarizing agonists are more desirable for the localization of the agonist binding site(s) on the AcChR. This chapter describes the interaction of an alkylating agonist, bromoacetylcholine (BrAcCh) with the membrane-bound and solubilized AcChR from T. californica. BrAcCh differs from MBTA in two respects in its physiological effects: first, in the absence of DTT, it acts as a reversible depolarizing agent, whereas MBTA acts as an inhibitor of cholinergic ligand induced depoarization; secondly, in the presence of DTT, it irreversibly activates, while MBTA irreversibly inhibits the receptor of Electrophorus (Karlin, 1969).

In the study described here it was found that BrAcCh binds specifically and reversibly to the non-reduced receptor preparation; this binding is competitive with AcCh. Following reduction with DTT the reagent irreversibly alkylates the AcChR. The number of sites alkylated is similar to the number of reversible binding sites for BrAcCh and corresponds to half the number of [^{125}I]-α-BuTx sites present in the preparation. Using [^{3}H] BrAcCh it was found that only the 40,000-

dalton subunit was covalently labeled. This result suggests that a major agonist binding site(s) resides on this polypeptide component of the AcChR protein complex. The polypeptide patterns of the alkylated receptor after proteolytic digestion have also been investigated.

EXPERIMENTAL

Materials:

Torpedo californica were obtained locally. Lyophilized venom of Bungarus multicinctus was obtained from Sigma Chemical Co. Na[^{125}I] was purchased from New England Nuclear Co. DE-81 DEAE discs were from Whatman, Ltd. S-acetylthiocholine, AcCh, DNPP, bromoacetylbromide and choline chloride were obtained from Aldrich Chemical Co., Inc. Lyophilized venom of Bungarus multicinctus, Carb, d-Tc, DTT and eserine were from Sigma Chemical Co., and [[^{3}H]-acetyl] AcCh and [^{3}H] choline chloride were from New England Nuclear Co. Reagents for gel electrophoresis were obtained from Pierce Chemical Co. All other chemicals were of the highest purity commercially available.

Preparation of Membrane-Bound and Solubilized, Purified AcChR

Crude AcChR-containing membrane fragments were prepared from homogenates of T. californica electroplaques by differential centrifugation. For the studies described in this chapter and Chapter 5, AcChR-enriched membrane fragments were prepared from these crude membrane fragments by further purification on sucrose gradients in zonal rotors (Duguid and Raftery, 1973; Reed et al., 1975). Recently, a much more rapid method has been employed to purify AcCh-R-enriched membrane fragments by a reorienting sucrose step gradient (Elliott et al, 1980). This method was used to prepare membranes for the studies described in Chapters 2-4. Buffer used throughout the preparation was 10 mM sodium phosphate, pH 7.4, 0.4 M NaCl, 1-5 mM EDTA and 0.02% NaN_3.

Highly purified AcChR was prepared by affinity chromatography after Triton solubilization as described previously (Schmidt and Raftery, 1972, 1973a, Vandlen et al, 1976).

Assay of AcChR Binding Activity by [^{125}I]-α-BuTx

α-BuTx was purified from lyophilized venom according to the method of Clark et al (1972) and was labeled with [^{125}I] by a procedure (Blanchard et al, 1979) modified from that of Vogel et al (1972). The monoiodo derivative was separated from other labeled species by CM-Sephadex chromatography. [^{125}I] α-BuTx binding to AcChR was carried out by the DEAE filter-disc assay method of Schmidt and Raftery (1973b). All membrane preparations were routinely assayed to determine whether they underwent an affinity change upon incubation with Carb (Lee et al, 1977). The initial rate of [^{125}I] α-BuTx binding to the AcChR was measured in the absence of agonist, and in the presence of 1 μM Carb, added either 30 min prior to, or at the same time as [^{125}I] α-BuTx, under conditions in which the toxin was in large excess over AcChR toxin binding sites. Only preparations with equal initial toxin binding rates observed in the absence of Carb and when Carb and toxin were added simultaneously were used for the studies presented here, i.e., preparations in the low affinity state. The toxin binding technique was also used to study the binding of unlabeled BrAcCh to AcChR.

Assay of Acetylcholinesterase Activity

Since BrAcCh is a substrate for acetylcholinesterase (AcChE) hydrolysis (Chiou and Sastry, 1968), eserine or diethylnitrophenyl phosphate (DNPP) was routinely added to the AcChR preparations to inhibit the AcChE activity, which was assayed by the method of Ellman et al, (1961) using S-acetylthiocholine as substrate. Alternatively, the method of Johnson and Russel (unpublished data) was employed to detect low levels of AcChE activity: to 100 µl of [[^{3}H]-acetyl] AcCh (1-1000 µM) in 25 mM potassium phosphate, pH 7.0, were added 10 µl of the sample whose AcChE activity was to be determined and the mixture was incubated at room temperature for 20 min. The reaction was stopped by adding 100 µl of a solution 0.1 M in chloroacetic acid, 2 M in NaCl and 0.5 M in NaOH. Esterase activity was determined by assaying the amount of [^{3}H] acetic acid selectively extracted into 3 ml of scintillation cocktail (10% isoamylalcohol in toluene, containing 1.14 mg POPOP and 18.95 mg PPO).

Preparation of Radiolabelled and Unlabelled BrAcCh

Bromoacetylcholine perchlorate was prepared from bromoacetylbromide and choline chloride according to the method of Chiou and Sastry (1968). The reaction product was recrystallized from 1:6 acetone-ethylacetate. The resulting colorless needles had a melting point of 103-103.5^{o}C and showed one NH_2OH-$FeCl_3$ positive spot (Hestrin, 1949) on thin-layer chromatography (n-BuOH-EtOH-H_2O-HOAc = 4:2:3:1 as solvent). [^{3}H]-Bromoacetylcholine perchlorate was synthesized from [^{3}H] choline by

the same procedure. The radioactive product cochromatographed with the unlabeled BrAcCh (R_f = 0.74) in the TLC system described above. Specific activities of [^{3}H] BrAcCh were 42 and 70 mCi/mmole for the two batches synthesized. The concentration of [^{3}H] BrAcCh was determined by hydroxylamine-ferric chloride determination of ester groups (Hestrin, 1949) using unlabeled BrAcCh as standard. Stock solutions of [^{3}H] BrAcCh in 1 mM Tris buffer, pH 7.2 were stored at -80^{o}C. It was found that under these conditions no significant hydrolysis occurred during a period of six months.

Measurements of Reversible Binding of ^{3}H-BrAcCh to Membrane-bound AcChR

To study reversible binding of [^{3}H] BrAcCh to membrane-bound AcChR various concentrations of [^{3}H] BrAcCh were incubated with AcChR-enriched membrane fragments in Torpedo Ringers (0.25 M NaCl, 5 mM KCl, 2 mM $MgCl_2$, 4 mM $CaCl_2$, 5 mM Tris-Cl, pH 7.4) for 20 min at 4^{o}C. Membrane fragments were then pelletted by centrifugation in a Beckman type 65 rotor at 49,000 rpm for 1 hour. Triplicate 100 µl aliquots of samples were withdrawn before and after centrifugation and these were counted in a Packard TriCarb Liquid Scintillation Spectrometer (Model 3375), using 10 ml of Aquasol as scintillant, to determine the total and free concentrations of [^{3}H] BrAcCh. [^{3}H] H_2O was used as external and internal standard to determine counting efficiency.

Covalent Labeling of Reduced AcChR with [^{3}H]-BrAcCh

DTT was added to the AcChR preparations (0.5-1 μM in α-BuTx sites) to a final concentration of 10 μM (for Triton solubilized, purified receptors) or 40 μM (for membrane-bound receptors). Reduction was performed at room temperature for 1 hour and various concentrations of [^{3}H] BrAcCh were then added and the reaction allowed to continue for another hour at 4^{o}C. Two 100 μl aliquots of reaction mixtures were pipetted onto DE-81 discs to adsorb the AcChR, and therefore the covalently attached [^{3}H] BrAcCh moieties. Unreacted [^{3}H] BrAcCh was then washed away with 10 mM sodium phosphate, pH 7.4, 0.1% Triton X-100, 50 mM NaCl for 10 min. This washing procedure was then repeated twice more. The discs were soaked in 800 μl of H_2O for 1 hour, shaken and counted in 10 ml of toluene-based scintillation fluid containing 25% triton X-100 and 0.55% Permablend III. For SDS-polyacrylamide gel electrophoresis the labeled product was dialyzed three times against fresh reaction buffer for four hours. SDS-gel electrophoresis with 8.75% or 12.5% acrylamide and 0.1% bisacrylamide was carried out according to Laemmli (1970). Gels were stained with CBB and scanned at 550 nm in a Gilford spectrometer. 1 mm slices of the gels were sliced on a Mickel gel slicer, dissolved in 0.5 ml H_2O_2 at 60-80^{o}C for 5-6 hours, and counted in 10 ml of the toluene-based scintillation cocktail described above.

Stability of BrAcCh was determined under the experimental conditions used for binding assays by determination of the ester content (Hestrin, 1949). No significant hydrolysis was observed for periods

up to four hours at room temperature. Similar stability was found with the covalently attached [^{3}H]-AcCh moieties on AcChR. No loss of radioactivity was detected after dialysis against Torpedo Ringers, pH 7.4 at 4^{o}C for over 16 hours.

RESULTS

(A) Reversible Interactions of Bromoacetylcholine with Membrane-Bound AcChR

$^{22}Na^+$ Flux. As will be described in Chapter 3, BrAcCh acts as a cholinergic agonist *in vitro* by inducing a rapid efflux of $^{22}Na^+$ from AcChR-enriched membrane vesicles. This result thus confirms the *in vivo* observations that BrAcCh is a depolarizing agonist.

Interconversion of AcChR Affinity State(s) by BrAcCh

In the absence of DTT, AcChR-enriched membrane fragments from *T. californica* underwent a change from low to high affinity state(s) upon incubation with BrAcCh. As shown in Figure 1A, the initial rate of [^{125}I) α-BuTx binding to the AcChR was only slightly affected by 200 nM BrAcCh when added at the same time as the radiotoxin. The binding curve deviated from that observed in the absence of BrAcCh as time progressed, indicating that a slow affinity change had occurred. Preincubation of AcChR with BrAcCh for 20 min greatly depressed the initial rate of receptor-toxin complex formation; BrAcCh thus induced a tighter binding state of AcChR with time. Such large effects have

FIGURE 1: A: Induction of AcChR Isomerization from Low to High Affinity State(s) by BrAcCh; (● - ●) To membrane-bound AcChR (6.2×10^{-8}M in α-BuTx sites) in Torpedo Ringers was added 5.0×10^{-7}M [^{125}I] α-BuTx and the time-course of AcChR α-BuTx complex formation was followed by the DEAE disc assay described in the Experimental Section. (Δ - Δ) Same as in (● - ●) except that 2×10^{-7}M Br-AcCh perchlorate was added simultaneously with [^{125}I] α-BuTx to the membrane suspension. (O - O) Same as in (● - ●) except that the AcChR was first pre-incubated with 2×10^{-7}M BrAcCh perchlorate at room temperature for 20 min before [^{125}I] α-BuTx addition.

B: Dependence of Initial Rates of [^{125}I] α-BuTx Binding on Bromoacetylcholine Perchlorate Concentration After Preincubation with Membrane-bound AcChR: Membrane-bound AcChR (3.4×10^{-8}M in α-BuTx sites) in Torpedo Ringers was preincubated with various concentrations of BrAcCh at room temperature for 20 min to reach equilibrium. 2.6×10^{-7}M [^{125}I] α-BuTx was then added and the initial rate of toxin binding was measured by DEAE disc assay. In all cases, the same amount of AcChR-toxin complex (C_∞) was found 15-20 hours after toxin addition. The pseudo-first order rate constants (k_{obs}) were determined from semilog plots ($\ln(C_\infty - C_t)$ vs. t, where C_t is the amount of AcChR-toxin complex formed at time t) by unweighted linear least squares fit. The apparent dissociation constant for BrAcCh was obtained by weighted linear least squares fit to the linearized form of Eqn. 1. Correction was made for the bound BrAcCh by an iterative procedure. (——) Fit of the experimental data to Eqn. 1, with $K_{app} = 17 \pm 4$ nM and $k_{obs} = 5.22 \times 10^{-3} s^{-1}$ in the absence of BrAcCh.

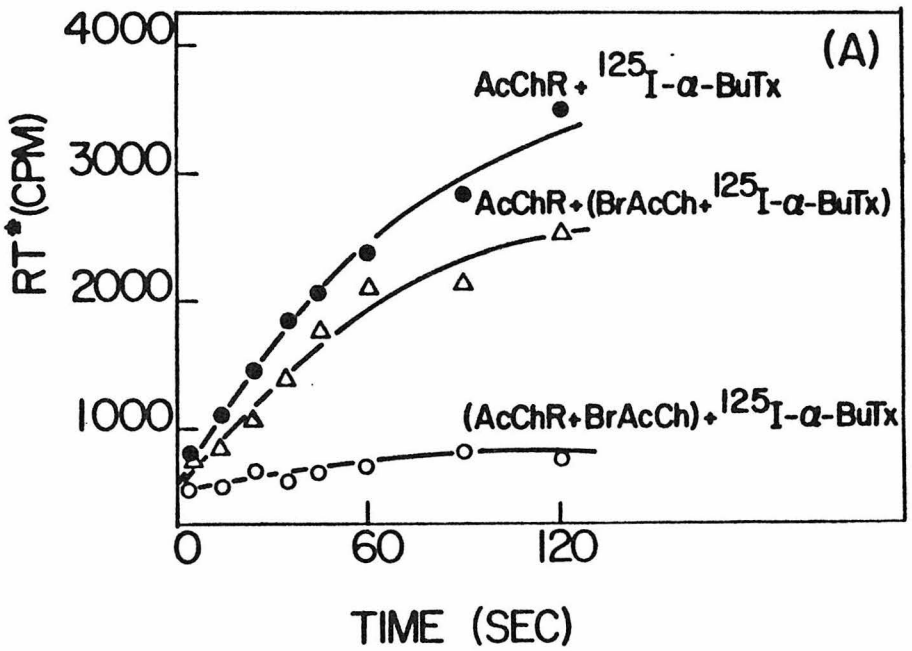
(A)
AcChR + 125I-α-BuTx
AcChR + (BrAcCh + 125I-α-BuTx)
(AcChR + BrAcCh) + 125I-α-BuTx
RT* (CPM)
4000
3000
2000
1000
0
60
120
TIME (SEC)

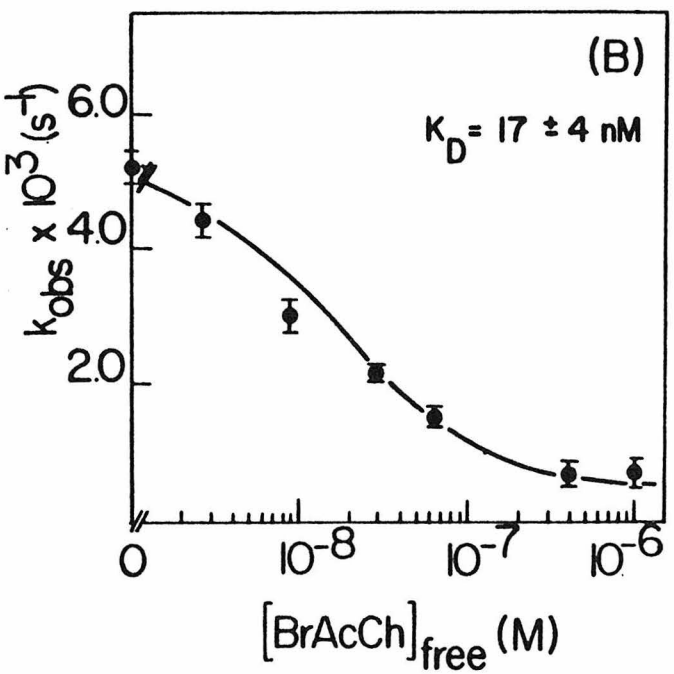
(B)
K_D = 17 ± 4 nM
k_obs x 10^3 (s^-1)
6.0
4.0
2.0
0
10^-8
10^-7
10^-6
[BrAcCh]_free (M)

previously been observed for a variety of agonists (Weber et al, 1975; Weiland et al, 1976, 1977; Colquhoun and Rang, 1976; Lee et al, 1977; Quast et al, 1978) and to a lesser extent for antagonists (Lee et al; Quast et al, 1978).

Equilibrium Binding Parameters Measured by Inhibition of Toxin Binding

Binding of [^{125}I] α-BuTx to membrane preparations under conditions in which the toxin was in large excess over the AcChR binding sites for the toxin followed simple pseudo-first order kinetics (Quast et al, 1978). Preincubation of the membrane-bound receptor with BrAcCh inhibited the initial toxin binding rate, but the kinetics remained pseudo-first order during the time period the reaction was followed. Figure 1B illustrates the observed pseudo-first order rate constant, k_{obs}, as a function of free BrAcCh concentration after preincubation. The data fit the following equation (Quast et al, 1978);

$$k_{obs} = \frac{kT_o}{1+[L]/K_{app}} \qquad (1)$$

where T_o is the total toxin concentration (T_o >> [AcChR]), k is the bimolecular rate constant of toxin binding to AcChR, [L] is the free BrAcCh concentration and K_{app} is the apparent dissociation constant for BrAcCh. The apparent dissociation constant for BrAcCh was found to be 17 ± 4 nM and the bimolecular rate constant (k) of toxin binding to this membrane preparation was $2.0 \times 10^4 M^{-1}s^{-1}$, in excellent agreement with the data of Quast et al, (1978) who determined a value of $2.0 \pm 0.2 \times 10^4 M^{-1}s^{-1}$.

Binding of Radioactive Ligand

The binding of [^{3}H] BrAcCh to membrane-bound AcChR was studied directly by centrifugation assay and as can be seen in Figure 2A, the binding curve was composed of two components: a saturable, specific binding hyperbola superimposed on a linear, non-specific binding component. Subtraction of the non-specific binding component from the total binding curve yielded the specific binding hyperbola. The ratio of the number of specifically bound [^{3}H] BrAcCh molecules to the number of α-BuTx sites was 0.51 ± 0.03. A Scatchard plot of data from similar experiments conducted with low receptor concentrations is shown in Figure 2B; a straight line was obtained with an x-intercept corresponding to 0.50 ± 0.02 [^{3}H] BrAcCh sites / α-BuTx sites. From the slope, the apparent dissociation constant of [^{3}H] BrAcCh to membrane-bound AcChR was found to be 16 ± 1 nM, in excellent agreement with the value obtained from the toxin binding inhibition technique (Fig. 1B). In addition, no cooperativity was detected in the binding; a Hill plot of the binding data gave a straight line with slope = 0.98 ± 0.02 (Figure 2C).

Inhibition of [^{3}H] BrAcCh Binding by AcCh

Binding of [^{3}H] BrAcCh to the receptor membrane fragments as detailed in Figure 2 was inhibited by the presence of AcCh. The data in Figure 3 represent binding studies conducted in the presence of several fixed concentrations of AcCh. Since the receptor concentration in these experiments was relatively large compared to the AcCh concentration, correction was made for the bound AcCh by an iterative non-

FIGURE 2: Reversible Binding of [^{3}H] Bromoacetylcholine Perchlorate to Membrane-Bound AcChR: A; Membrane fragments (8.06×10^{-6}M in α-BuTx sites) in Torpedo Ringers were incubated with indicated concentrations of [^{3}H] BrAcCh at 4^{o}C for 20 min. The amount of [^{3}H] BrAcCh bound was measured as described in the experimental section. (●) The observed bound [[^{3}H] BrAcCh]. (---) linear least squares fit of the non-specific binding component. (O) Specific binding component obtained by subtracting the non-specific binding component from the observed $[[^3H]\ BrAcCh]_{bound}$. B and C: Scatchard plot and Hill plot. [AcChR] = 2.29×10^{-7}M. (——) linear least squares fit of data. n = total concentration of BrAcCh sites, b = concentration of bound ligand and f = concentration of free ligand.

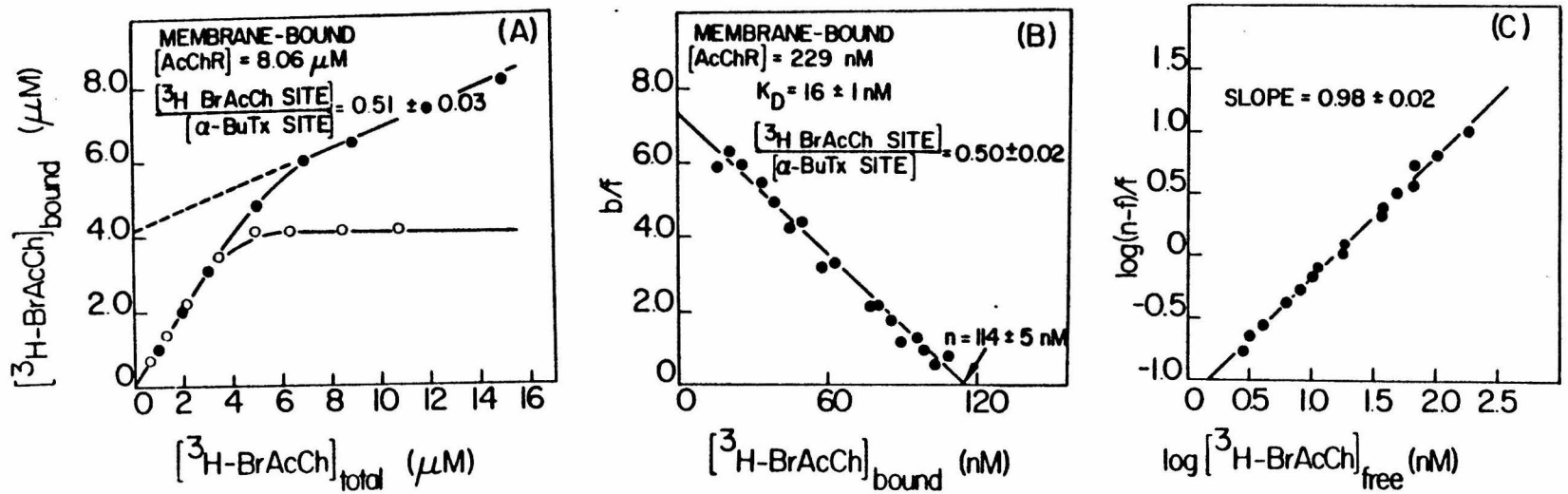
MEMBRANE-BOUND
[AcChR] = 8.06 μM
[3H BrAcCh SITE] / [α-BuTx SITE] = 0.51 ± 0.03
(A)
[3H-BrAcCh]bound (μM)
[3H-BrAcCh]total (μM)
0 2 4 6 8 10 12 14 16
0 2.0 4.0 6.0 8.0
MEMBRANE-BOUND
[AcChR] = 229 nM
KD = 16 ± 1 nM
[3H BrAcCh SITE] / [α-BuTx SITE] = 0.50±0.02
n = 114 ± 5 nM
(B)
b/f
[3H-BrAcCh]bound (nM)
0 60 120
0 2.0 4.0 6.0 8.0
SLOPE = 0.98 ± 0.02
(C)
log(n-f)/f
log [3H-BrAcCh]free (nM)
0 0.5 1.0 1.5 2.0 2.5
-1.0 -0.5 0 0.5 1.0 1.5

FIGURE 3: Inhibition of [^{3}H] BrAcCh Binding to Receptor Membrane Preparation by AcCh: To membrane fragments (2.29×10^{-7}M in α-BuTx sites) in Torpedo Ringers were added various concentrations of AcCh (40, 80, 120 nM). For a fixed concentration of AcCh, a series of [^{3}H] BrAcCh binding studies, as described in Figure 2, were carried out. The reciprocal of bound [^{3}H] BrAcCh is plotted versus the reciprocal of free [^{3}H] BrAcCh; (■) observed data points; (●) non-linear least squares fit of the data to a competitive model, with correction for free [AcCh] by an iterative method. The fit gives K_{app} for BrAcCh = 15 ± 1 nM and K_I for AcCh = 8±1 nM.

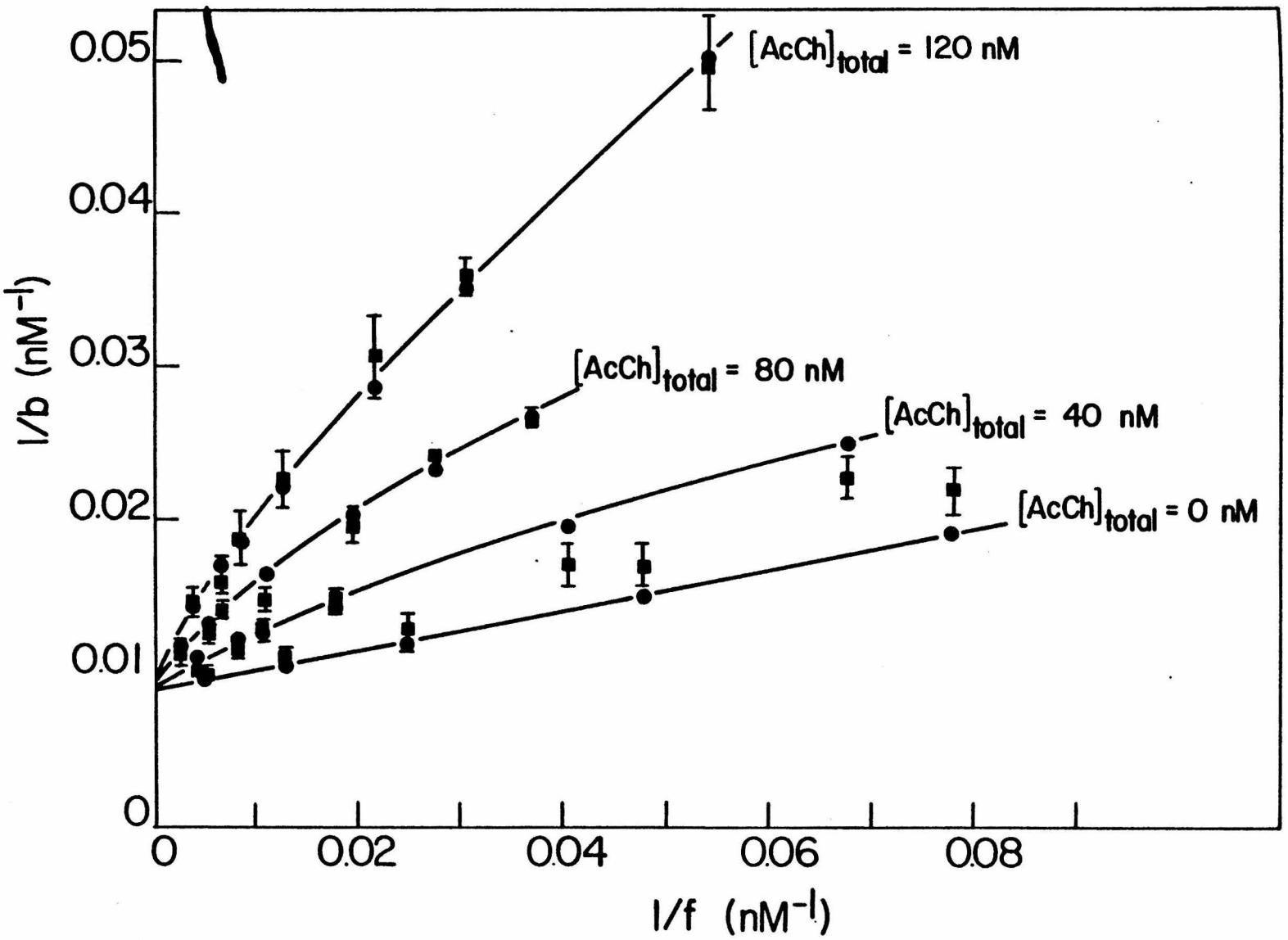
0.05
0.04
0.03
0.02
0.01
0
1/b (nM⁻¹)
[AcCh]total = 120 nM
[AcCh]total = 80 nM
[AcCh]total = 40 nM
[AcCh]total = 0 nM
0
0.02
0.04
0.06
0.08
1/f (nM⁻¹)

linear least squares fit. The parameters obtained from such a fit were 15 ± 1 nM for the dissociation constant of BrAcCh and 8 ± 1 nM for the dissociation constant of AcCh; this value for the K_d of AcCh agrees very well with previously published values of direct measurements of the binding of this ligand to membrane preparations (Weber and Changeux, 1974).

(B) Covalent Labeling of Reduced AcChR by Bromoacetylcholine

Stoichiometry

After reduction of the AcChR with DTT BrAcCh was found to covalently modify the receptor. The amount of irreversibly bound [^{3}H] BrAcCh was determined from the radioactivity associated with an extensively dialyzed reaction mixture or by the DEAE disc method described in the Experimental Section. Figure 4 shows the extent of labeling for both membrane-bound and Triton-solubilized, purified AcChR. In both cases, the curves consisted of a saturable binding component superimposed on a small, linear, non-specific phase. Preincubation of the AcChR with excess α-BuTx completely inhibited the saturable uptake and provided a convenient measure of non-specific binding; subtraction of this non-specific component from the observed total binding curve gave the specific binding component. From the radioactivity incorporated, a stoichiometry of 0.50 ± 0.02 [^{3}H] BrAcCh sites per α-BuTx site was obtained for both solubilized, purified and membrane-bound AcChR. In the absence of DTT, no specific irreversible labeling could be detected (Figure 4 Curve C).

FIGURE 4: Covalent Labeling of Reduced AcChR by [^{3}H] BrAcCh: A: Triton-solubilized Purified AcChR B: Membrane-bound AcChR. Curve A: AcChR (5.7×10^{-7}M in α-BuTx sites) was first reduced by DTT. Various concentrations of [^{3}H] BrAcCh were then added to start the labeling reaction. The amount of [^{3}H] BrAcCh covalently attached to the receptor was determined by DEAE disc assay as described in the experimental section. Curve B: AcChR was preincubated with excess unlabeled α-BuTx for 3-5 hours before reduction and alkylation. Curve C: Same as in Curve A, except that DTT was replaced by buffer. (---) Subtraction of Curve B from Curve A to obtain the specific binding component.

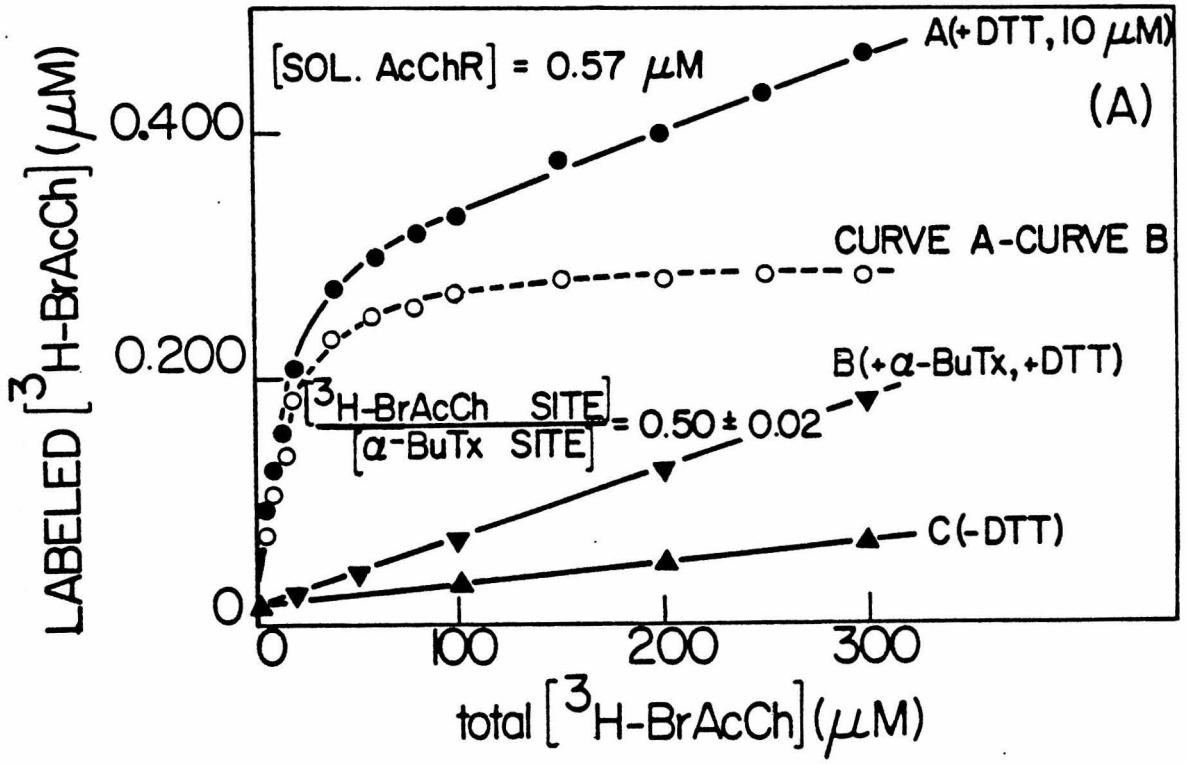
[SOL. AcChR] = 0.57 μM
A(+DTT, 10 μM)
(A)
CURVE A-CURVE B
B(+α-BuTx, +DTT)
[3H-BrAcCh SITE] / [α-BuTx SITE] = 0.50 ± 0.02
C(-DTT)
LABELED [3H-BrAcCh] (μM)
total [3H-BrAcCh] (μM)
0.400
0.200
0
0
100
200
300

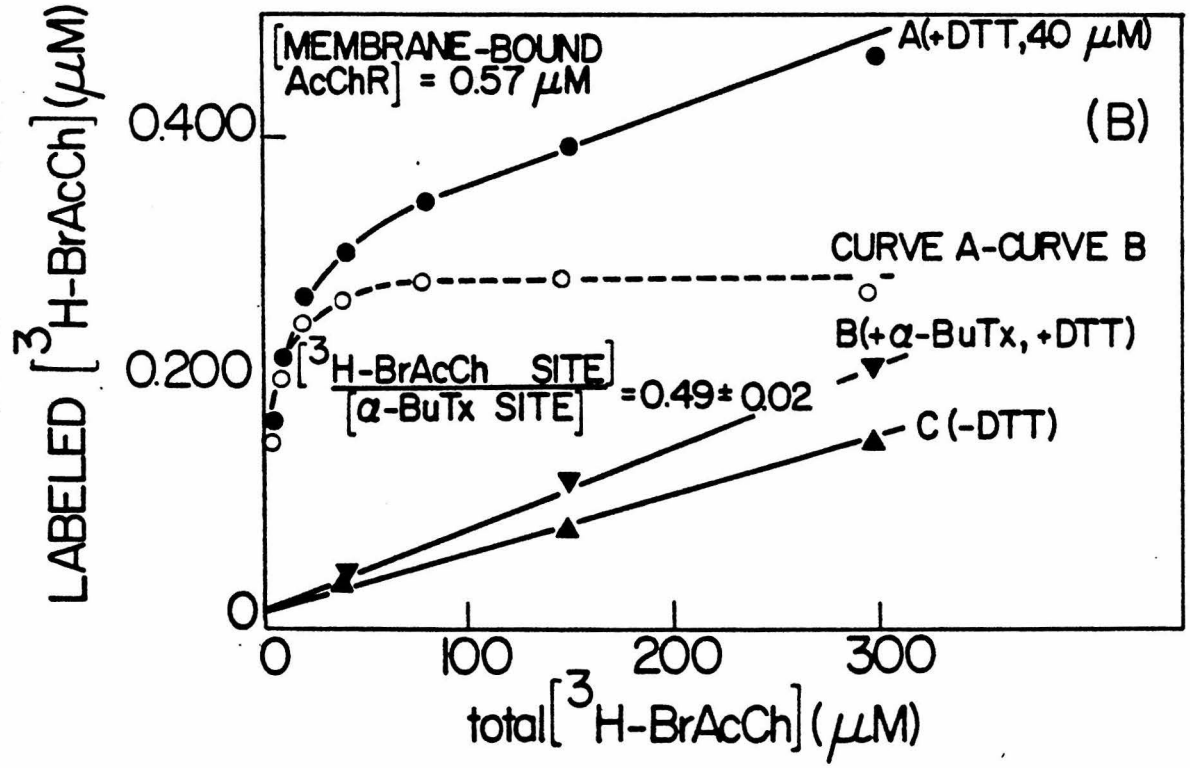
[MEMBRANE-BOUND AcChR] = 0.57 μM
A(+DTT, 40 μM)
(B)
CURVE A-CURVE B
B(+α-BuTx, +DTT)
[3H-BrAcCh SITE] / [α-BuTx SITE] = 0.49 ± 0.02
C(-DTT)
LABELED [3H-BrAcCh] (μM)
total [3H-BrAcCh] (μM)
0.400
0.200
0
0
100
200
300

Protection Studies

When the reduction and alkylation of membrane-bound AcChR by [^{3}H] BrAcCh was carried out in the presence of $8x10^{-4}$M AcCh, the naturally occurring agonist for the AcChR, or of $5x10^{-5}$M d-Tc, a potent antagonist, the extent of labeling was appreciably reduced (Figure 5). Exposure of AcChR containing membranes to unlabeled BrAcCh prior to introduction of [^{3}H] BrAcCh also inhibited the incorporation of radioactivity. Similar results were obtained with Triton solubilized, purified AcChR (data not shown).

SDS-Polyacrylamide Gel Electrophoresis and the Site of [^{3}H]-BrAcCh Labeling

Only four polypeptide components of 40,000, 50,000, 60,000 and 65,000 dalton M.W. are present in the solubilized, purified AcChR preparations while the AcChR membrane preparations purified on sucrose gradients contain numerous other polypeptides in addition to these four components. Both preparations, following covalent labeling with [^{3}H]-BrAcCh and SDS gel electrophoresis, revealed a prominent, single peak of radioactivity associated with the 40,000 dalton polypeptide. The protective effect exerted by cholinergic ligands and α-BuTx was evident from the decreased incorporation of radioactivity into this receptor subunit (Fig. 6).

FIGURE 5: Protection of AcChR from [^{3}H] BrAcCh Labeling by Cholinergic Ligands. The labeling reaction was carried out with a receptor membrane preparation as in Figure 4B, Curve A, except that 8 x 10^{-4}M AcCh (▽), 5 x 10^{-5}M d-Tc (▲) and a 10 fold excess of unlabeled BrAcCh (O) were added immediately before [^{3}H] BrAcCh addition.

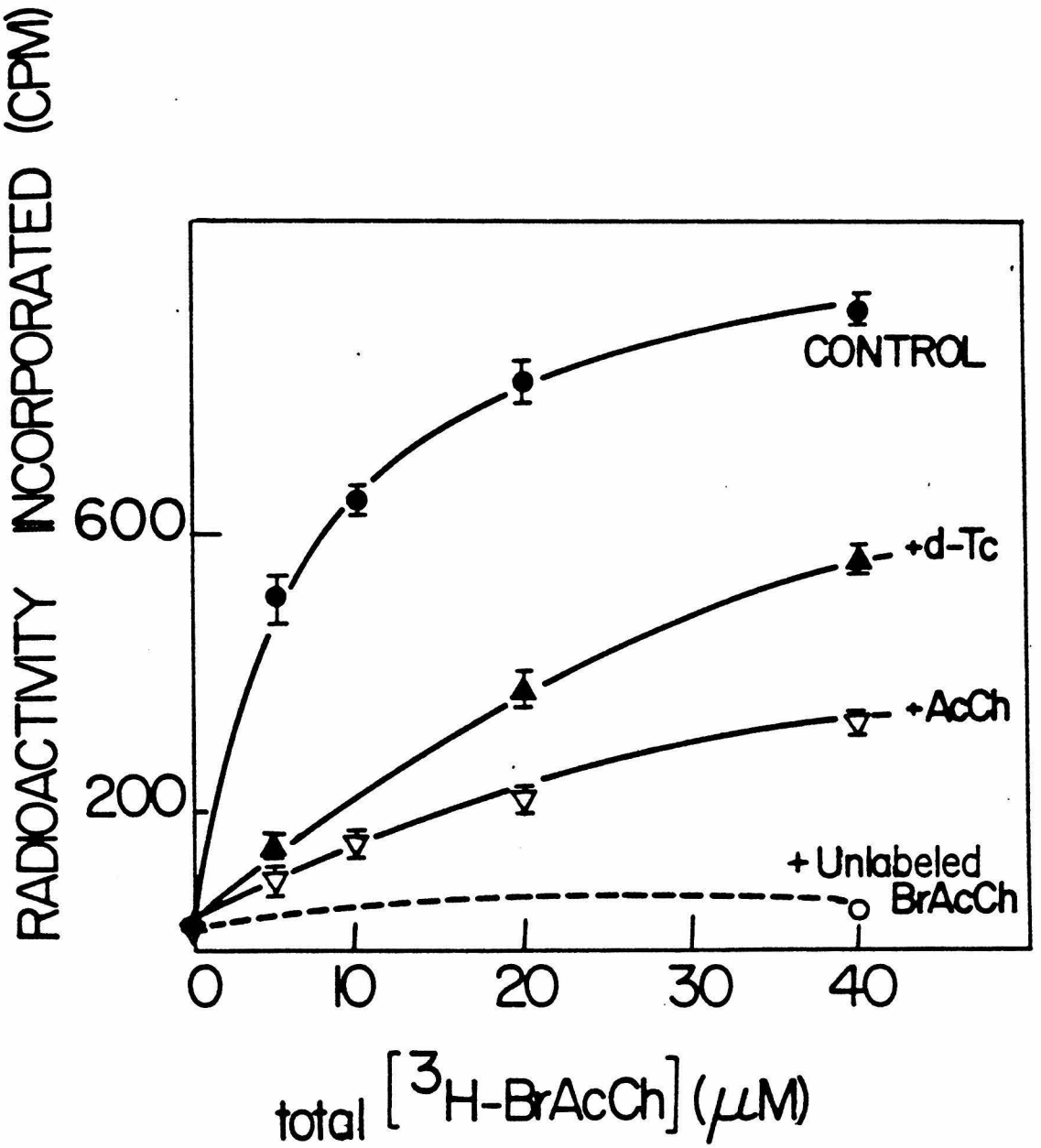
RADIOACTIVITY INCORPORATED (CPM)
600
200
CONTROL
+d-Tc
+AcCh
+ Unlabeled BrAcCh
0
10
20
30
40
total [3H-BrAcCh] (μM)

FIGURE 6: SDS-Polyacrylamide Gel Electrophoresis of [^{3}H] BrAcCh Labeled AcChR: The radioactivity incorporated is plotted as a function of gel slice number. CBB stained 12.5% (top) and 8.75% (bottom) SDS polyacrylamide gels are shown. (■) Labeled, Triton solubilized, purified AcChR. (●) Labeled membrane-bound AcChR; (○) membrane-bound AcChR labeled in the presence of 5 x 10^{-5}M d-Tc; (Δ) in the presence of 8 x 10^{-4}M AcCh and (□) in the absence of DTT or in the presence of a large excess of unlabeled BrAcCh or α-BuTx.

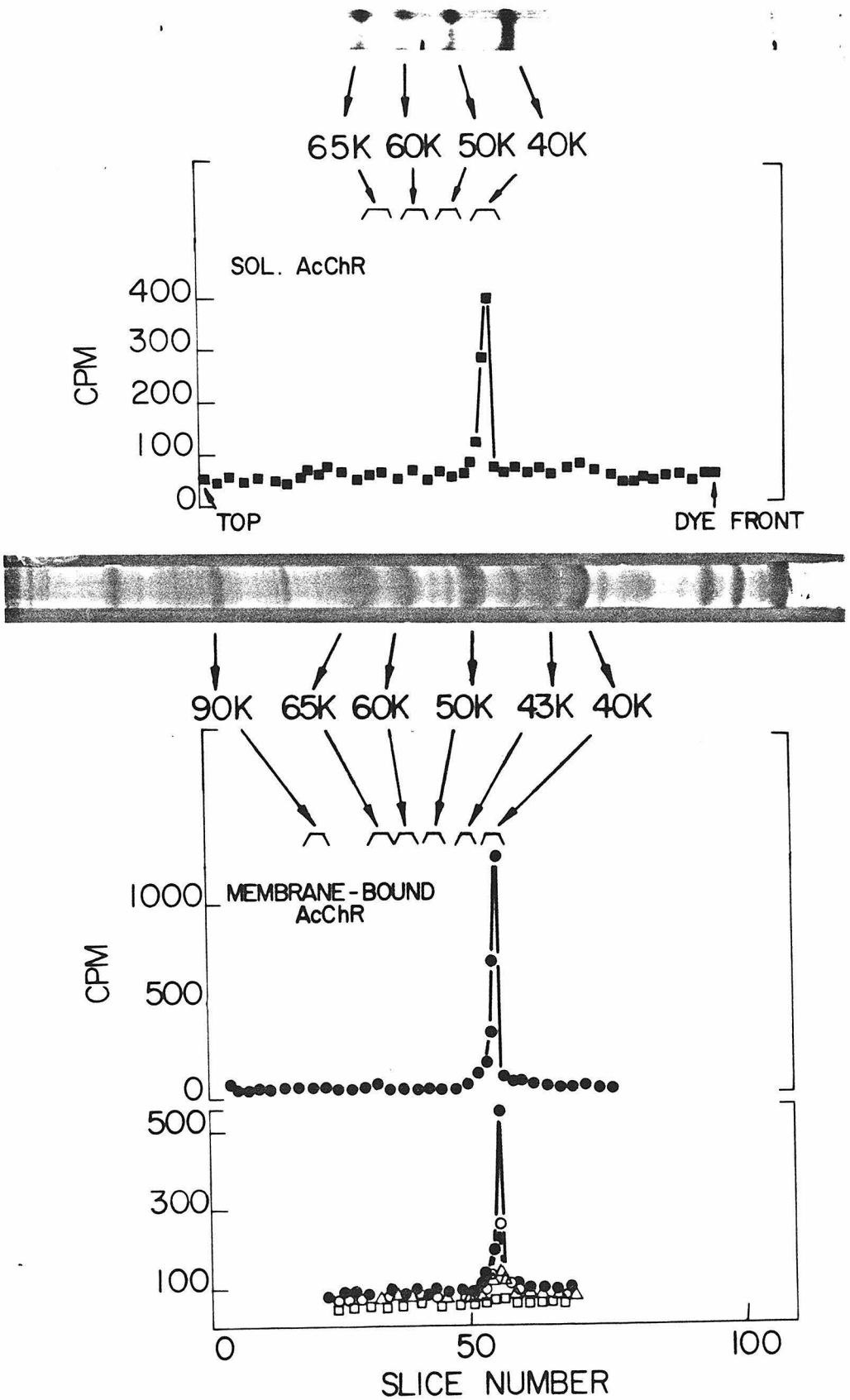
65K 60K 50K 40K
SOL. AcChR
CPM
400
300
200
100
0
TOP
DYE FRONT
90K 65K 60K 50K 43K 40K
MEMBRANE-BOUND
AcChR
1000
500
0
500
300
100
0
50
100
SLICE NUMBER

Toxin Binding to Alkylated AcChR

The effect of BrAcCh alkylation on the binding of [^{125}I] α-BuTx to the AcChR was investigated and as shown in Figure 7, the initial rate of [^{125}I] α-BuTx binding to both purified and membrane-bound AcChR was greatly suppressed after alkylation with BrAcCh. The total extent of receptor-toxin complex formed 15-20 hours after toxin addition was 45 - 60% (for purified AcChR) and 12 - 26% (for membrane-bound AcChR) of that found for non-alkylated receptor.

Proteolytic Digestion of AcChR Labeled with [^{3}H]-BrAcCh

Recently membrane preparations of highly purified AcChR have been obtained by a method of alkaline extraction which contain only four major constituents (the 40,000, 50,000, 60,000 and 65,000-dalton polypeptides, see Chapter 3). This type of preparation also gives similar labeling pattern when alkylated by [^{3}H]-BrAcCh. Extensive tryptic digestion of the alkylated membranes gives rise to two major low M.W. bands along with several minor bands on a SDS gel electrophoretogram (Figure 8). The lower M.W. component of the two major degradation products (Band II in Figure 8) was found to contain the label. The label was also found in a polypeptide of similar M.W. when digestion was carried out with alkylated AcChR after Triton solubilization. Denaturation of the alkylated AcChR by SDS before digestion, however, results in a much more complete degradation and the label electrophoresed with a component at the dye front. The 40,000 dalton subunit in the native AcChR complex can thus be cleaved by trypsin to yield a relatively

FIGURE 7: Effect of BrAcCh Alkylation of AcChR on the Initial [^{125}I] α-BuTx Binding Rate; (▲) To AcChR (3.1×10^{-9}M) in Torpedo Ringers was added [^{125}I] α-BuTx and the formation of receptor-toxin complex was followed by DEAE disc assay. (□) Same as in (▲) for AcChR alkylated with 80 μM BrAcCh, or 200 μM (○), 40 μM (●), and 300 μM (■) BrAcCh. (a) Triton-solubilized AcChR, $[^{125}\text{I}\ \alpha\text{-BuTx}]_{total} = 2.5 \times 10^{-7}$M. (B) Membrane-bound AcChR, $[^{125}\text{I}\ \alpha\text{-BuTx}]_{total} = 6.25 \times 10^{-7}$M.

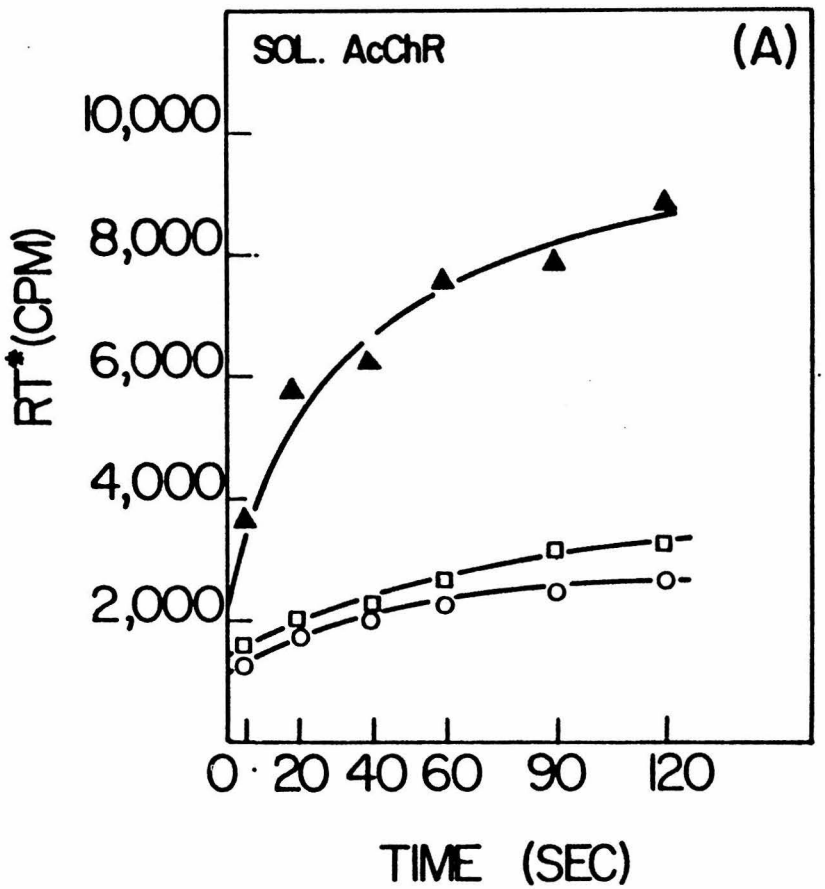
SOL. AcChR
(A)
10,000
8,000
6,000
4,000
2,000
RT*(CPM)
0 20 40 60 90 120
TIME (SEC)

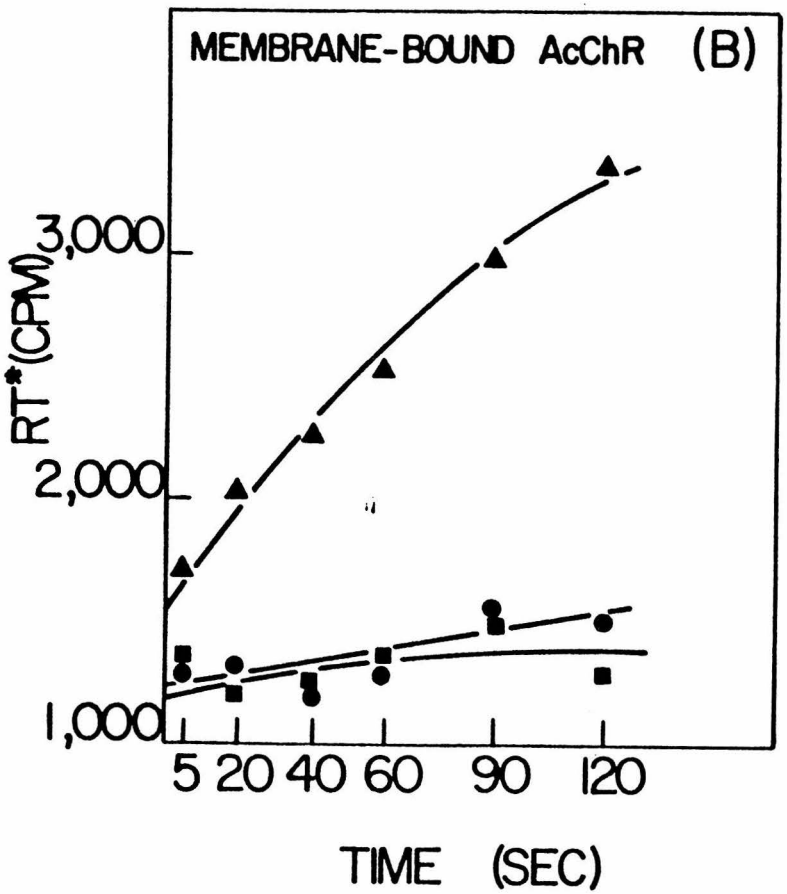
MEMBRANE-BOUND AcChR
(B)
3,000
2,000
1,000
RT*(CPM)
5 20 40 60 90 120
TIME (SEC)

FIGURE 8: Proteolytic Digestion of Base-extracted AcChR Membranes Labeled with [^{3}H]-BrAcCh: Base-extracted membrane preparations (Chapter 3) were reduced with 20 μM DTT and labeled with 40 μM [^{3}H]-BrAcCh. (Top): CBB staining and distribution of radioactivity of a 8.75% SDS polyacrylamide gel of the alkylated AcChR. (Middle): Staining and labeling patterns obtained after digestion of the alkylated receptors with trypsin (1 mg/ml). (Bottom): After digestion with papain (20 μg/ml).

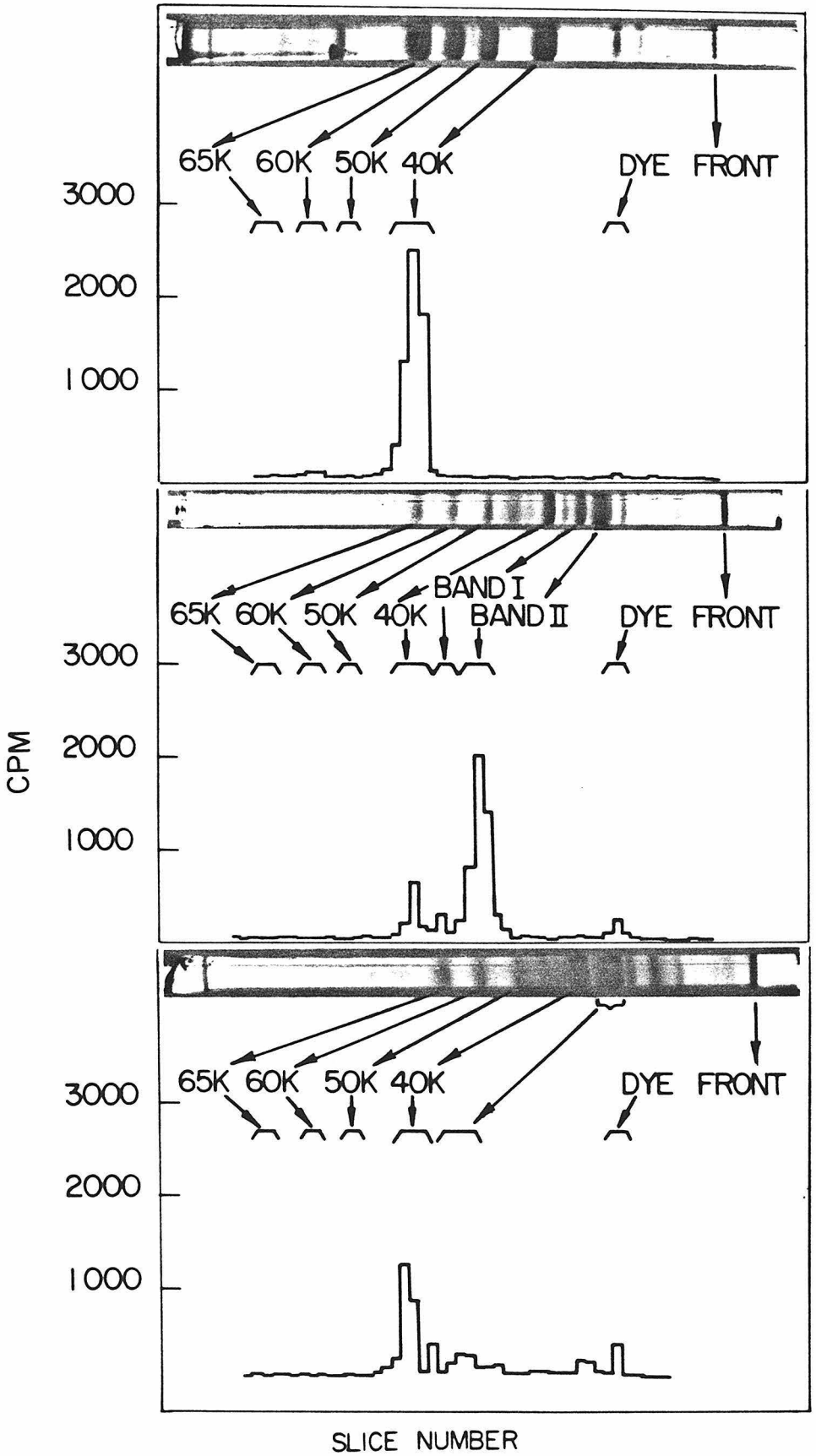
65K
60K
50K
40K
DYE FRONT
3000
2000
1000
BAND I
65K
60K
50K
40K
BAND II
DYE FRONT
3000
2000
1000
65K
60K
50K
40K
DYE FRONT
3000
2000
1000
CPM
SLICE NUMBER

large polypeptide component (Band II in Fig. 8) containing the tight agonist binding site(s). This component is further digested into smaller pieces when the protein complex is unfolded.

A much more nonspecific degradation of the alkylated membranes was observed with papain. A considerable amount of the radiolabel is retained in the 40,000 dalton subunit and the remaining radioactivity was distributed among many of the degradation products (Fig. 8).

DISCUSSION

Identification of the ligand binding site(s) of the AcChR with bromoacetylcholine is desirable for the following reasons. The reagent reversibly depolarizes the non-reduced electroplaque of Electrophorus electricus and stimulates the Torpedo AcChR in vitro by rapidly releasing the vesicle-entrapped $^{22}Na^{+}$ (Chapter 3). Reduction of the eel electroplaque followed by BrAcCh addition results in an activation of the cell which persists after the excess reagents are washed away. These results suggested that BrAcCh acts as an irreversible affinity alkylating reagent with the additional, exceptional property of being a receptor activator. In this respect it has an advantage over previously used affinity reagents, namely, MBTA (Weill et al, 1974), DAPA (Witzemann and Raftery, 1977) or α-BuTx (Hucho, 1976; Witzemann and Raftery, 1977); all of which bind to the 40,000 dalton Torpedo californica receptor subunit.

In this study, various aspects of the reversible interaction of

BrAcCh with membrane-bound AcChR were investigated and compared to those of the natural agonist, AcCh. The two reagents show striking similarity in their interaction with AcChR. Furthermore, alkylation of AcChR by BrAcCh is competitively inhibited by the reversible ligands. These results suggest that AcCh and BrAcCh are likely to bind to the same AcChR site(s) and that this site(s) can be localized by the irreversible alkylation of reduced receptor with BrAcCh.

BrAcCh was judged to bind to the unreduced membrane-bound AcChR reversibly by the following criteria: (i) The initial rate of [^{125}I] α-BuTx binding to the AcChR was inhibited by preincubating the receptor with BrAcCh (Figure 1B). The total number of receptor-toxin complexes formed 15-20 hours after toxin addition was, however, unaffected by BrAcCh, the reaction being eventually driven to the receptor-toxin complex by the irreversible inhibitor α-BuTx. (ii) Direct binding studies with [^{3}H] BrAcCh revealed a specific, saturable uptake by the AcChR (Figure 2A). (iii) In the absence of DTT, no irreversible labeling of the AcChR by [^{3}H] BrAcCh was found after dialysis or by DEAE disc assay (Figure 4 Curve C). These results suggest that [^{3}H] BrAcCh binds reversibly to the nonreduced AcChR membrane preparation.

The half-maximal initial rate of toxin binding was observed in the presence of 17 nM BrAcCh (Figure 1A), indicating tight binding at equilibrium of BrAcCh to the receptor-containing membranes. A similar dissociation constant was obtained by direct binding of the tritiated derivative (K_D = 16 ± 1 nM, Figure 2B). This affinity, measured at equilibrium, is 600-fold higher than that recorded for the physiological

response ($K_{Act.} \simeq 10$ μM, Karlin, 1973). This difference may be explained by the finding that BrAcCh induced a slow transition of the membrane-bound AcChR from a low to a high affinity state(s) upon preincubation (Figure 1A), a process suggested to be a possible in vitro parallel of physiological desensitization (Weber et al, 1975; Weiland et al, 1976, 1977; Colquhoun and Rang, 1976; Lee et al, 1977; Quast et al, 1978). Similarly, the capability to induce receptor affinity change and strong equilibrium binding are also observed with AcCh (Raftery et al, 1975; Schimerlik and Raftery, unpublished). The similarities are also evidenced by the competitive nature of binding of these two ligands to AcChR (Figure 3).

Reduction of the AcChR with DTT prior to [^{3}H] BrAcCh addition converted the reversible binding to an irreversible one, presumably by specific alkylation of a sulfhydryl group(s) generated near the binding site (Figure 4). The incorporated radioactivity could not be dialyzed or washed away, suggesting a covalent linkage to the receptor. The amount of non-specific labeling by [^{3}H] BrAcCh, as measured with reduced toxin-blocked receptor, was higher than that measured with unreduced receptor (Figure 4 Curve B and C). This is to be expected since reduction may produce more free sulfhydryl groups available for alkylation. When alkylation of the AcChR by [^{3}H] BrAcCh was carried out in the presence of AcCh or d-Tc, the radioactivity incorporated after 1 hour labeling was appreciably decreased (Figure 5); presumably these ligands compete with BrAcCh for the same anionic binding site for

quaternary ammonium groups and thus lower the rate of alkylation and the extent of labeling after one hour.

Both Triton-solubilized and membrane-bound AcChR are labeled by [^{3}H]-BrAcCh in a single subunit of M.W. 40,000 dalton (Figure 6). This subunit therefore contains a major agonist binding site(s). A similar labeling pattern was recently obtained for purified AcChR from Narcine brazielensis (Chang et al, 1977) and T. californica (Damle et al, 1978).

The number of BrAcCh sites in the nonreduced receptor membrane preparation, measured by direct binding, was found to be half of that for α-BuTx (Figure 2B). Based on our lowest estimate of the Torpedo californica AcChR molecular weight of 270,000 (Martinez-Carrion et al, 1976) for the 9S form (Raftery et al, 1972) and the fact that the dimeric 13S form (Raftery et al, 1972) is the predominant form in the membrane preparation by virtue of S-S bonds formed between 65,000 - 67,000 dalton subunits (Suarez-Isla and Hucho, 1977; Chang and Bock, 1977; Hamilton and Karlin, 1977; Witzemann and Raftery, 1978) it is estimated that four α-BuTx molecules and two BrAcCh molecules bind strongly to this receptor dimer. No cooperativity was detected for this binding (n_H = 0.98 ± 0.02, see Figure 2C). Similar stoichiometry of binding has also been observed previously in this laboratory for binding of AcCh (Moody et al, 1973) and Carb (Raftery et al, 1975).

The amount of specific labeling by [^{3}H] BrAcCh was measured using α-BuTx-labeled AcChR as a control. It was found that BrAcCh irreversibly alkylated the reduced AcChR with the same stoichiometry (BrAcCh site/

α-BuTx site = 0,5) as found from direct binding measurements to non-reduced receptor. The present results thus suggest that each ligand binding site has one reactive disulfide in its vicinity and that alkylation by BrAcCh occurs with one SH-group of each of the reduced disulfide bond(s).

Although all the affinity labeling studies thus far reported show that there are twice as many α-BuTx sites present in the AcChR preparation as can be covalently labeled by BrAcCh or MBTA (Karlin et al, 1975; Damle et al, 1978; Moore and Raftery, 1979), values ranging from 1 to 2 have been reported for the ratio of the number of α-BuTx sites to that of reversible ligand (such as Carb or AcCh) sites (Weber and Changeux, 1974; Raftery et al, 1975; Quast et al, 1978; Dunn et al, 1980). The origin of this apparent discrepancy is not as yet clear. It is possible that loss of α-BuTx sites has occurred during some of the preparation procedures which results in the 1:1 stoichiometry of toxin: ligand sites.

The ion permeability of the DTT-reduced, BrAcCh-alkylated AcChR membrane vesicle preparations has been investigated by the $^{22}Na^{+}$ flux technique (Chapter 3). In the absence of added agonists the alkylated AcChR vesicle preparations did not show high permeability to $^{22}Na^{+}$, indicating that the covalently attached BrAcCh molecules, although they transiently increase the cation permeability, did not indefinitely keep the receptor in an active state capable of translocating ions (possibly due to desensitization). Upon addition of 100 μM Carb, however, the modified AcChR vesicles rapidly released their entrapped $^{22}Na^{+}$.

Similar findings have very recently been reported by Delegeane and McNamee (1980), who in addition found that the concentration of Carb required for a 50% maximal $^{22}Na^+$ efflux response was higher in the affinity-labeled membranes. These authors attributed the results to the existence of two classes of independent functional sites on the AcChR, each corresponding to one α-BuTx site; affinity labeling by BrAcCh specifically activated and desensitized one class of binding sites while the remaining class of sites could be independently activated by Carb. To explain the higher requirement of Carb concentration for $^{22}Na^+$ flux response of the affinity-labeled membranes, they assumed that either the second site had an inherently different Carb affinity or alkylation of the first site induced a change in the second site. Although such a two-site model provides an explanation of the observed data, other possibilities exist. Since the membrane vesicles have a high-density of AcChR on their surface and only a small fraction of the total AcChR present on each vesicle is needed to elicit a full $^{22}Na^+$ flux response (Chapter 3), it is possible that the observed $^{22}Na^+$ flux response of the alkylated membranes to added Carb was produced by a small percentage of unmodified AcChR due to incomplete reaction with BrAcCh. Such flux would require a higher concentration of Carb to achieve the maximal response because the remaining population of active AcChR was small and a higher degree of activation was thus needed. Until the flux response of the alkylated membranes is determined by a more quantitative method (such as that described in Chapter 4), the origin of the Carb-induced permeability change of these

membranes cannot be unequivocally determined.

Tryptic digestion of the BrAcCh-labeled AcChR in the membrane-bound form and Triton-solubilized state results in a relatively simple degradation pattern of polypeptides on a SDS gel electrophoretogram. Only one major band was found to contain the label. This band is similar in molecular weight to a tryptic fragment of 27,000 dalton recently purified by Bartfeld and Fuchs (1979) from an α-BuTx affinity column. The fragment has a sedimentation coefficient of 8.0S and retains the pharmacological and myasthenic activity of the intact AcChR. Since this polypeptide(s) contains the BrAcCh label, it is clear that at least part of it comes from the 40,000 dalton subunit. In view of the large sedimentation coefficient and the sequence homology between the four AcChR subunits (Raftery et al, 1980), it is possible that this polypeptide(s) also results from subunits other than the 40,000 dalton component. It would be of interest in the future to test this hypothesis and to study the ability of this polypeptide(s) to mediate ion translocation across the membrane. The peptide fragment which contains the BrAcCh label can also be isolated for the amino acid sequence study of the active site.

REFERENCES

1. D. Bartfeld and S. Fuchs (1979) Biochem. Biophys. Res. Commun. 89, 512.
2. E. Bertels-Bernal, T. L. Rosenberry, and H. W. Chang (1976) Mol. Pharmacol. 12, 813.
3. D. Ben-Haim, E. M. Landau, and I. Silman (1973) J. Physiol. 234, 305.
4. S. G. Blanchard, U. Quast, K. Reed, T. Lee, M. I. Schimerlik, R. Vandlen, T. Claudio, C. D. Strader, H.-P.H. Moore, and M. A. Raftery (1979) Biochemistry 18, 1875.
5. R. S. L. Chang, L. T. Potter, and D. S. Smith (1977) Tissue and Cell 9, 623.
6. H. W. Chang and E. Bock (1977) Biochemistry 16, 4513.
7. C. Y. Chiou and B. V. R. Sastry (1968) Biochem. Pharmacol. 17, No. 1, 805.
8. D. G. Clark, D. D. Macmurchie, E. Elliott, R. G. Wolcott, A. M. Landel, and M. A. Raftery (1972) Biochemistry 11, 1633.
9. D. Colquhoun and H. P. Rang (1976) Mol. Pharmacol. 12, 519.
10. D. Colquhoun, F. Dreyer, and R. E. Sheridan (1979) J. Physiol. 293, 247.
11. V. N. Damle, M. McLaughlin, and A. Karlin (1978) Biochem. Biophys. Res. Commun. 84, 845.
12. A. M. Delegeane and M. G. McNamee (1980) Biochemistry 19, 890.
13. J. R. Duguid and M. A. Raftery (1973) Biochemistry 12, 3593.

14. S. M. J. Dunn, S. G. Blanchard, and M. A. Raftery (1980) Biochemistry, submitted.

15. J. Elliott, S. G. Blanchard, W. Wu, J. Miller, C. D. Strader, P. Hartig, H.-P. Moore, J. Racs, and M. A. Raftery (1980) Biochemical J 185, 667.

16. G. L. Ellman, K. D. Courtney, V. Andres, and R. M. Featherstone (1961) Biochem. Pharmacol. 7, 88.

17. S. C. Froehner, A. Karlin, and Z. W. Hall (1977) Proc. Natl. Acad. Sci. USA 74, 4685.

18. S. L. Hamilton, M. McLaughlin, and A. Karlin (1977) Biochem. Biophys. Res. Commun. 79, 692.

19. S. Hestrin (1949) J. Biol. Chem. 180, 249.

20. F. Hucho, P. Layer, H. R. Kiefer, and G. Bandini (1976) Proc. Natl. Acad. Sci. USA 73, 2624.

21. N. Kalderon and I. Silman (1971) Isr. J. Chem. 9, 12.

22. A. Karlin (1969) J. Gen. Physiol. 54, 245S.

23. A. Karlin and D. Cowburn (1973) Proc. Natl. Acad. Sci. USA 70, 3636.

24. A. Karlin (1973) Fed. Proc. 32, 1847.

25. A. Karlin, C. L. Weill, M. G. McNamee, and R. Valderrama (1975) Symposium Quant. Biol. 40, 203.

26. U. K. Laemmli (1970) Nature 227, 680.

27. T. Lee, V. Witzemann, M. Schimerlik, and M. A. Raftery (1977) Arch. Biochem. Biophys. 183, 57.

28. M. Martinez-Carrion, M. A. Raftery, J. K. Thomas, and V. Sator (1976) J. Supramol. Struct. 4, 373.

29. T. Moody, J. Schmidt, and M. A. Raftery (1973) Biochem. Biophys. Res. Comm. 53, 761.

30. H.-P.H. Moore and M. A. Raftery (1979) Biochemistry 18, 1862.

31. U. Quast, M. I. Schimerlik, T. Lee, V. Witzemann, S. Blanchard, and M. A. Raftery (1978) Biochemistry 17, 2405.

32. M. A. Raftery, J. Bode, R. Vandlen, D. Michaelson, J. Deutsch, T. Moody, M. J. Ross, and R. M. Stroud (1975) in Protein-Ligand Interactions (H. Sund and G. Blauer, eds.) Walter de Gruyter, Berlin and New York, 328.

33. M. A. Raftery, M. W. Hunkapiller, C. D. Strader, and L. E. Hood (1980) Science, submitted.

34. K. Reed, R. Vandlen, J. Bode, J. Duguid, and M. A. Raftery (1975) Arch. Biochem. Biophys. 167, 138.

35. J. Schmidt and M. A. Raftery (1972) Biochem. Biophys. Res. Commun. 49, 572.

36. J. Schmidt and M. A. Raftery (1973a) Biochemistry 12, 852.

37. J. Schmidt and M. A. Raftery (1973b) Anal. Biochem. 52, 349.

38. I. Silman and A. Karlin (1969) Science 164, 1420.

39. B. A. Suarez-Isla and F. Hucho (1977) FEBS Letters 75, 65.

40. R. Vandlen, J. Schmidt, and M. A. Raftery (1976) J. Macromol. Sci. Chem. A10, 73.

41. Z. Vogel, A. J. Sytkowski, and M. W. Nirenberg (1972) Proc. Natl. Acad. Sci. USA 69, 3180.

42. M. Weber and J. P. Changeux (1974) Mol. Pharmacol. 10, 15.

43. M. Weber, T. David-Pfeuty, and J. P. Changeux (1975) Proc. Natl. Acad. Sci. USA 72, 3443.

44. G. Weiland, B. Georgia, V. T. Wee, C. F. Chignell, and P. Taylor (1976) Mol. Pharmacol. 12, 1091.

45. G. Weiland, B. Georgia, S. Lappi, C. F. Chignell, and P. Taylor (1977) J. Biol. Chem. 252, 7648.

46. C. L. Weill, M. G. McNamee, and A. Karlin (1974) Biochem. Biophys. Res. Commun. 61, 997.

47. V. Witzemann and M. A. Raftery (1977) Biochemistry 16, 5862.

48. V. Witzemann and M. A. Raftery (1978) Biochem. Biophys. Res. Commun. 81, 1025.

CHAPTER TWO

Osmotic Properties of Membrane Vesicles from *T. californica*: Preparation of AcChR-Enriched Membrane Vesicles Suitable for *in vitro* Ion Flux Studies

INTRODUCTION

In Chapter 1 the polypeptide component of 40,000 dalton MW in the AcChR preparations has been shown to contain a strong agonist binding site(s). To characterize the physiological function of AcChR and to define other structural components essential for such function, assay systems have been developed for measuring the chemical excitability in vitro. The system most commonly used involves loading of AcChR-containing membrane vesicles with radiotracer ions (such as $^{22}Na^{+}$) and monitoring the stimulation of ion efflux by agonists after filtering the vesicles on Millipore filters (Kasai and Changeux, 1971 and Chapter 3). Assay systems such as this and the one to be described in Chapter 4 require the formation of sealed vesicles with a large interior volume. Failure to prepare the vesicles properly may result in small vesicle interior volume and hence variability in the ion flux response. In the work described in this chapter we therefore investigated the osmotic properties of Torpedo membrane fragments with a view towards understanding and improving the methods for preparation of sealed AcChR vesicles suitable for in vitro ion flux studies.

Preparations of AcChR in the native membrane-bound state are currently obtained at three levels of purity. "Crude membrane preparations" are obtained from homogenates of Torpedo electroplaques by differential centrifugation. Further purification of the crude membrane fragments by centrifugation on sucrose-density gradients yields "AcChR-enriched membrane preparations" (Duguid and Raftery, 1973;

Elliott et al, 1980). "Highly purified membrane preparations" are prepared from the AcChR-enriched membrane preparations by a method of alkaline extraction (Neubig et al, 1979; Elliott et al, 1979 and Chapter 3). The studies described here were designed to trace the fate of the vesicular properties of Torpedo membrane fragments during the various treatments in the purification procedure, with special emphasis on the effect of osmotic shock. We find that large, transient pores form in the vesicles during osmotic shock which rapidly and spontaneously reseal.

EXPERIMENTAL

Membrane Preparations

Crude membranes were prepared from electric organs of freshly killed Torpedo californica or from organs that had been frozen in liquid nitrogen immediately after dissection and stored at -80°C. The organs were first cut into pieces approximately 5 g each and suspended in 1 ml of ice-cold 400 mM NaCl, 10 mM sodium phosphate, 1 mM EDTA, pH 7.4 buffer per gram of organ. These were homogenized in a Waring Laboratory Blender at full speed for 2 x 1 min. The mixture was rehomogenized in a Brinkmann Polytron at full speed for 1 min. The homogenate was then centrifuged in a Sorvall GSA rotor at 5000 rpm for 10 min. The supernatant was collected, passed through two layers of cheesecloth, and centrifuged at 16000 rpm for 1 hour in a Beckman type 35 rotor. The supernatant was discarded and the pellets were resuspended in the same NaCl-sodium phosphate-EDTA buffer (0.2 ml per g of organ), using a Virtis-23 homogenizer at full speed for 2 x 20 sec. The final suspension of the membranes was made in a small volume (∿0.03 ml per g of organ) of Ca^{+2}-free Torpedo Ringers containing 400 mM NaCl (400 mM NaCl, 5 mM KCl, 2 mM $MgCl_2$, 5 mM Tris, 0.02% NaN_3, pH 7.4) to maintain isotonicity. Resuspension was accomplished with a Virtis-23 homogenizer at medium speed for 2 x 20 sec. The entire isolation was done at 4°C, and the homogenization and suspension of membranes were carried out under argon.

Membrane fragments enriched in AcChR were prepared from the crude

membranes by sucrose gradient centrifugation in a Beckman VTi 50 vertical rotor (Elliott et al, 1980). Membranes recovered from the middle band of the gradients were pooled and centrifuged for 1 hour at 30,000 rpm in a Beckman Type 35 rotor following a two-fold dilution into 10 mM Tris-Cl, pH 7.4. The membranes were resuspended with a Virtis-23 homogenizer in the same buffer.

Highly purified membranes were prepared in buffer of low ionic strength from the AcChR-enriched membranes after base treatment as described in Chapter 3.

Preparation of [^{14}C]-glucagon and Assay of Protease Activity

Radiolabeled glucagon was prepared by reductive methylation as follows. 20 mg of glucagon in 3 ml 0.2 M borate buffer, pH 10.7 was mixed with 0.4 mg $NaBH_4$. 0.6 mg [^{14}C]-HCHO was slowly added to the mixture in 5 aliquots over 30 min at 0^{o}C. [^{14}C]-glucagon was separated from the reagents by a Sephadex G-10-120 column equlibrated in 1 mM NH_4HCO_3, pH 10.7. Protease activity was assayed according to the method of Jusic et al (1976). Incubation of the enzyme and substrate was carried out at 37^{o}C for 30 min. Reaction was quenched by a mixture of BSA-TCA and the radioactivity remaining in the supernatant was assayed.

Assay of Vesicle Entrapped Radioactive Solutes

To measure vesicle entrapped radioactivity, the membrane mixture was diluted, if necessary, with isotonic nonradioactive buffer and

aliquots were filtered through two layers of Millipore filters (plain, white, 0.8 μm pore size, 25 mm dia.) mounted on a Millipore manifold apparatus followed by washing with 2x7.5 ml of isotonic buffer. ^{3}H- and ^{14}C- radioactivities were measured in the toluene-based liquid scintillation cocktail described in Chapter 1 while $^{22}Na^{+}$ and ^{125}I- radioactivities were measured in a Beckman gamma counter.

Osmotic Shock and Resealing of Membrane Vesicles

To study the vesicle resealing process crude membrane preparations in 400 mm NaCl buffer were used. The various components were added and mixed with a Vortex mixer at the times indicated. Note that the final solution compositions were identical in all experiments, only the order of addition of the various components was altered.

EXPERIMENT	TIME			
	0 SEC	10 SEC	20 SEC	30 SEC
Shock-Entrapment	Add 50λ of Membrane homogenate to 90λ of 33 μCi/ml $^{22}NaCl$ in distilled water	Add 10λ of 4 M NaCl	Add 4 ml of 400 mM NaCl	--------
Control	Add 50λ of Membrane homogenate to 100λ of 400 mM NaCl containing 29.7 μCi/ml $^{22}NaCl$	-------	Add 4 ml of 400 mM NaCl	--------
Entrap-Release	Add 50λ of Membrane homogenate to 90λ of 33 μCi/ml $^{22}NaCl$ in distilled water	Add 10λ of 4 M NaCl	Add 3.6 ml of distilled water	Add 400λ of 4 M NaCl

At 40, 50, 60 and 70 seconds, 1 ml of the solution was washed on Millipore filters with 0.4 M NaCl-1 mM EDTA-10 mM Na phosphate, pH 7.4.

Measurement of Transmembrane Potential by Fluorescence

For these studies, crude membranes were prepared in 400 mM K methylsulfate-10 mM K Hepes, pH 7.4. Fluorescence was measured in a Perkin-Elmer MPF-4 Spectrofluorometer. Because of the tendency of the dye molecules to adsorb to the glass cuvettes, measurements were made using polystyrene cuvettes (Evergreen Scientific) and with constant stirring. Stock solutions of 3,3'-dipropylthiadicarbocyanine ($diSC_3$-(5)), gramicidin (Sigma) and valinomycin (Sigma) were in ethanol. $DiSC_3$-(5) was a generous gift of Dr. S. Parsons.

RESULTS

Ca^{2+}-Activated Protease Activity in the Crude Homogenate of Torpedo Electroplaques

To design better methods for the preparation of functional AcChR vesicles, we first investigated the possible existence of protease activity in the AcChR source materials. Fig. 1 illustrates the presence of Ca^{2+}-activated protease activity in the crude homogenate of Torpedo electric organs. [^{14}C]-glucagon was hydrolyzed by the crude Torpedo homogenate to a greater extent in the presence of Ca^{2+} than in its absence as evidenced by the higher level of TCA non-precipitable radioactivity after digestion. Trypsin (80 ug) hydrolyzed nearly all the available substrate. Since in the presence of EDTA the level of hydrolyzed radioactivity by the homogenate was significantly higher than that of the control, it is possible that Ca^{2+}-independent as well as Ca^{2+}-activated proteases are present in the crude homogenate. Ca^{2+} activated phospholipase activity is also present (Wu and Raftery unpublished). EDTA and protease inhibitors such as PMSF are thus normally included in the homogenization buffer for the preparation of AcChR. Usually EDTA is also included in the subsequent purification procedure to suppress Ca^{2+}-activated protease and phospholipase activities.

Figure 1. Ca^{2+}-Activated Protease Activity in the Crude Homogenate of Torpedo Electroplaque. TCA precipitable radioactivity was plotted against the total amount of substrate, ^{14}C-glucagon, added. (▲-▲) Trypsin (80 µg) in the absence of Ca^{2+} or EDTA; (●+▼) Crude Torpedo homogenates after filtration through cheese cloth (65 µl) assayed in the presence of 2 mM $CaCl_2$ (●-●) or 8 mM EDTA (▼-▼).

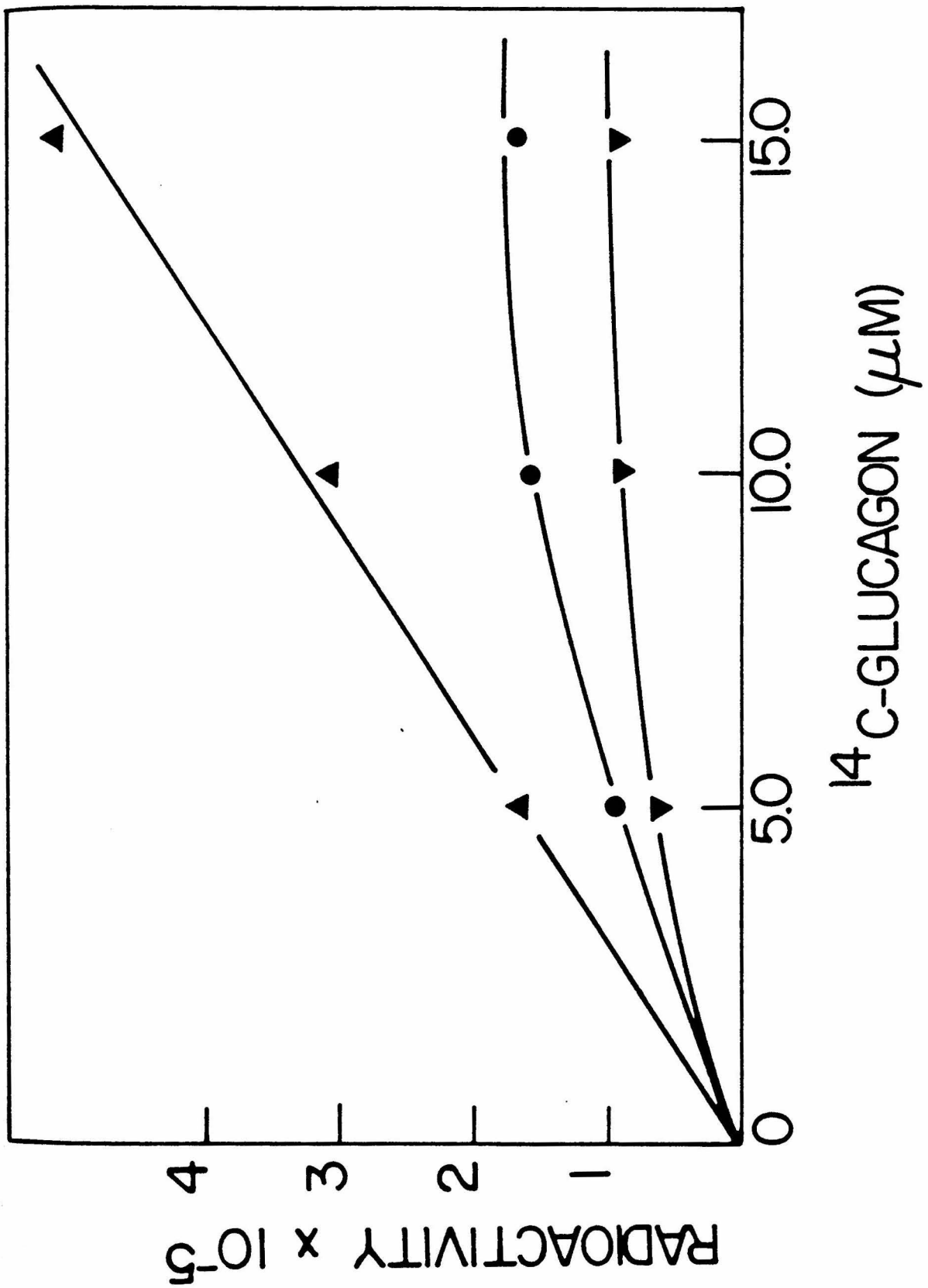
RADIOACTIVITY x 10^{-5}
4
3
2
1
0
5.0
10.0
15.0
^{14}C-GLUCAGON (μM)

The Vesicular Nature of Crude AcChR Membrane Fragments

Crude AcChR membrane fragments were isolated from the homogenate of electric organs under isotonic conditions with Torpedo plasma (400 mM NaCl-buffer (Brock and Eceles, 1958)) by differential centrifugation. Following negative staining these membranes exhibited under the electron microscope vesicle structures widely ranged in size. Only a small fraction of the vesicles showed the characteristic rosette structures of AcChR on their surface (Strader et al, 1979); most of the AcChR was found to be associated with larger vesicles of diameters ranging from 1000 Å to 10,000 Å. A large percentage of the vesicles form with the outside-out orientation (synaptic face accessible to the bulk solution) (Hartig and Raftery, 1979).

The presence of vesicular structures in electron micrographs does not demonstrate vesicle intactness because membrane defects may not be morphologically obvious. Fig. 2 shows that a significant fraction of the membrane vesicles does form sealed compartments because they are capable of entrapping a radionuclide, $^{22}Na^{+}$, upon prolonged incubation with this slightly permeable solute. These vesicles are easily osmotically shocked; the entrapped $^{22}Na^{+}$ was rapidly released upon dilution into hypotonic buffers (Fig. 2, lower trace).

If the membranes form sealed vesicles, one should be able to establish a transmembrane potential under proper conditions. Fig. 3 illustrates that such is the case. To measure the membrane potential, we have employed a membrane-potential sensitive fluorescence dye, diSC_3-(5) (see Scheme I). Simms et al (1974) have shown that this

Figure 2. Entrapment of $^{22}Na^{+}$ in Crude Torpedo Membrane Vesicles. Crude membrane vesicles (8-13 μM in α-BuTx sites) in calcium free Torpedo Ringers containing 400 mM NaCl was incubated with 4.1 μM $^{22}NaCl$ for 6-12 hours at 4°C. (● - ●) At time zero the mixture was diluted 20 fold into nonradioactive isotonic buffer and 200 μl aliquots were washed by the Millipore filter method at times indicated. (▲ - ▲) same as in (● - ●) except that the vesicles were osmotically shocked by diluting into 20 fold distilled water at t = 0.

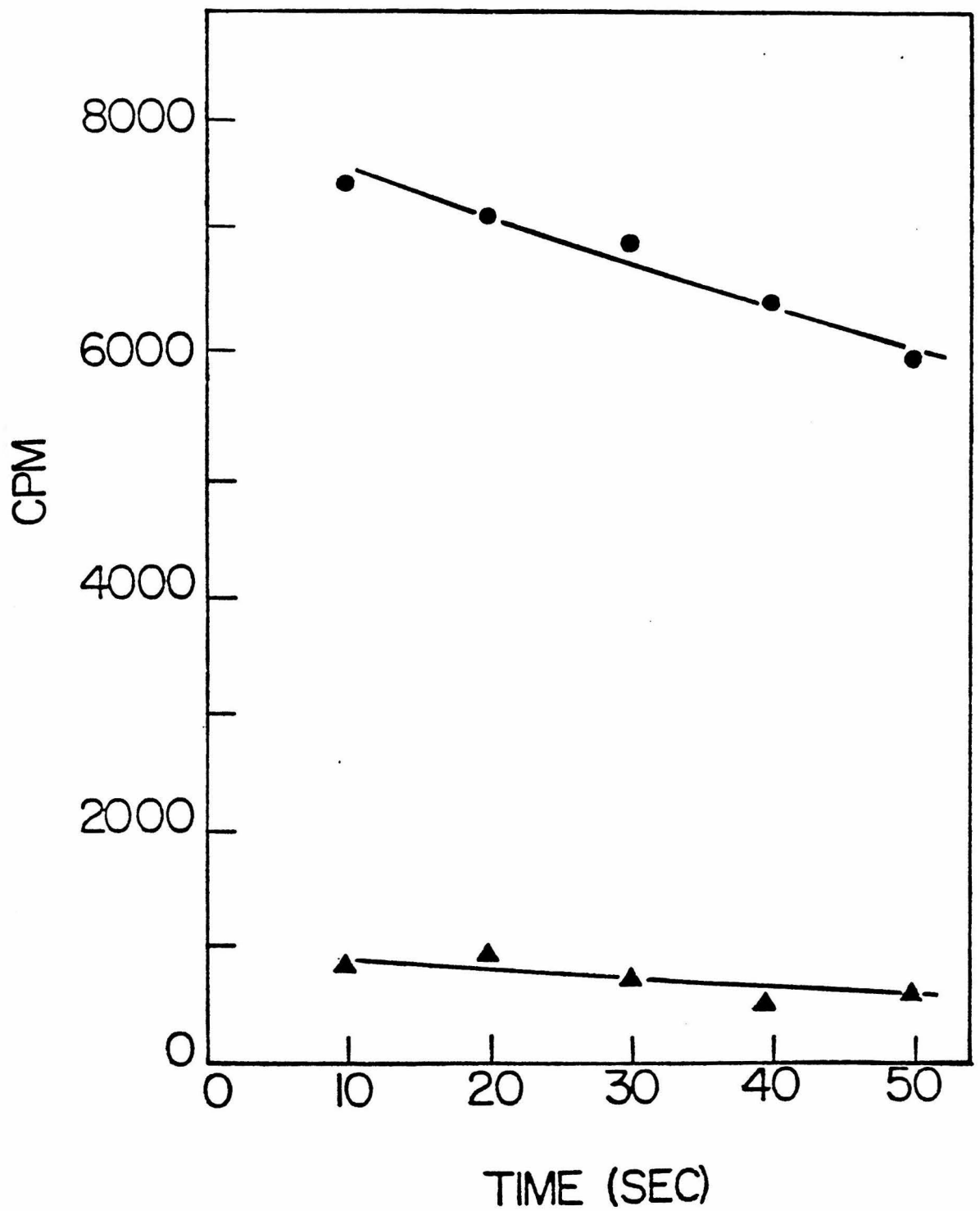
8000
6000
4000
2000
0
CPM
0
10
20
30
40
50
TIME (SEC)

Scheme I. The molecular structure of 3,3'-dipropylthiadicarbocyanine iodide

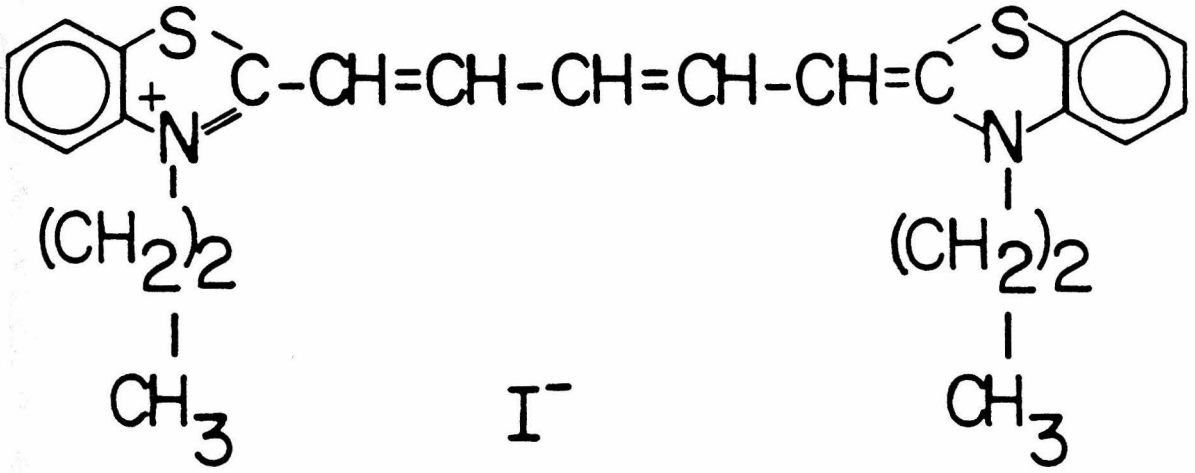

diS-C_3-(5)

dye responds to negative membrane potentials on a time scale of seconds with a large decrease in fluorescence. To establish transmembrane potential, crude membrane vesicles of high internal K^+ concentration were prepared in buffers containing 400 mM K^+ and an impermeant anion, methylsulfate. When the exterior medium was rapidly changed to 400 mM Na methylsulfate a large decrease in $diSC_3$-(5) fluorescence was observed, while in a control experiment with K^+ on both sides of the membranes $diSC_3(5)$ still exhibited high fluorescence (Fig. 3A,B). Addition of the ionophore gramicidin did not significantly affect the control level of fluorescence but greatly increased the fluorescence for the vesicle preparation containing internal K^+ and external Na^+. As shown in Fig. 3C,D, valinomycin did not produce the large effect caused by gramicidin. The membrane vesicles are thus more permeable to K^+ than to Na^+; polarization of the vesicles (inside negative) can be generated by placing K^+ ions inside and Na^+ ions outside the vesicles and by using an impermeant anion as the counter ion. Gramicidin increases the membrane's permeability to both K^+ and Na^+ ions (McLaughlin and Eisenberg, 1975) and hence depolarizes the membrane.

Since K^+ is the only dominant permeant ion in the absence of added ionophores, addition of the K^+-specific ion carrier, valinomycin, does not change the membrane potential. When the membranes were prepared with Cl^- as the counter ion on both sides, however, increasing the K^+ permeability by addition of valinomycin shifted the membrane potential to a more negative value inside, indicating that Cl^- is also permeable to the vesicle membrane and that both K^+ and Cl^- contributed

Figure 3. Transmembrane Potential Across Torpedo Membrane Vesicles Measured by $diSC_3$-(5). Membrane vesicles prepared in 400 mM K methylsulfate - 10 mM K Hepes, pH 7.4 were diluted 60 fold at time indicated by arrows 'M' into 400 mM K methylsulfate - 10 mM K Hepes, pH 7.4 (A & C) or 400 mM Na methylsulfate - 10 mM Na Hepes, pH 7.4 (B & D) containing 6 μM $DiSC_3$-(5) and the fluorescence of the mixture was immediately followed (Excitation at 680 nm and emission at 695 nm). At time indicated by the arrows, gramicidin (arrows 'G') or valinomycin (arrows 'V') was added to a final concentration of 3 μg/ml or 2 μg/ml, respectively, and fluorescence recording was continued.

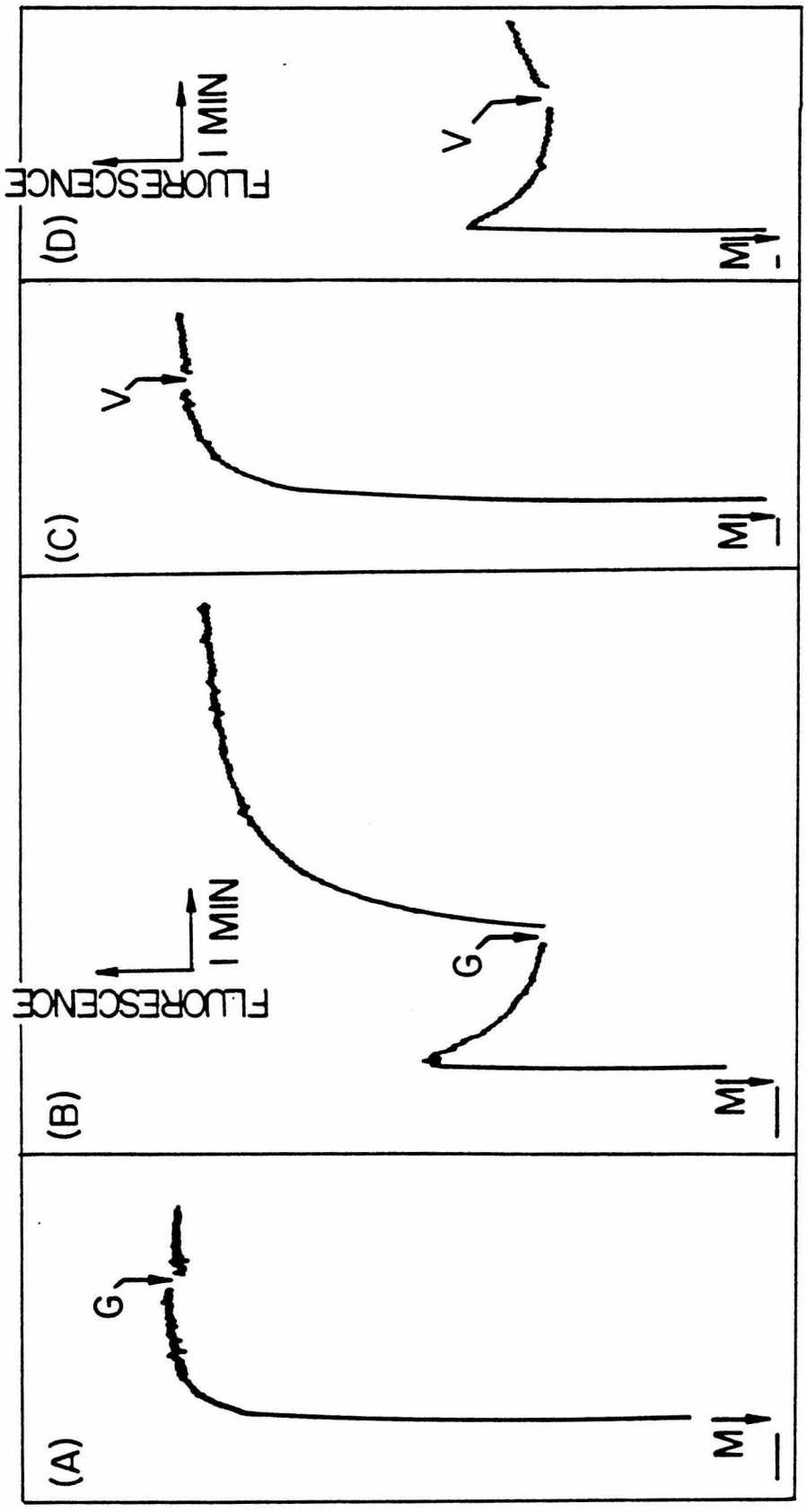
(A)
G
M
(B)
FLUORESCENCE
1 MIN
G
M
(C)
V
M
(D)
FLUORESCENCE
1 MIN
V
M

to the resting membrane potential under such conditions.

Selection of AcChR-containing Membrane Vesicles by Osmotic Shock and Sucrose-Density Gradient Centrifugation

Although the crude membrane preparation described above exhibits the desirable properties of sealed vesicles suitable for ion flux assay *in vitro*, it represents a very impure preparation with a great number of contaminating vesicles. Further purification of AcChR-containing vesicles can be achieved by sucrose-density gradient centrifugation, because the receptor membrane fragments exhibit exceptionally high equilibrium density (∿1.18 g/ml, Duguid and Raftery, 1973). In the form of fully inflated intact vesicles, however, the overall density of the AcChR vesicles, taking into account their interior space, is much lower (∿1.03 g/ml) and not markedly different from other vesicles (Hartig and Raftery, 1979). An additional osmotic shock step was therefore included before the sucrose-density gradient centrifugation (Elliott *et al*, 1980) in order to disrupt the vesicles. It was assumed that osmotic shock damaged the membranes and allowed equilibration of the vesicle interior with the sedimentation medium and the vesicles eventually sedimented at the intrinsic AcChR membrane density (1.18 mg/ml).

Vesicle Resealing Processes Following Osmotic Shock

If the AcChR vesicles remained broken after osmotic shock as discussed in the preceding paragraph, the resulting purified vesicles from the sucrose gradient centrifugation would not be useful for ion flux

studies. We have found that this is not the case. Following washing with buffers of low ionic strength, the membranes harvested from the high density regions of the sucrose gradient were capable of entrapping $^{22}Na^{+}$ (see below). The presence of sealed membrane vesicles was also demonstrated by measuring the percentage of a membrane pellet's volume which was accessible to membrane-permeant or to membrane-impermeant radionuclides. It has been previously shown that intact vesicles are impermeable to sucrose (Hartig and Raftery, 1979). Equal amounts of membranes from reorienting gradients were centrifuged in the presence of $^{3}H_2O$ or ^{14}C-sucrose. The supernatants were removed completely and the pellet was counted. The pellet containing ^{14}C-sucrose entrapped 17% fewer counts than that containing $^{3}H_2O$ suggesting that 17% of the total water space of the pellet was sequestered inside of membrane vesicles. These results suggest that resealing processes may have occurred after the vesicles were osmotically shocked. The following experiments were designed to test this hypothesis.

If intact Torpedo vesicles form transient pores during osmotic shock which spontaneously reseal, they should entrap radioactive substances from the external shocking solution inside the resealed compartments. Subsequent Millipore filtration of a suspension of vesicles would allow them and their contents to be retained on the filters while the bathing solution is removed. The entrapment of ^{22}Na in Torpedo homogenates containing intact vesicles upon osmotic shock was demonstrated by this method (Figure 4). The radioactive substances which were entrapped by the shock and resealing processes were released

Figure 4. Entrapment of ^{22}Na in Crude Torpedo Membrane Vesicles Upon Osmotic Shock. Membrane vesicles prepared in 400 mM NaCl-buffer were osmotically shocked into ^{22}Na-containing medium. The entrapped radioactivity was then measured by Millipore filtration (see table in Experimental). (●) entrapment by osmotic shock; (□) control experiment without osmotic shock; (○) release by osmotic shock. The vesicles with entrapped ^{22}Na were subjected to a second osmotic shock into non-radioactive medium and released their contents.

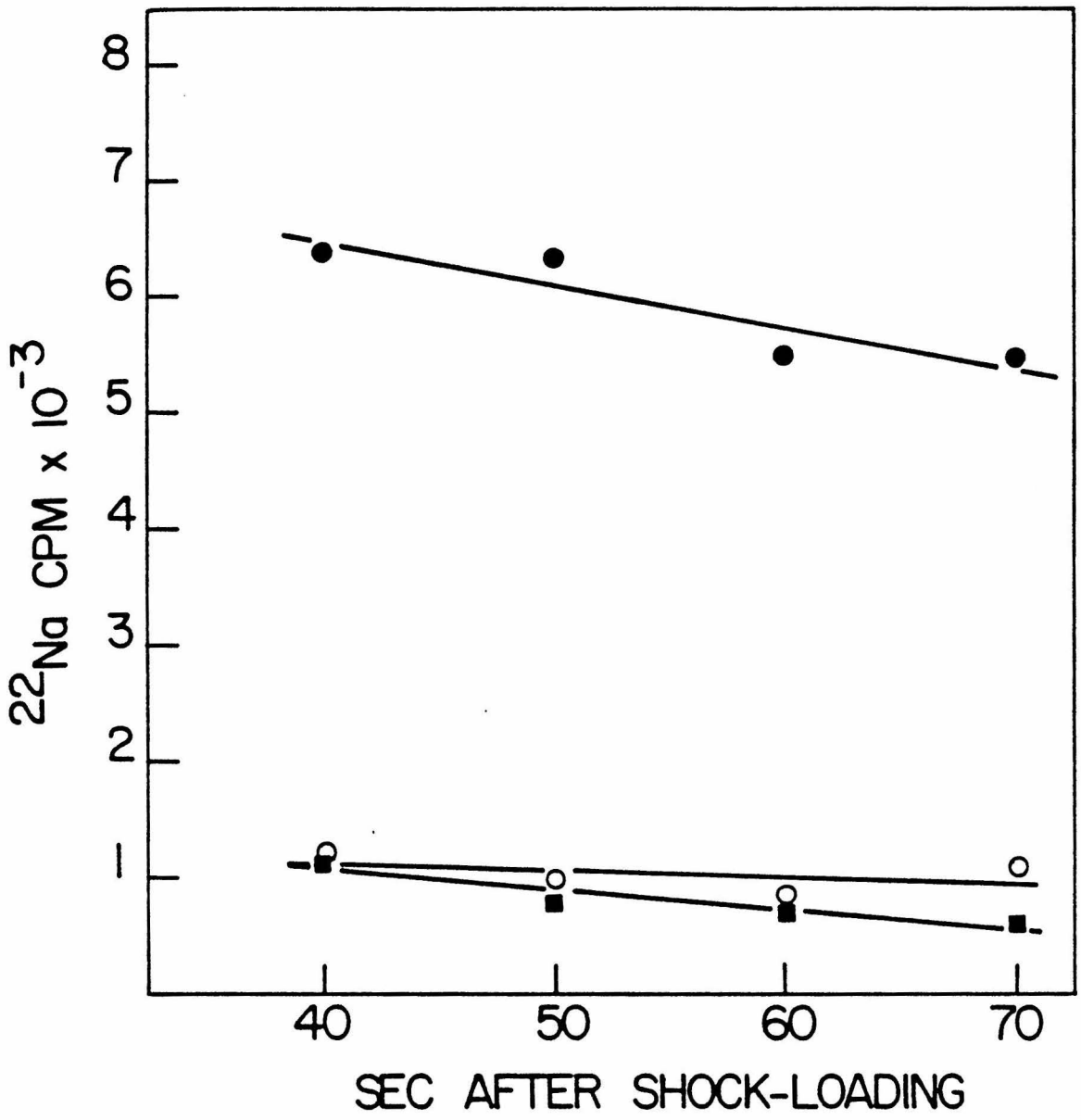
8
7
6
5
4
3
2
1
^{22}Na CPM x 10^{-3}
40
50
60
70
SEC AFTER SHOCK-LOADING

by a second osmotic shock (Figure 4, (O)). Control experiments for adsorption of radioactive substances to the vesicle exterior and for vesicle permeability to the radioactive substance were conducted by supplementing the shock solution with salt before its addition to the vesicles so that no osmotic shock occurred (Figure 4). All experiments were arranged so that the compositions of the solutions applied to the Millipore discs were identical; only the order of addition of the components was varied.

Addition of the ionophore gramicidin D to vesicles containing shock-entrapped ^{22}Na rapidly caused its release (Figure 5 (O)) whereas addition of the ionophore to the control (Figure 5, (●)) had no effect. ^{22}Na was clearly entrapped in the vesicle interior by a resealing process that followed the formation of transient pores during osmotic shock.

The effect of cooling on the shock-induced loading and resealing processes was investigated by conducting the experiment at $4^{o}C$. Under these conditions, ^{22}Na was still entrapped during osmotic shock but the amount retained decreased slightly (to 70% of the value at $25^{o}C$, results not shown). At both $4^{o}C$ and $25^{o}C$ the vesicle resealing process was complete within 5 seconds, as shown by an experiment in which vesicles were shocked in distilled water and ^{22}Na was added 5 seconds later (with the Millipore filtration technique, 5 seconds is the minimum time required for solution transfer and mixing). The level of ^{22}Na retained in this experiment was the same as the control level of non-specific adsorption (results not shown), demonstrating complete resealing

Figure 5. Release of the $^{22}Na^{+}$ Entrapped by Osmotic Shock Using Gramicidin. (○) Vesicles were loaded with $^{22}Na^{+}$ by osmotic shock as in Figure 1 (●); at the time indicated by the arrow, gramicidin D (in EtoH) was added to a final concentration of 8 μg/ml. (▲) same as above except that EtoH without gramicidin was added. The concentration of EtoH was 0.8% in the final mixture. (●) control experiment without osmotic shock. Addition of gramicidin at the time indicated by the arrow did not affect this baseline.

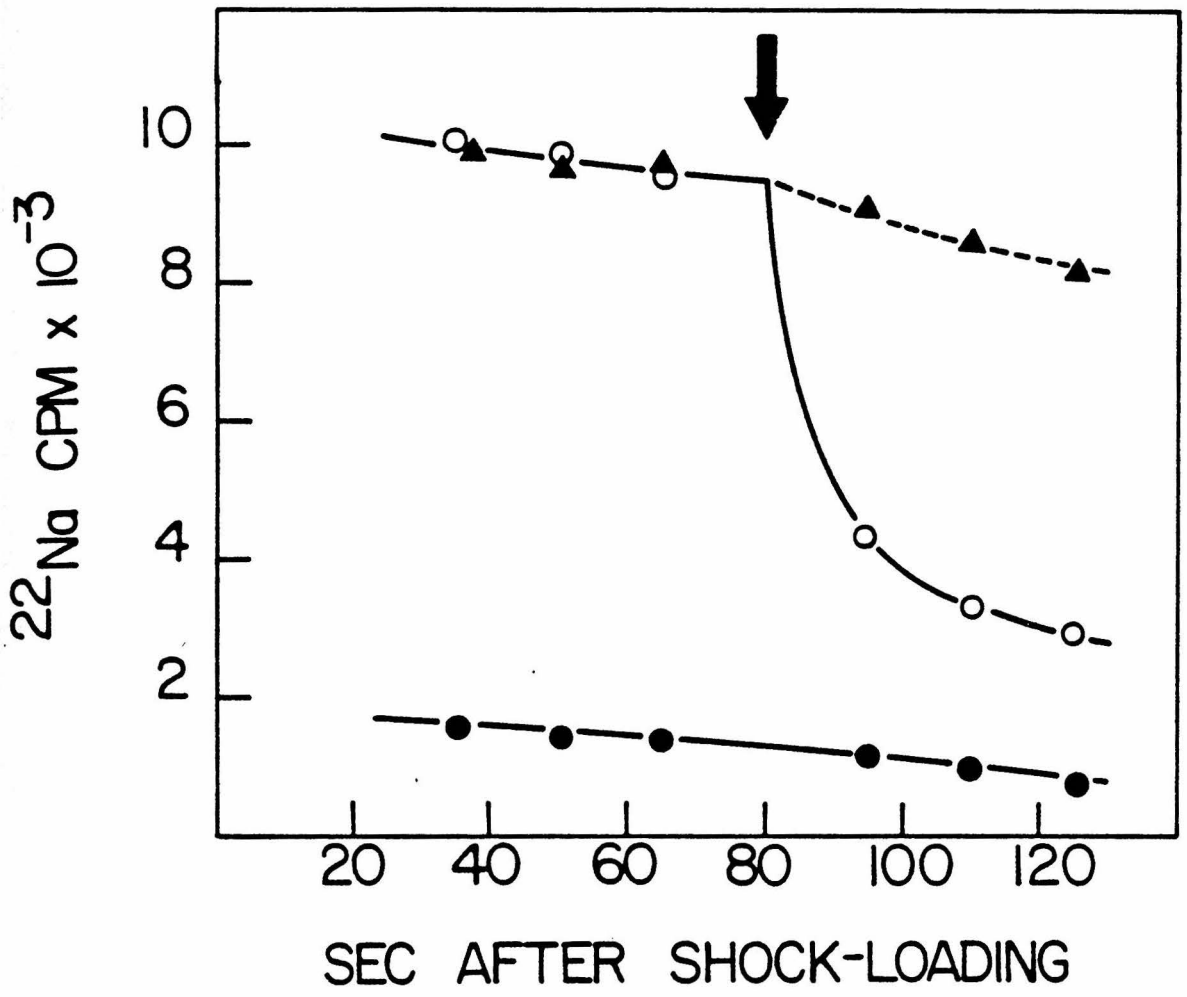
^{22}Na CPM x 10^{-3}
10
8
6
4
2
20
40
60
80
100
120
SEC AFTER SHOCK-LOADING

within 5 seconds. We tested the size and charge specificities of the transient pores that form during osmotic shock by including a variety of radioactive substances in the shock solution. Both $^{125}I^-$ and ^{14}C-sucrose were efficiently entrapped during osmotic shock. The transient pores formed during osmotic shock therefore showed no charge specificity since anions, cations and neutral species were all entrapped. Figure 6 demonstrates the effect of molecular weight on the entrapment process; equal volumes of membranes were shocked into solutions containing the indicated radiolabeled compounds (total cpm were identical). Three curves were obtained as described for Figure 4 and the average value for each curve was plotted in the form of a bar graph (Figure 6).

The vesicles shock-loaded $^{22}Na^+$ most efficiently. The level of entrapped counts decreased for ^{14}C-sucrose and [^3H] inulin ($\overline{MW}$ = 5000) and fell off drastically for the dextran polymer with an average molecular weight of 70,000 daltons. It thus appeared that the loading efficiency decreases as the molecular weight of the molecules increases.

When the same experiments as those shown in Figure 6 were carried out for [^{125}I] α-BuTx ($\overline{MW}$ ∿8000) on vesicles pre-saturated with excess unlabeled toxin to block all the specific binding sites, the level of entrapped radioactivity was 10 times higher than that of $^{22}Na^+$. The entrapped radioactivity can be released by a second shock and therefore is not due to toxin irreversibly bound to the interior of the vesicle membranes. This preferential accumulation of α-BuTx in the interior of the vesicles may be due to strong protein lipid interactions. Extremely high protein trapping efficiency has also been reported in some liposome systems (Sessa and Weismann, 1968).

Figure 6. Effect of Molecular Weight on the Efficiency of Loading of Vesicles by Osmotic Shock. The three curves, as in Figure 4, were measured for four different radioactive substances: $^{22}Na^{+}$, ^{14}C-sucrose, [^{3}H]-inulin and ^{14}C-dextran. The bar graph represents the average of the four points as determined in Figure 4.

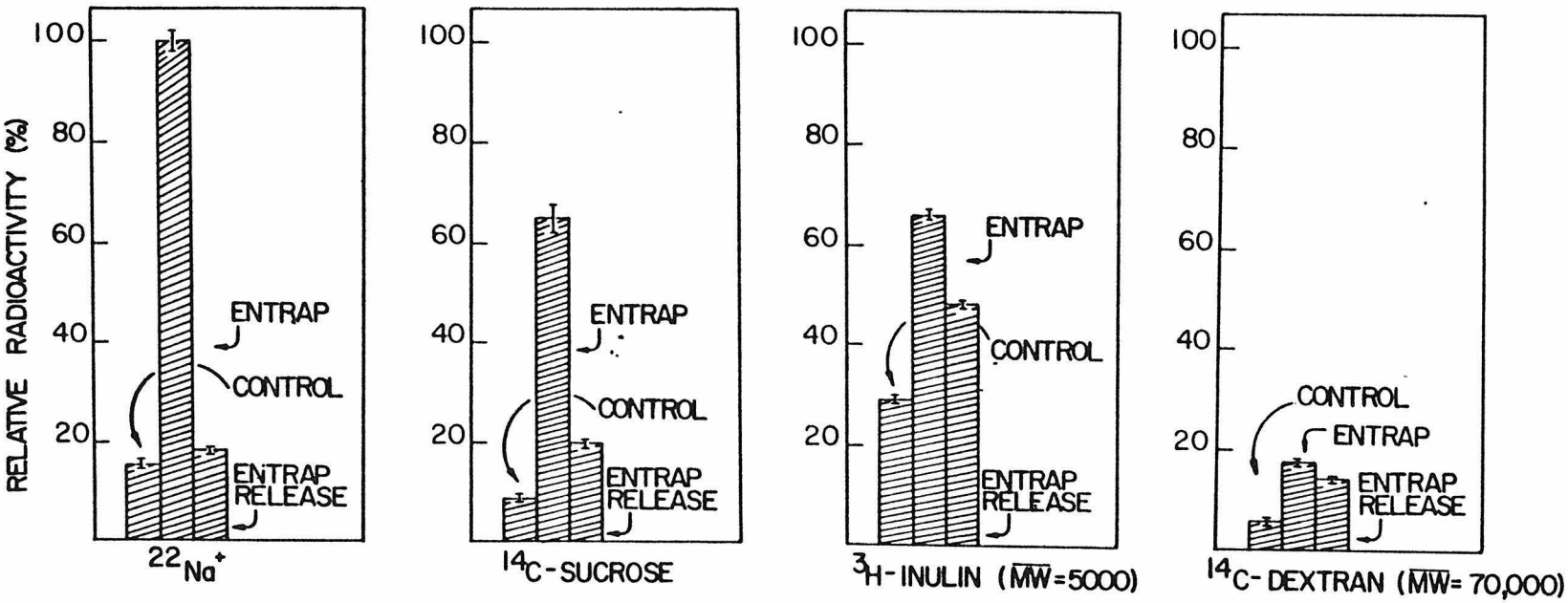
RELATIVE RADIOACTIVITY (%)
100
80
60
40
20
ENTRAP
CONTROL
ENTRAP RELEASE
$^{22}Na^{+}$
^{14}C-SUCROSE
^{3}H-INULIN ($\overline{MW}$=5000)
^{14}C-DEXTRAN ($\overline{MW}$= 70,000)

These studies therefore show that transient pores form in the Torpedo membrane vesicles during osmotic shock which spontaneously reseal. The processes occur not only with contaminating vesicles in the preparation but also with AcChR-containing vesicles, since the shock-loaded $^{22}Na^{+}$ was released by addition of cholinergic agonists (Fig. 7). The AcChR vesicles thus remain apparently active after the osmotic shock and resealing processes.

Let us consider why osmotically shocked AcChR vesicles sediment on sucrose density gradients in the high density region corresponding to that of pure AcChR membranes, yet apparently behave as resealed, intact vesicles in the above experiments. The most likely explanation is that following osmotic shock the vesicles spontaneously resealed, entrapping a low osmotic strength medium, which then shrunk and collapsed under the high osmotic pressure of the sucrose gradient (in 400 mM NaCl) to a high density form with little interior volume. This explanation is consistent with the observation that when these membranes were harvested from the sucrose gradient and suspended in a buffer containing 400 mM NaCl they retained very little $^{22}Na^{+}$, as expected for collapsed, shrunken vesicles having little interior volume. When resuspended in buffers of decreasing ionic strength, the vesicles appeared to expand and exhibit increasing interior volume (data not shown). A large interior volume was thus obtained when membranes harvested from the sucrose gradient were washed and suspended in a low salt buffer such as 10 mM NaCl-10mM TrisCl, pH 7.4 (see Chapter 3).

Figure 7: Carb Induced Efflux of ^{22}Na Entrapped in Purified AcChR Vesicles by Osmotic Shock. (O - O) Entrapment of $^{22}Na^{+}$ in AcChR vesicles by osmotic shock as described in Fig. 4. (■-■) Control experiment without osmotic shock. (● - ●) same as in (O - O) except that 100 μM Carb was included in the dilution buffer at t = 20 sec.

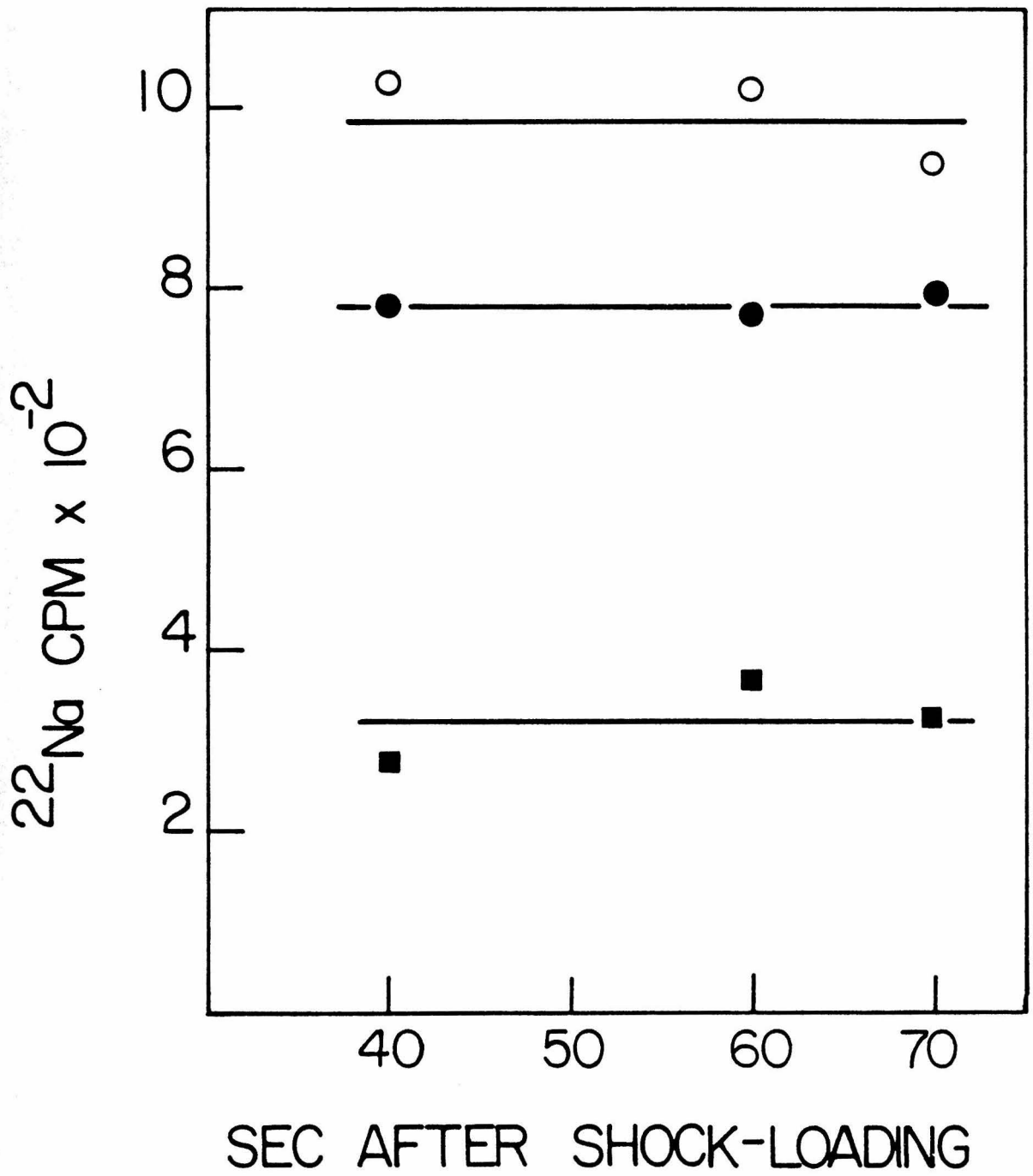
10
8
6
4
2
^{22}Na CPM x 10^{-2}
40
50
60
70
SEC AFTER SHOCK-LOADING

Shrinkage of Vesicles in Hypertonic Medium

As will be described in Chapter 3, the AcChR-enriched membrane preparation can be further purified by a method of alkaline extraction to yield a highly purified membrane preparation. To achieve the best result, the extraction is carried out in solutions of low ionic strength. The resulting membranes still exhibit the sealed vesicle structure with large interior volume and low interior osmolarity. In hypertonic medium, the vesicles shrink to a form with very little interior volume as indicated by the low equilibrium level of entrapped $^{22}Na^{+}$ radioactivity (Fig. 8).

Thus, the Torpedo membrane vesicles can be repeatedly osmotically shocked. Each time they are shocked they retain lower salt concentrations in the vesicle interior. The vesicles shrink when suspended in solutions of higher osmotic strength. To obtain optimal interior volume for ion flux studies, the AcChR-enriched preparations and highly purified membranes should be suspended in solutions of low osmolarity to prevent vesicle shrinkage due to low interior osmotic strength.

Loading of Impermeant Solutes into Vesicles

For ion flux studies such as those described in Chapter 4 as well as other studies concerning the AcChR topology in the membrane, it is sometimes desirable to load various solutes into the vesicle interior. Solutes which are permeable to the membranes can be loaded into the vesicles by prolonged incubation. For impermeant solutes, however,

Figure 8. Shrinkage of AcChR Vesicles with Low Interior Osmolarity in Hypertonic Medium. Base-extracted membranes were prepared in 10 mM Na Hepes, pH 7.4 as described in Experimental. Aliquots of membranes were incubated with $^{22}Na^{+}$ in 10 mM Na Hepes, pH 7.4 (● - ●) or in 400 mM NaCl- 10 mM Na Hepes, pH 7.4 (O - O) 12 hours at 4°C. Vesicle entrapped radioactivity was assayed by the Millipore method in the same buffer as the incubation media.

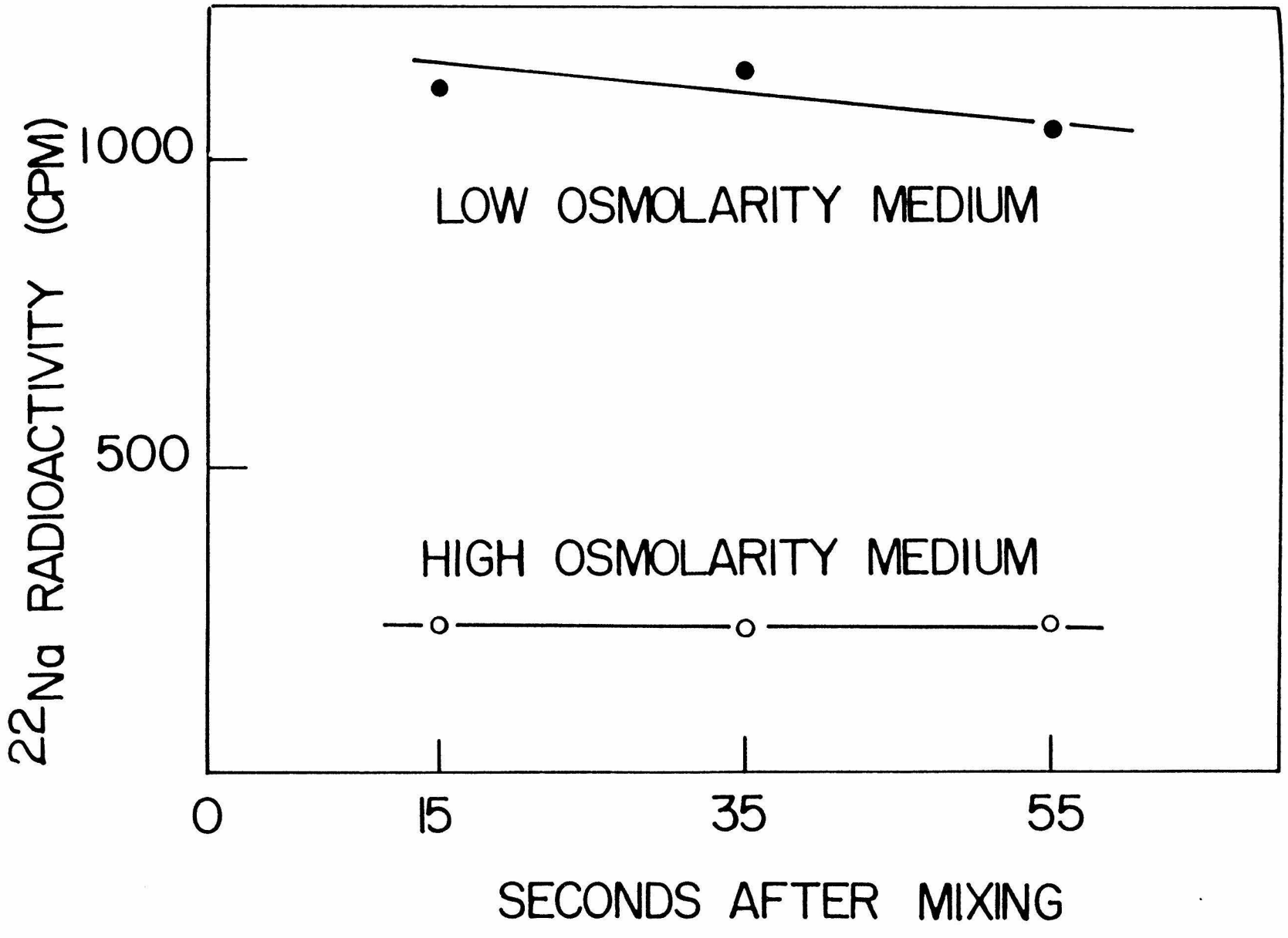
^{22}Na RADIOACTIVITY (CPM)
1000
500
LOW OSMOLARITY MEDIUM
HIGH OSMOLARITY MEDIUM
0
15
35
55
SECONDS AFTER MIXING

methods which produce temporary tears in the membranes are required. For vesicles of high interior osmotic strengh (such as the crude AcChR membrane preparation), osmotic shock into hypotonic solutions containing the solutes can be used since it produces transient holes in the membranes as discussed earlier. The AcChR-enriched and highly purified membranes, however, cannot be osmotically shocked efficiently because of their low interior osmolarity. An alternative method, "freeze-thaw" cycles, proved to be an easy and efficient way to load impermeant solutes into vesicles which cannot be readily osmotically shocked. As shown in Fig. 9, [^{3}H]-inulin was entrapped within the highly purified AcChR vesicles when a mixture of the vesicles and the radio-solutes was quickly frozen in liquid N_2 and gradually thawed at 0^{o}C. Presumably ice crystals formed during rapid freezing caused temporary tears in the membrane allowing solutes to permeate which then spontaneously reseal. A second "freeze-thaw" cycle does not increase the amount of entrapped radioactivity. Furthermore, the amount of entrapped [^{3}H]-inulin is comparable to that of $^{22}Na^{+}$ loaded by prolonged incubation, indicating that a single "freeze-thaw" cycle is sufficient to allow complete equilibration of the vesicle interior with the incubation media.

Figure 9. Freeze-Thaw Cycles for Loading Impermeant Solutes into Vesicles. 300 µl base-extracted membranes (∿25 µM in α-BuTx sites) were mixed with 30 µl of ^{3}H-inulin (∿200 µCi/ml) and rapidly frozen in a liquid N_2 bath. The mixture was gradually thawed in an ice bath over a period of one hour. The vesicle entrapped radioactivity was assayed by the Millipore method. (O - O) entrapped radioactivity measured after one and two freeze-thaw cycles. (Δ - Δ) control experiment. All the steps were identical except that the membranes were incubated with ^{3}H-inulin at 0°C without freeze-thaw cycles.

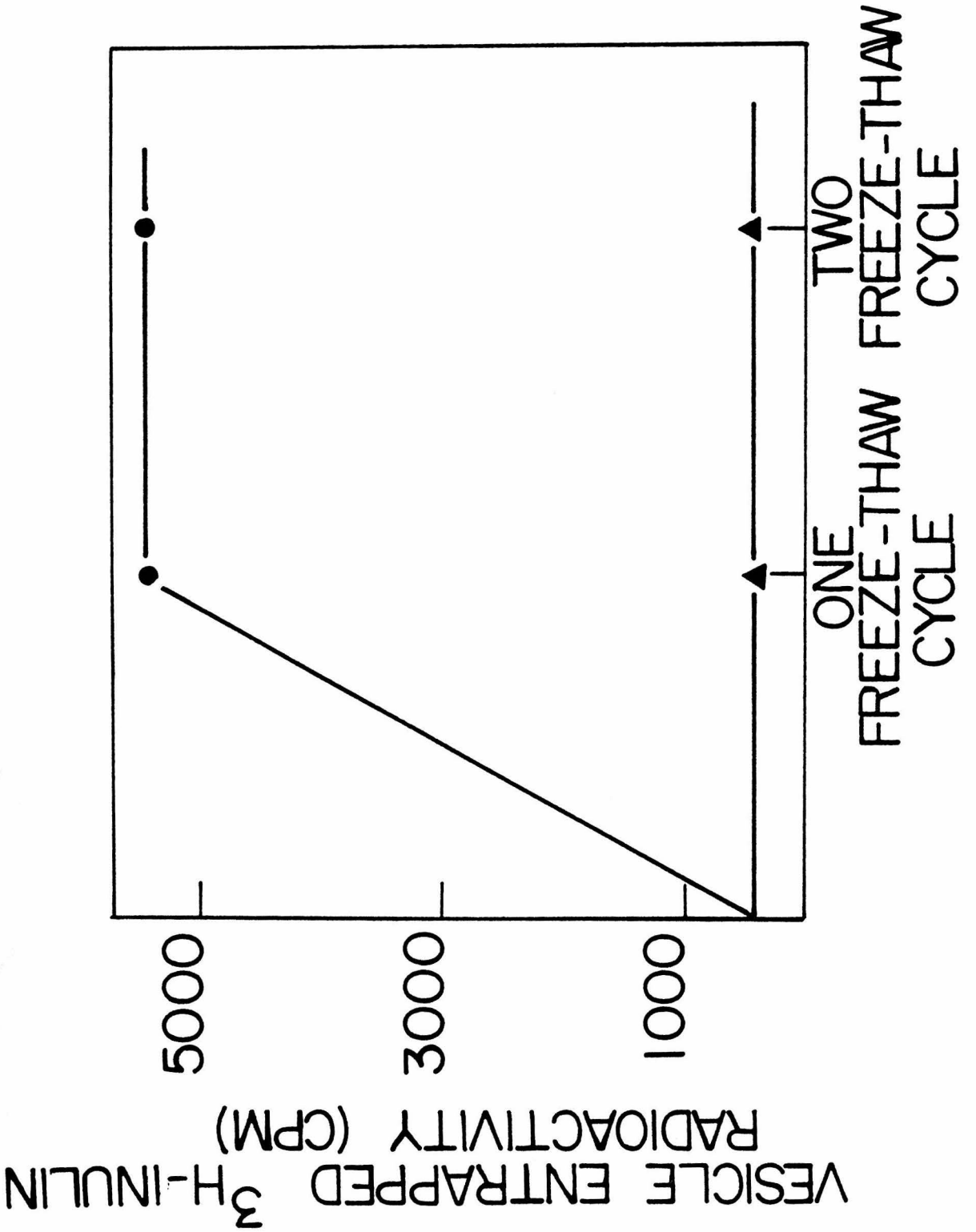
VESICLE ENTRAPPED ^{3}H-INULIN
RADIOACTIVITY (CPM)
5000
3000
1000
ONE FREEZE-THAW CYCLE
TWO FREEZE-THAW CYCLE

DISCUSSION

In some systems, osmotically shocked vesicles will reseal spontaneously (Wallach and Schmidt-Ulrich, 1977) while others remain mostly broken under certain conditions (Bodemann and Passow, 1972). In Torpedo californica membrane vesicles the present studies show that osmotic shock causes formation of pores through which interior contents are lost and small molecules from the exterior can enter. These transient pores are not likely to consist of stretched natural pores such as AcChR ion channels because, unlike AcChR channels, the pores do not discriminate between anions, cations and neutral species. Also, α-BuTx treatment of membrane vesicles did not block the osmotic shock induced effects even though α-BuTx effectively blocks AcChR function in Torpedo membranes (Lee, 1972). In addition, the pores induced by osmotic shock are permeable to molecules of up to 7800 M_r.

The lack of entry of 70,000 M_r dextran may be a reflection of resealing time as well as of the size of cutoff of these transient pores. It may be that the transient pores reseal before the large extended dextran polymer can significantly diffuse into the vesicle interior. More refined experiments will be required to make this distinction.

Following osmotic shock, Torpedo vesicles reseal within less than 5 seconds, the fastest attainable time using our experimental conditions. Such rapid resealing of the pores occurred both at 4^oC and 25^oC. Despite this lack of an observable temperature effect, fluid-phase membrane lipid may be a requirement for the resealing process. Torpedo californica lives in deepwater environments with temperatures near 4^oC

(Bennett, 1970). Thus, it is likely that the vesicle membranes remain fluid at 4°C. It is likely that the transient pores consist of large tears in the membrane induced by osmotic rupture, which rapidly and spontaneously re-anneal. Such pores have been observed by electron microscopy of erythrocyte membrane vesicles (Seeman et al, 1973).

The ability of osmotically shocked Torpedo vesicles to spontaneously reseal explains why so many different types of electroplaque membrane preparations are vesicular, capable of maintaining asymmetric ion composition across their bilayer for in vitro ion flux studies. Large inflated crude membrane vesicle preparations can be obtained with interior solutions of high osmotic strength (isotonic to Torpedo plasma, equivalent to ∿400 mM NaCl). The AcChR-enriched membranes harvested from the high density regions of the sucrose density gradient and the highly purified AcChR membranes obtained after alkaline extraction, however, retain large interior volume only when suspended in solutions of low osmolarity since they incorporate solutions of low osmotic strength during the osmotic shock step in the purification procedure; under high osmotic pressure they tend to shrink and collapse into a form with little interior volume and of high density (approaching that of pure AcChR membranes, ∿1.18 mg/ml). AcChR vesicles can be sequentially shocked and resealed for several cycles, each time incorporating solutions of lower osmotic strength into the vesicle interior and thus becoming more resistant to subsequent osmotic shock. Because of the spontaneous resealing process, osmotic shock procedure can be used to introduce impermeable solutes into a vesicle interior of high osmotic

strength. For vesicles more resistant to osmotic shock, the 'freeze-thaw' cycles prove to be an efficient method for such a purpose. With this information on the osmotic behavior of AcChR membrane vesicles it will be easier to design preparative biochemical methods for studies utilizing the vesicle properties of the AcChR membranes.

REFERENCES

1. M. V. L. Bennett (1970), Ann. Rev. Physiol. 32, 471.
2. H. Bodemann and H. Passow (1972), J. Membrane Biol. 8, 1.
3. L. G. Brock and R. M. Eccles (1958), J. Physiol. 142, 251.
4. J. R. Duguid and M. A. Raftery (1973), Biochemistry 12, 3593.
5. J. Elliott, S. G. Blanchard, W. Wu, J. Miller, C. D. Strader, P. R. Hartig, H.-P. H. Moore, J. Racs, and M. A. Raftery (1980), Biochemical J. 185, 667.
6. J. Elliott, S. M. J. Dunn, S. G. Blanchard, and M. A. Raftery (1979), Proc. Natl. Acad. Sci. 76, 2576.
7. P. R. Hartig and M. A. Raftery (1979), Biochem. 18, 1146.
8. M. Jusic, S. Seifert, E. Weiss, R. Haas, and P. C. Heinrich (1976), Arch. Biochem. Biophys. 177, 355.
9. M. Kasai and J.-P. Changeux (1971), J. Membrane Biol. 6, 1.
10. C. Y. Lee (1972) Ann. Rev. Pharmacol. 12, 265.
11. S. McLaughlin and M. Eisenberg (1975), Ann. Rev. Biophys. Bioeng. 4, 335.
12. R. R. Neubig, E. K. Krodel, N. D. Boyd, and J. B. Cohen (1979), Proc. Natl. Acad. Sci. 76, 690.
13. P. Seeman, D. Cheng, and G. H. Iles (1973), J. Cell Biol. 56, 519.
14. G. Sessa and G. Weissmann (1968), J. Lipid Res. 9, 310.
15. P. J. Simms, A. S. Waggoner, C.-H. Wang, and J. F. Hoffman (1974), Biochemistry 13, 3315.

16. C. D. Strader, J.-P. Revel, and M. A. Raftery (1979), J. Cell Biol. 83, 499.

17. D. F. H. Wallach and R. Schmidt-Ulrich (1977), Methods in Cell Biology 15, 235 (Ed. D. M. Prescott, Academic Press, New York).

CHAPTER THREE

Rapid Cation Translocation in *Torpedo* Membrane Vesicles: I. Acetylcholine Receptor Mediated $^{22}Na^{+}$ Efflux and Correlation of Polypeptide Composition with Functional Events

INTRODUCTION

In the study of neuromuscular transmission at the molecular level it is important to relate the structural components of AcChR to receptor functionality. Of the two major events leading to membrane depolarization, namely AcCh binding and cation translocation, the first has been extensively studied in *in vitro* preparations. As discussed in Chapter 1, a major AcCh binding site(s) has been localized on the 40,000 dalton polypeptide component of the AcChR. The subsequent events leading to membrane permeability changes and the structural constituents mediating cation translocation, however, have been characterized to a much lesser extent. In this and the following chapters, we have therefore employed the various sealed membrane vesicle preparations from *T. californica* characterized in Chapter 2 to study such functional events of the receptor and to define the molecular species essential in controlling the membrane cation permeability.

Following detergent solubilization, and affinity column chromatography for purification of quatenary ammonium binding activity, the *Torpedo* AcChR preparation appears to be composed of four polypeptides of M.W. 40,000, 50,000, 60,000 and 65,000 daltons (Raftery *et al*, 1976). Such a preparation, however, does not provide a convenient system for identifying the molecular entities involved in the permeability control because the membrane barrier across which ion translocation can be monitored has been disrupted. Preparations of AcChR in its native membrane-bound state are thus more useful for such purposes (Chapter 2). When

prepared by centrifugation procedures from the crude homogenates of Torpedo electroplaques, these contain in addition to the four polypeptides of the solubilized, purified preparation many other polypeptides, notably those of M.W. 43,000 and 90,000 daltons (Elliott, et al, 1980). Recently, a membrane preparation has been obtained by Sobel et al (1978) from T. marmorata which consists of only two major polypeptide constituents, namely, those of M.W. 40,000 and 43,000 daltons. Based on studies of interactions with local anesthetics and histrionicotoxin, the authors suggested that the polypeptide of 43,000 daltons carries the binding sites for substances (such as local anesthetics) known to interact with AcChR-associated ion channels and therefore may represent the putative ionophore. In their model, the 'AcCh regulator' is composed of two allosterically linked, distinct protein entities, the 'AcCh receptor' and the 'AcCh ionophore'. The former resides in the polypeptide of 40,000 daltons and binds cholinergic agonists, antagonists and snake α-toxins. The latter, on the other hand, is made up of another class of polypeptide chains (ppssibly of M.W. 43,000 daltons) which carries both the ion channel and the local anesthetic binding sites. According to these authors, the polypeptides of higher M.W. (such as those of 50,000, 60,000, 65,000 daltons) normally associated with the AcChR preparations may be contaminants which copurify with the receptor. Using a photoaffinity derivative of the local anesthetic procaine amide, Blanchard and Raftery (1979) found that the 43,000 dalton polypeptide was selectively labeled and thus might contain a binding site for

procaine amide.

More recently the hypothesis of Sobel et al (1978) has been challenged by the finding that treatment of the AcChR-enriched membrane preparations (which contain many polypeptides in addition to the polypeptides of 40,000, 50,000, 60,000 and 65,000 daltons) at alkaline pH selectively extracts a substantial fraction of the 43,000, 90,000 dalton and many other polypeptide components from the membranes (Neubig et al, 1979; Elliott et al, 1980); the resulting membrane preparations contain four major constituent polypeptides of M.W. 40,000, 50,000, 60,000 and 65,000 daltons and exhibit binding affinities for certain local anesthetics that are indistinguishable from those of untreated membranes (Neubig et al, 1979; Elliott et al, 1979). Since local anesthetics may act at sites other than those directly involved in the ion translocation mechanism, more direct methods to measure the receptor function are required to solve this apparent controversy and to identify those peptide chains which make a contribution to the functioning of the receptor.

One approach to study the AcChR-mediated cation permeability is to utilize the vesicular properties of the in vitro membrane preparations (Chapter 2) and to monitor efflux of $^{22}Na^{+}$ preloaded in these vesicles in response to addition of cholinergic ligands (Kasai and Changeux, 1971a). A filtration method can be employed to remove the external $^{22}Na^{+}$. The first use of such a method was by Kasai and Changeux (1971a) who observed stimulation of cation efflux from crude membrane vesicles derived from Electrophorus electricus by cholinergic ligands. The

efflux process, however, has a half-time of ∿7 min and is far slower than the millisecond response time observed *in vivo*. This slow response has nevertheless been extensively characterized with respect to various pharmacological agents (Kasai and Changeux, 1971b; Hess *et al*, 1976). In the work described in this chapter, we have first studied the $^{22}Na^{+}$ flux from the crude, sealed *Torpedo* membrane vesicles prepared according to Chapter 2 in response to cholinergic agonists. The observed efflux process is considerably faster than those previously reported and is complete within the first time point obtainable by the filtration method (∿10 sec). Moreover the response has many properties similar to those characterized in vivo; it exhibits the expected cholinergic ligand specificities, desensitization upon prolonged incubation with the agonist Carb and blockage by the toxins α-BuTx and H_{12}-HTX which are considered to be specific inhibitors of ligand binding and ion-translocation respectively. This rapid efflux is thus more closely related to the physiological phenomenon than is the slow response previously analyzed by others and provides a convenient *in vitro* assay for AcChR mediated permeability change.

The quantitative use of the method described above to define the structural components required for AcChR function is complicated by the lack of kinetic data for the rapid flux response due to the slowness of the filtration technique. Only a flux amplitude consisting of a time-integrated release of vesicle entrapped $^{22}Na^{+}$ can be measured after all flux processes have terminated. The limited number

of vesicle-entrapped $^{22}Na^{+}$ ions to be transported and the high transport number associated with each activated ion channel *in vivo* lead us to the expectation that a full flux amplitude can be produced by only a small active fraction of the total AcChR population present on the vesicle surface. Consequently flux responses measured in this manner do not directly quantitate the number of active receptors in a given preparation. We have therefore employed a method of partial inactivation to assess the number of active AcChR. This method involves random inactivation of variable fractions of AcChR channels by the irreversible binding of α-BuTx. The dependence of flux amplitude on the extent of this inactivation serves as an indication of the size of the functional AcChR population. Using this method we have compared the flux responses of AcChR enriched membranes and of membranes from which polypeptides of 43,000 daltons and 90,000 daltons have been substantially removed by base extraction. The results indicate that the 43,000, 90,000 daltons, and certain other polypeptides substantially removed by base extraction are not essential for AcChR-mediated ion flux and that the full flux response occurs with preparations composed of essentially the four polypeptides of 40,000, 50,000, 60,000 and 65,000 daltons.

EXPERIMENTAL

Membrane Vesicle Preparations

Crude membrane vesicles were prepared from homogenates of Torpedo electroplaques in buffers isotonic to Torpedo plasma as described in Chapter 2. AcChR-enriched membrane preparations were membranes harvested from the high density regions of sucrose density gradients and suspended in buffers of low osmotic strength (also see Chapter 2). Except for the initial studies using crude membrane vesicles, most of the preparations used were routinely treated with 5 mM iodoacetamide and 10 mM PMSF included in the first homogenization medium.

Base Extraction of AcChR-enriched Membrane Vesicles

For base treatment, membranes harvested from the sucrose gradients (15-18 μM in α-BuTx sites) were diluted ten-fold into room temperature distilled water and the pH adjusted to 11 with 0.2 N NaOH. The membranes were stirred at $4^{o}C$ for 1 hr and centrifuged at 39,000 x g for 45 min. The supernatant and a soft pellet that sedimented on top of the hard pellet were removed. The hard pellet was resuspended in 10 mM NaCl-10 mM Tris-Cl, pH 7.4 at 1.5 - 1.8 μM and the pH was again adjusted to 11. The membranes were immediately pelleted as before and resuspended (∿13 μM) in the same buffer. α-BuTx binding was totally recovered in the various fractions. Also, the α-BuTx association rate constant and the $t_{1/2}$ of the Carb-induced affinity change were unaltered (Elliott et al, 1980). For AcChR enriched membranes, where removal of non-receptor

proteins was not desired, the same treatments were followed except that the pH was kept at 7.4 throughout.

The concentration of α-BuTx sites in the membrane preparations was routinely assayed by the DEAE disc method of Schmidt and Raftery (1973). Protein was assayed according to the procedure of Lowry et al (1951) with bovine serum albumin as the standard. The specific activity of a typical membrane preparation was 0.3 - 0.6 nmol α-BuTx sites/mg protein, 1.0-1.25 nmol/mg and 4.0-6.0 nmol/mg for crude membranes, AcChR enriched membranes and base-treated, highly purified membranes respectively.

$^{22}Na^{+}$ Flux Assay

To measure agonist-induced cation efflux, the membrane vesicle preparations (12-30 μM in α-BuTx sites) in the assay buffer were incubated with 4.1 μM $^{22}NaCl$ (Amersham, 4.4 Ci/mmole) for 6-12 hours at $4^{o}C$ to allow equilibration of the $^{22}Na^{+}$ inside and outside the vesicles. The flux assay was started by a 20-fold dilution of the radioactive membrane suspension into nonradioactive assay buffer at room temperature with or without a cholinergic effector(s). The mixture was immediately vortexed and at desired time intervals 200 μl aliquots were transferred with an Eppendorf pipet onto two layers of Millipore filters (plain, white, 0.8 μM pore size, 25 mm dia.) which had been presoaked in the assay buffer and mounted on a Millipore manifold apparatus. The filters were immediately washed with 2 x 7.5 mls of nonradioactive assay buffer (room temperature) and counted in a Beckman gamma counter with the counting windows optimized for ^{22}Na. The flux data were fit to single

exponential curves. In those figures for which data points were averaged time points of 10, 20, 30 and 40 sec after dilution were taken. As already discussed in Chapter 2, buffers of different ionic composition were used for the various preparations to maximize vesicle interior volume. For crude membrane vesicles, the assay was carried out in 400 mM Na Cl, 5 mM KCl, 2 mM $MgCl_2$, 5 mM Tris, 4 mM $CaCl_2$, 0.02% NaN_3, pH 7.4 whereas 10 mM TrisCl, pH 7.4 or 10 mM NaCl-10 mM TrisCl, pH 7.4 was used for the AcChR-enriched and the base-extracted, highly purified membrane vesicles.

Partial Inactivation Studies

For partial toxin blockage, the AcChR-enriched or highly purified membranes were diluted to 1.15 μM with 400 mM NaCl-1 mM EDTA-10 mM Na-phosphate, pH 7.4 to decrease the α-BuTx binding rate. The reaction was initiated by rapid addition of an equal volume of α-BuTx in the same buffer to a well-stirred membrane suspension. The mixture was incubated at room temperature for 65 min to allow 99% completion of the reaction (measured bimolecular rate constant = $2.2 \times 10^4 M^{-1} s^{-1}$). Aliquots of the reaction mixture were withdrawn to determine the residual α-BuTx sites with [^{125}I] α-BuTx. The membranes were washed with and resuspended in 10 mM NaCl-10mM TrisCl, pH 7.4. Flux studies of these partially inactivated membranes were carried out in 10 mM NaCl-10mM TrisCl, pH 7.4 as described above except that time points were taken 10 min after dilution to reduce non-specific background efflux.

Gel Electrophoresis

8.75% polyacrylamide gels were run in 0.1% SDS and were stained for protein with 0.05% (w/v) Coomassie Brilliant Blue in 10% acetic acid, 25% methanol and destained in the same solution without the dye. Gel strips cut from slabs were scanned at 550 nm using a Gilford 240 spectrophotometer equipped with a linear-transport accessory.

H_{12}-HTX was a generous gift of Dr. Y. Kishi.

RESULTS

Rapid $^{22}Na^+$ Flux Response of Torpedo Membrane Vesicles to Cholinergic Agonists

Crude AcChR membrane preparations from Torpedo californica electroplaques loaded with $^{22}Na^+$ exhibit a rapid component of sodium efflux upon addition of Carb. Figure 1 demonstrates the loading of membrane preparations by incubation in ^{22}Na containing buffer. The time to completion of loading varies from 2 to 6 hours from preparation to preparation. Figure 2 demonstrates that a rapid flux component which was essentially complete within 10 seconds was induced by Carb addition. The shaded area in Figure 2 indicates a zone of uncertainty in these measurements. The active cation efflux signal falls somewhere within this zone. With the filtration techniques we are unable to measure time points less than 10 seconds after mixing.

Agonist-induced cation efflux in these preparations presumably arises from a subpopulation of sealed vesicles. As has been discussed in Chapter 2, the membrane vesicles are very sensitive to osmotic shock. As much as 88% of the entrapped $^{22}Na^+$ was released by this treatment (Fig. 2, lower trace). Therefore, 12% or less of the total counts were non-vesicular in origin. Within the same experiment the level of ^{22}Na retention following osmotic shock approximately equals the retention immediately after introduction of ^{22}Na in the loading solution. This baseline level of ^{22}Na retention presumably represents tightly bound

FIGURE 1. Time Course of Loading Torpedo Membrane Vesicles with $^{22}Na^{+}$

To a membrane preparation (8-13 μM in α-BuTx sites) in calcium free Torpedo Ringers containing 400 mM NaCl was added 4.1 μM $^{22}NaCl$. These were well mixed and incubated on ice. At the indicated times after the addition, 25 μl of the mixture was diluted into 500 μl of assay buffer at room temperature. At 10 sec after the dilution, a 200 μl aliquot was pipetted onto Millipore filters and washed. The amount of entrapped $^{22}Na^{+}$ was determined by the radioactivity retained on the filters.

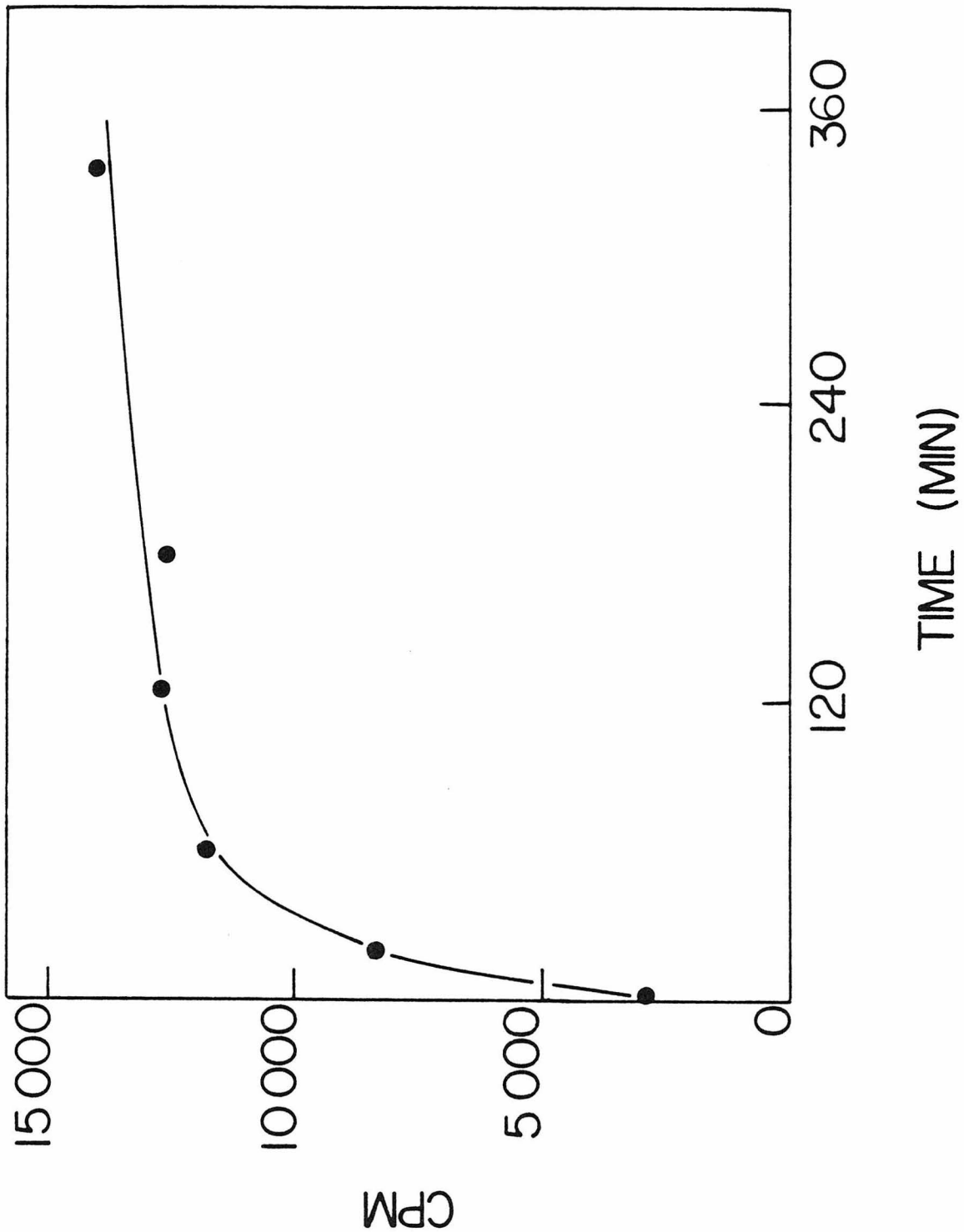
15000
10000
5000
0
CPM
120
240
360
TIME (MIN)

FIGURE 2. Release of Loaded $^{22}Na^{+}$ from the Crude Membrane Preparation by Carb and Osmotic Shock. A membrane preparation loaded with $^{22}Na^{+}$ was diluted 20-fold into dilution buffer (●), or dilution buffer plus 100 μM Carb (■) and the time course was followed by the Millipore filter method. The osmotic shock experiment (▲) was done by a 20-fold dilution into distilled water followed by immediate addition of 400 mM NaCl to the mixture. Solid lines indicate single exponential fits to the normalized data. The shaded area indicates a zone of uncertainty in these measurements.

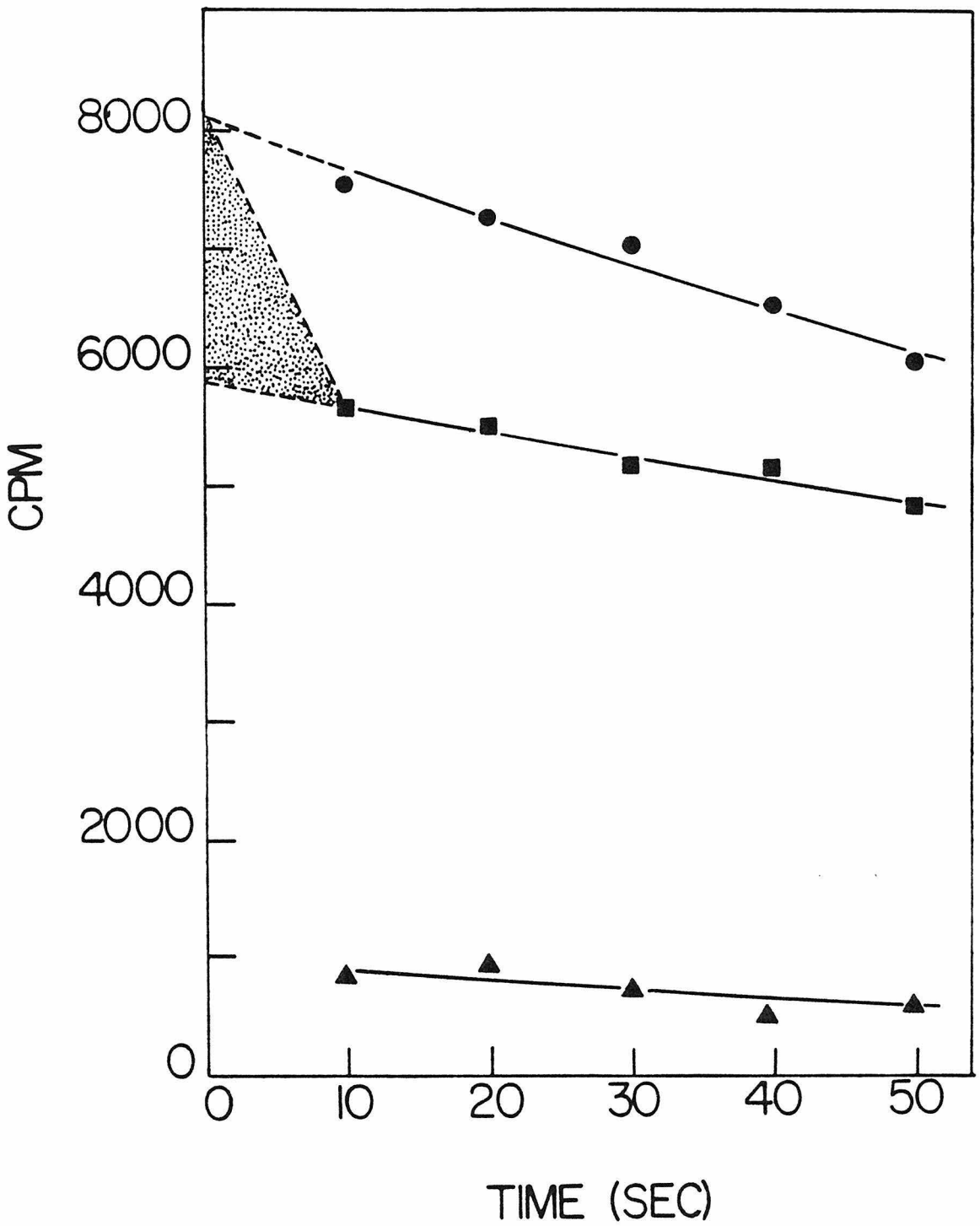
8000
6000
4000
2000
0
CPM
0
10
20
30
40
50
TIME (SEC)

and filter-trapped sodium. In contrast to the results obtained by Hess et al (1978) on eel membranes, rapid, agonist-induced efflux from Torpedo membrane vesicles occurs when buffers of the same ionic composition are used both inside and outside the vesicles. This active efflux is not sensitive to the divalent cation content of the buffer; buffers containing calcium and magnesium, magnesium alone, or EDTA with no divalent cations present all produce active efflux.

Pharmacological Characteristics of the in vitro Flux Response

Active efflux from our Torpedo membrane preparations displays many of the properties of the in vivo response. Figure 3A demonstrates the blockage of efflux by α-BuTx. The toxin has no effect in the absence of Carb but completely blocks the Carb-induced rapid efflux. Figure 3B illustrates the effect of desensitization on the efflux; preincubation of membranes with 100 μM Carb for 30 minutes blocks agonist-induced rapid efflux without affecting the background signal. Figure 3C shows the effect of H_{12}-HTX on the rapid efflux. Incubation of membranes with 5 μM H_{12}-HTX for 5 minutes did not affect the background signal, whereas incubation with 5 μM or 20 μM H_{12}-HTX blocked 30% and 57% respectively of the Carb-induced efflux. Figure 3D shows that Torpedo membranes isolated in the presence of iodoacetamide exhibit agonist-induced efflux to the same extent as untreated membranes. The acetylcholine receptor is largely or entirely in dimeric form in iodoacetamide treated membranes (Witzemann and Raftery, 1978).

FIGURE 3. Effect of (A) α-BuTx (B) Desensitization and (C) H_{12}-HTX on Carb-induced Fast Cation Flux. (A) Membranes were first reacted with a six-fold excess of α-BuTx at $0^{o}C$ for 45 min before 20-fold isotonic dilution into assay buffer (●) or buffer plus 100 μM Carb (□). The bottom curve (■) shows the control experiment done by isotonic dilution of non-toxinated membranes into 100 μM Carb. (B) Membranes were preincubated with 100 μM Carb at $0^{o}C$ for 30 min before isotonic dilution into assay buffer (●) or buffer plus 100 μM Carb (□). (■) isotonic dilution of membranes into 100 μM Carb without preincubation with Carb. (C) Membranes were diluted 20-fold into assay buffer with or without H_{12}HTX and incubated at $0^{o}C$ for 5 min. At time zero, buffer or Carb (100 μM) was added and efflux of $^{22}Na^{+}$ was followed. (●) no HTX, no Carb; (○) 5 μM HTX, no Carb; (■) no HTX, Carb; (▲) 5 μM HTX, Carb; (□) 20 μM HTX, Carb. (D) Membranes were isolated with 5 mM iodoacetamide added for the initial homogenization. After loading with ^{22}Na these membranes were diluted 20-fold into dilution buffer (●) or into buffer plus 100 μM Carb (■).

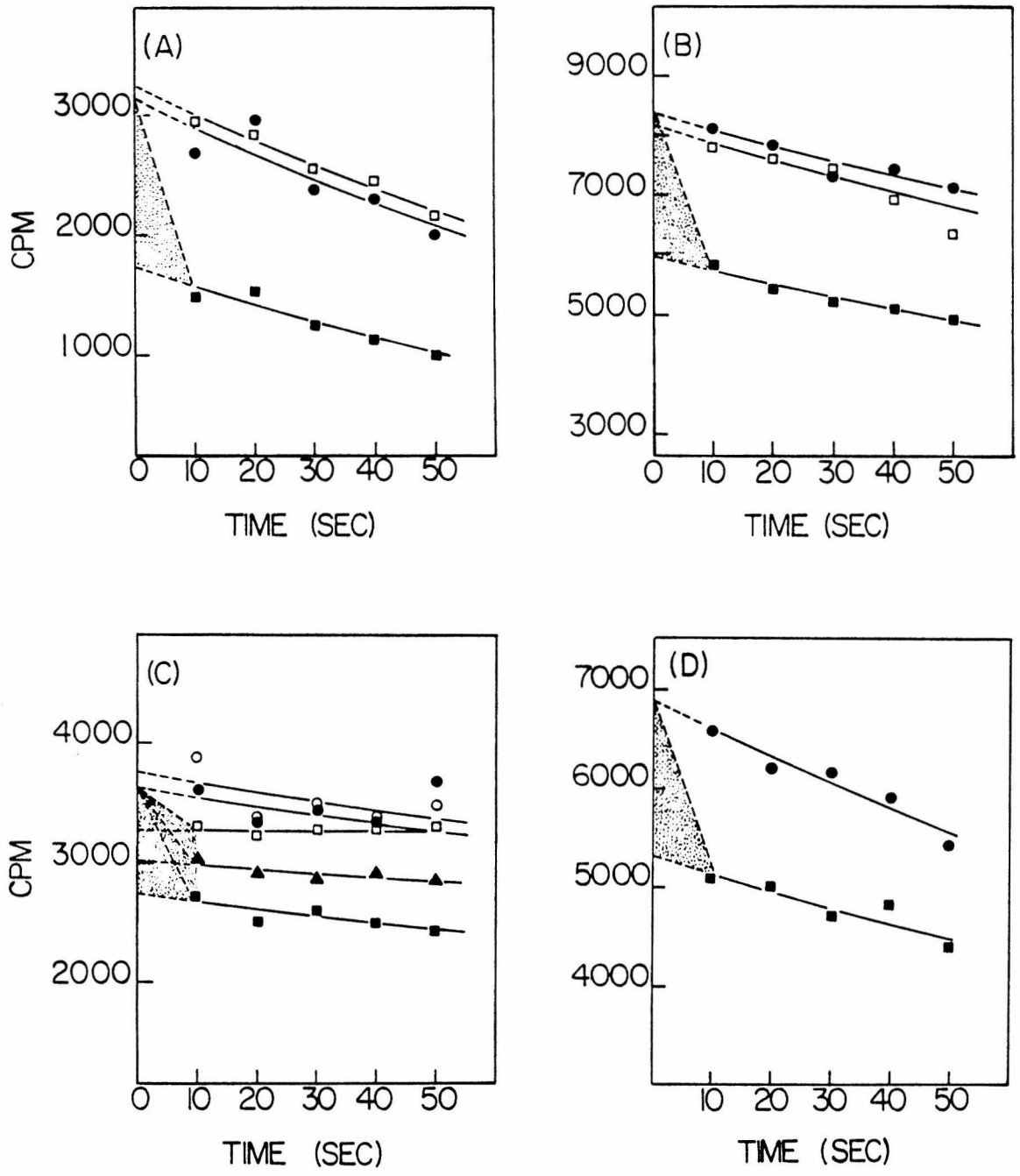
(A)
3000
2000
1000
CPM
0 10 20 30 40 50
TIME (SEC)
(B)
9000
7000
5000
3000
0 10 20 30 40 50
TIME (SEC)
(C)
4000
3000
2000
CPM
0 10 20 30 40 50
TIME (SEC)
(D)
7000
6000
5000
4000
10 20 30 40 50
TIME (SEC)

Figure 4 illustrates the observed flux amplitude as a function of the concentration of Carb. The observation that different concentrations of Carb do not elicit the same flux amplitude is indicative of the presence of a time-dependent inactivation process which terminates the flux process before all the entrapped $^{22}Na^{+}$ is emptied. Since the integrated flux amplitude is a complicated function of both channel activation and inactivation processes, such a 'dose-response' curve does not represent simple binding hyperbola and the midpoint of the curve cannot be taken as the dissociation constant for the ligand binding.

Ligand Specificity of $^{22}Na^{+}$ Efflux in the AcChR-enriched Membrane Preparations

In the previous paragraphs we have demonstrated that the crude Torpedo membrane preparations catalyze a rapid cation efflux upon addition of the agonist Carb. Membranes more enriched in AcChR can be obtained from high density regions of sucrose gradients. Under conditions for optional vesicle interior volume (Chapter 2), these membranes also exhibit the characteristic rapid $^{22}Na^{+}$ efflux in response to Carb. As shown in Fig. 5A, the % of entrapped $^{22}Na^{+}$ released by Carb is considerably higher than that for crude membranes, indicating enrichment of the AcChR-containing vesicles in this preparation. The cholinergic ligands, AcCh, BrAcCh and S-acetylthiocholine, all produced the agonist specific flux response (Fig. 5B,C,D). Inhibition of the acetylcholinesterase activity in the membrane preparations by 10^{-6}M eserine does not affect the signal, suggesting that

FIGURE 4. $^{22}Na^{+}$ Flux Amplitude as a Function of Carb Concentration. The relative response as measured by the total amplitude of the fast efflux component is plotted as a function of Carb concentration in the dilution buffer.(The data represent three independent measurements with three different membrane preparations).

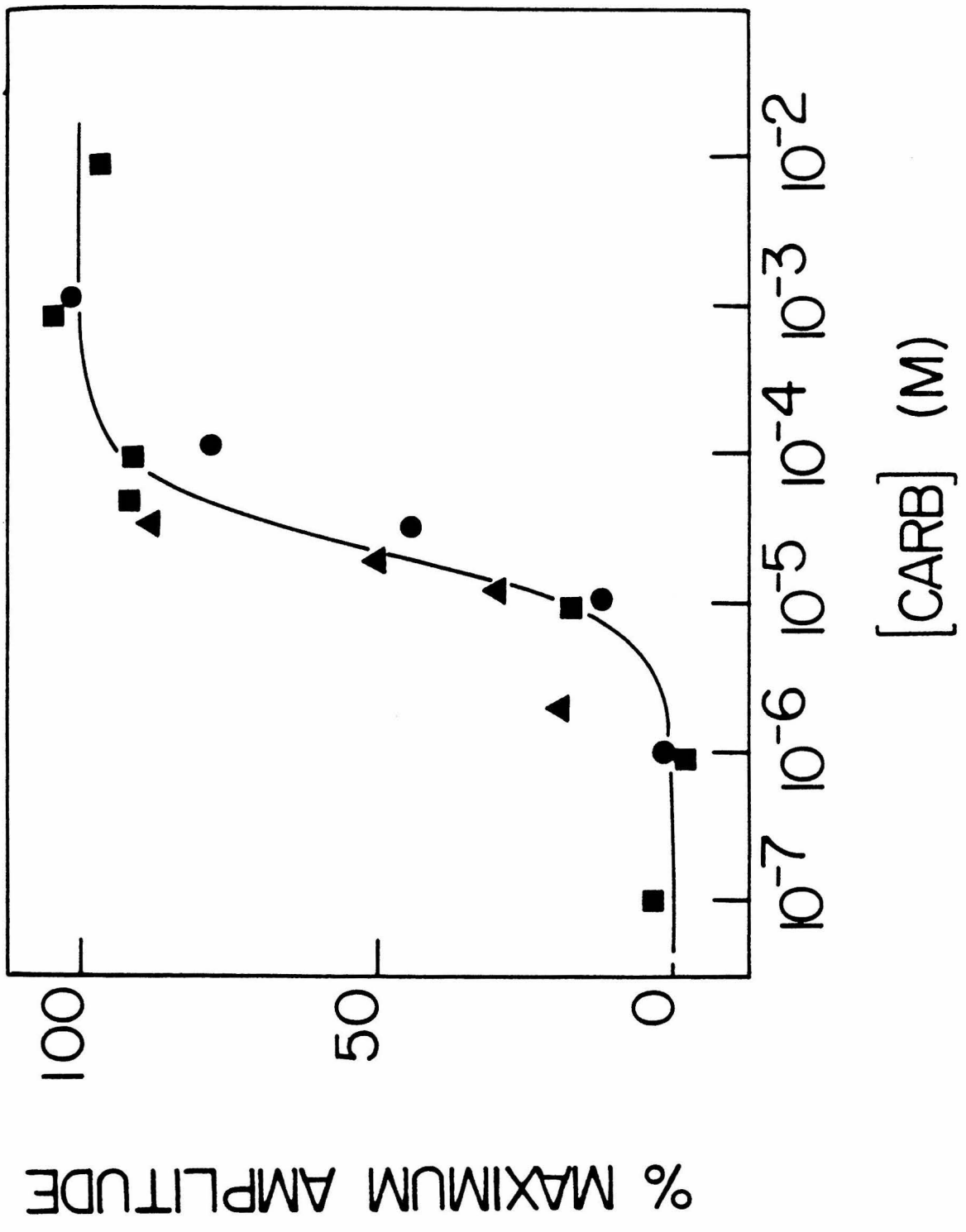
% MAXIMUM AMPLITUDE
100
50
0
10^{-7} 10^{-6} 10^{-5} 10^{-4} 10^{-3} 10^{-2}
[CARB] (M)

FIGURE 5. Cholinergic Ligand Specificity of $^{22}Na^{+}$ Flux Response in AcChR-enriched Membrane Vesicles. AcChR-enriched membrane vesicles in 10 mM Na Hepes pH 7.4 were preincubated with $^{22}Na^{+}$ for 12 hours at $4^{o}C$. $^{22}Na^{+}$ efflux was measured by the Millipore method. Efflux processes by (A) 0 μM Carb (● - ●) or 100 μM Carb (O - O); (B) 100 μM BrAcCh (● - ●) or 100 μM BrAcCh but pretreating the membranes with excess α-BuTx (O - O); (C) 100 μM d-Tc (▼ - ▼) or 100 μM Deca (▲ - ▲) or 100 μM AcCh (● - ●); (D) 10 μM choline (▲ - ▲) or 1 mM Choline (● - ●) or 100 μM S-Acetylthiocholine (▼ - ▼). Esterase activity was not inhibited in these experiments.

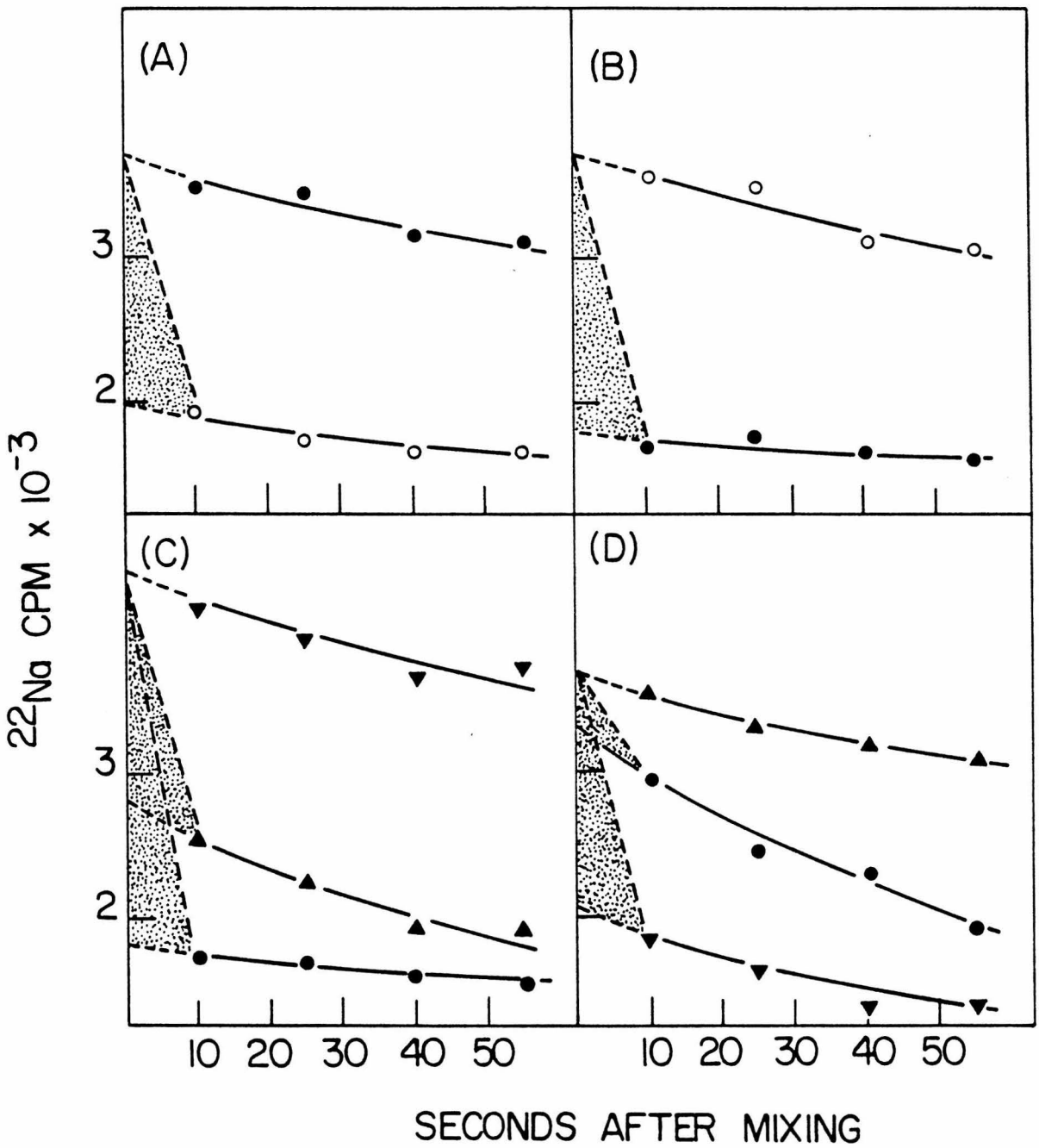
(A)
(B)
(C)
(D)
3
2
3
2
^{22}Na CPM x 10^{-3}
10 20 30 40 50
10 20 30 40 50
SECONDS AFTER MIXING

generation of the flux response is fast compared to the complete hydrolysis of these agonists (present at 100 μM). The observed response is not produced by the hydrolyzed product, choline or thiocholine, because hydrolysis of the ligands by esterases before addition to the membrane preparations abolishes the observed response. Higher concentrations of eserine or DNPP, on the other hand, totally inhibited the Carb-produced flux response (Fig. 6), either by perturbing the vesicle membrane or by other processes interfering with the receptor function. The antagonist d-tubocurare (d-Tc) at 100 μM does not stimulate $^{22}Na^{+}$ efflux (Fig. 5c). Decamethonium at the same concentration produces a partial release of $^{22}Na^{+}$. No flux response was observed with low concentrations of choline. At concentrations in the mM range, however, choline induces a slow $^{22}Na^{+}$ efflux and thus behaves as a weak agonist.

Qualitative Comparison of Active $^{22}Na^{+}$ Efflux in AcChR-Enriched and Selectively Extracted Membrane Preparations

Recently, the alkaline pH treatment originally used for selective extraction of erythrocyte membranes (Steck and Yu,1973) has been applied to purified Torpedo membranes (Neubig et al, 1979; Elliott et al, 1980). Treatment at pH 11 removed a large fraction of the 43,000 and 90,000 dalton polypeptide and many minor polypeptides from the membranes and produced a preparation greatly enriched in the four constituent polypeptides of 40,000, 50,000, 60,000 and 65,000 daltons (Fig. 7). Treatment at lower pH values was less effective in removing these components. A considerable amount of the polypeptides of M.W. $90x10^{3}$

FIGURE 6. Effect of Esterase Inhibitors on $^{22}Na^{+}$ Flux Response and Acetylcholinesterase Activity in the AcChR-enriched Membrane Preparations. AcChR-enriched membrane preparations (15-20 μM in α-BuTx sites) were treated with the amount of esterase inhibitors indicated for 30 min at $4^{o}C$ and aliquots were assayed for acetylcholinesterase activity (see Chapter One) and Carb induced $^{22}Na^{+}$ flux response. Data are presented as the percentage of maximal activity determined for the untreated membrane preparations.

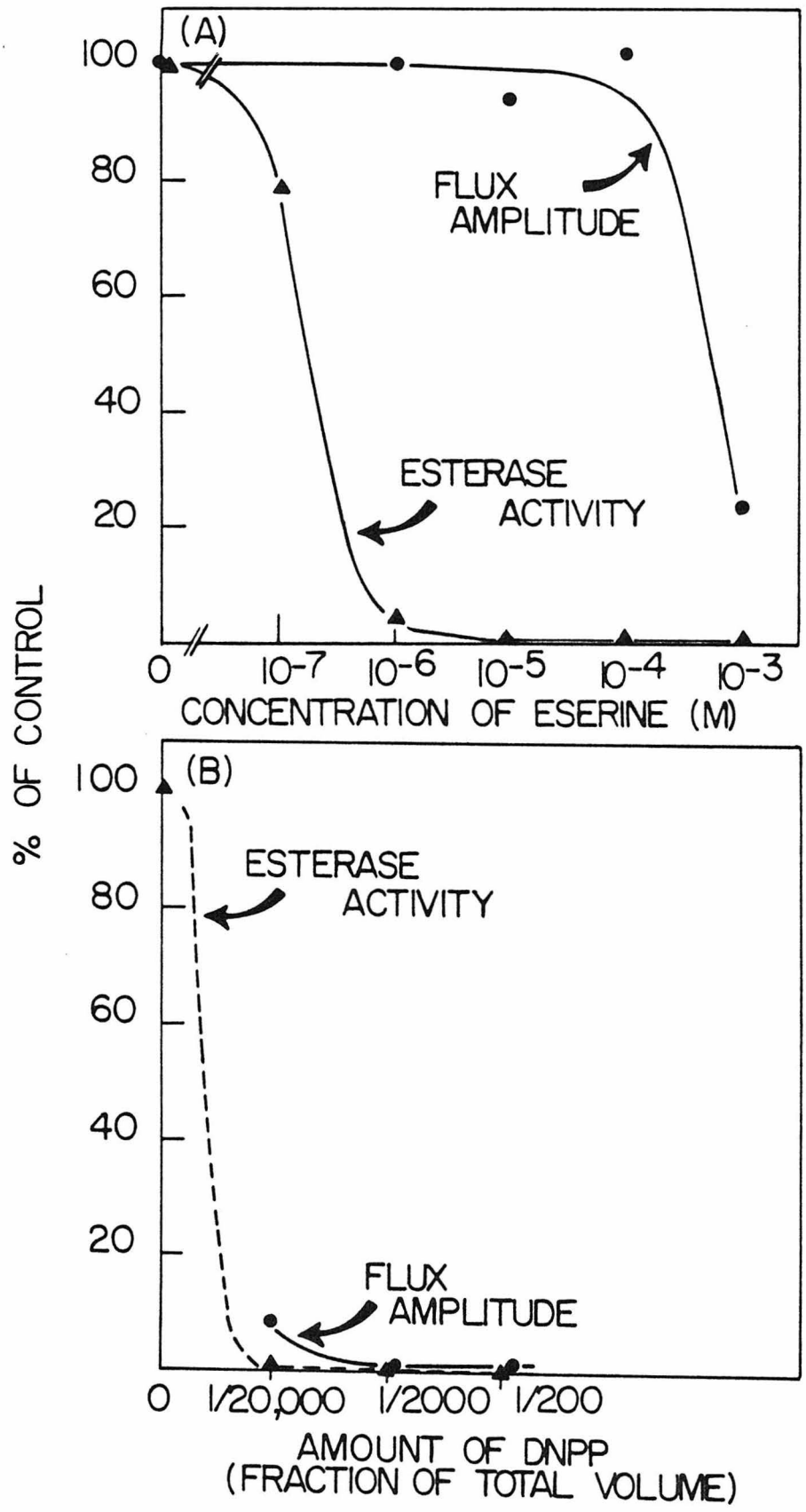
(A)
100
80
60
40
20
FLUX
AMPLITUDE
ESTERASE
ACTIVITY
0
10-7
10-6
10-5
10-4
10-3
CONCENTRATION OF ESERINE (M)
% OF CONTROL
(B)
100
80
60
40
20
ESTERASE
ACTIVITY
FLUX
AMPLITUDE
0
1/20,000
1/2000
1/200
AMOUNT OF DNPP
(FRACTION OF TOTAL VOLUME)

FIGURE 7. Polypeptide Composition of the Various Fractions During Base Extraction of AcChR-enriched Membranes. AcChR-enriched membrane preparations were treated twice at pH 11 as described in Experimental. The polypeptide components in the various fractions were analyzed by 8.75% SDS polyacrylmide gel electrophoresis. Left to right: CBB stained gels of membranes before treatment, membranes after treatment, polypeptides removed in the supernatant and polypeptides removed in the soft pellet which sedimented on top of the extracted membranes.

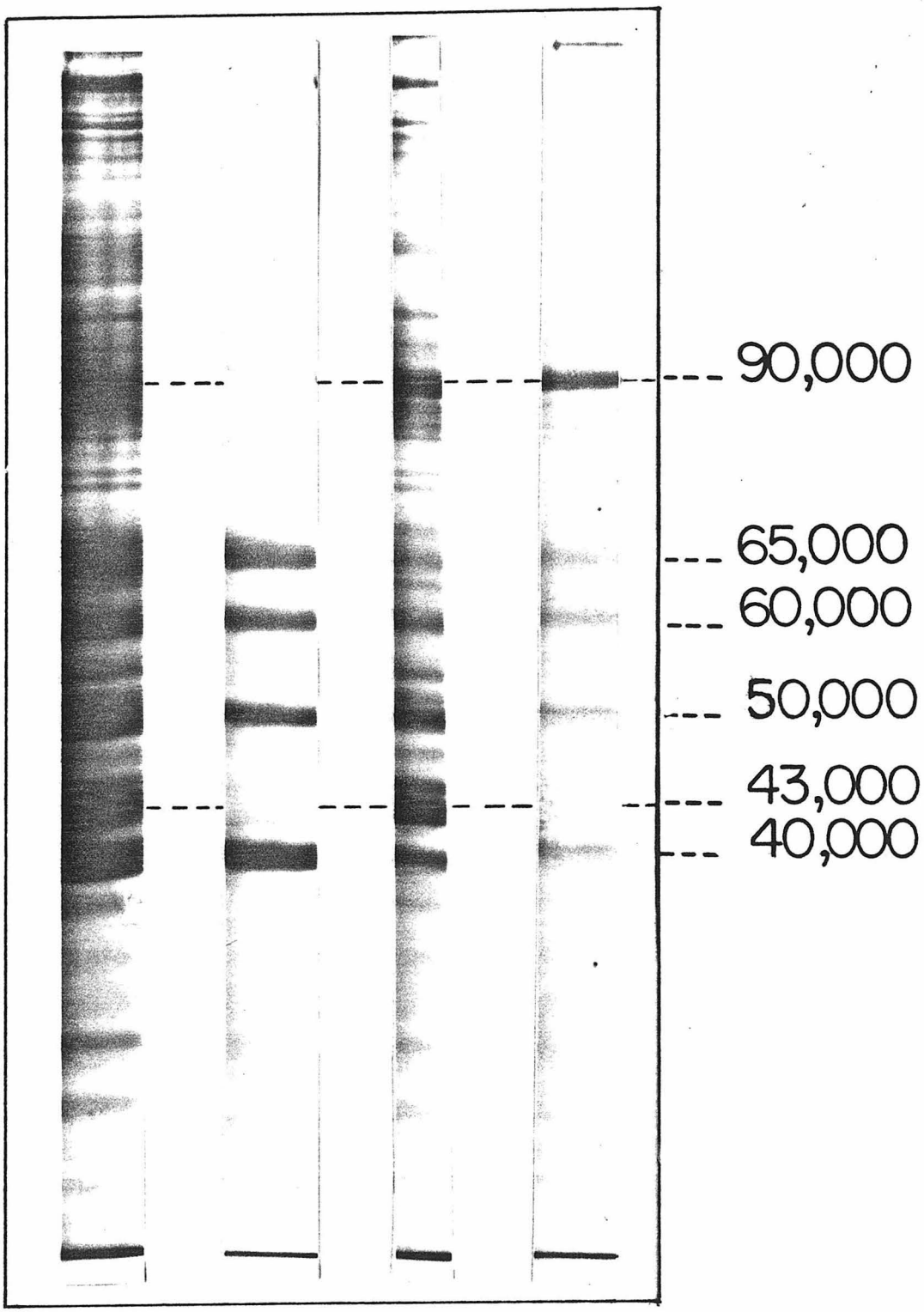
90,000
65,000
60,000
50,000
43,000
40,000

daltons and M.W. less than $40x10^3$ daltons (Fig. 7, right column) occur in a particulate fraction that sediments on top of the dense membrane pellet following treatment at pH 11. This lighter particulate fraction can be discarded.

Following prolonged incubation with ^{22}Na at 4^oC alkaline pH treated membranes retained the isotope when the external ^{22}Na was removed by the Millipore assay method. The apparent total vesicular volume (retained ^{22}Na) decreased as the pH value of the treatment was raised (Figure 8). All of the treated membrane fractions responded to the agonist Carb by rapidly releasing entrapped ^{22}Na and the percentage of retained counts released remained relatively constant (or increased in some preparations) as the pH of the treatment was raised. Thus the removal of the 43,000 and 90,000 dalton-polypeptide and additional major and minor components by pH 11 treatment does not obviously hinder agonist-induced cation efflux amplitude.

Sodium efflux from pH 11 treated membranes exhibited the expected pharmacology for a nicotinic cholinergic receptor preparation, as also demonstrated for untreated membranes. The data in Figure 9 demonstrate that the Carb-induced Na^+ efflux from pH 11 treated membranes is completely blocked by α-BuTx and is also eliminated by prior desensitization of the AcChR by Carb. The pH 11 treated membranes have been shown to bind the toxin, HTX, with similar affinity, kinetics and stoichiometry to that of untreated membranes (Elliott et al, 1979). As shown in Fig. 10 the treated membranes also exhibit a dose-dependent blockage of sodium efflux by HTX. After correcting for depletion due to bound HTX the free HTX

FIGURE 8. Effect of pH Treatment on Apparent Vesicle Volume. Equal aliquots of membranes were treated at the indicated pH values and loaded with $^{22}NaCl$ at pH 7.4. Counts retained in vesicles were determined from the average of 4 data points from the Millipore flux assay following dilution into 10 mM Tris-Cl pH 7.4 ± 100 μM Carbamylcholine.

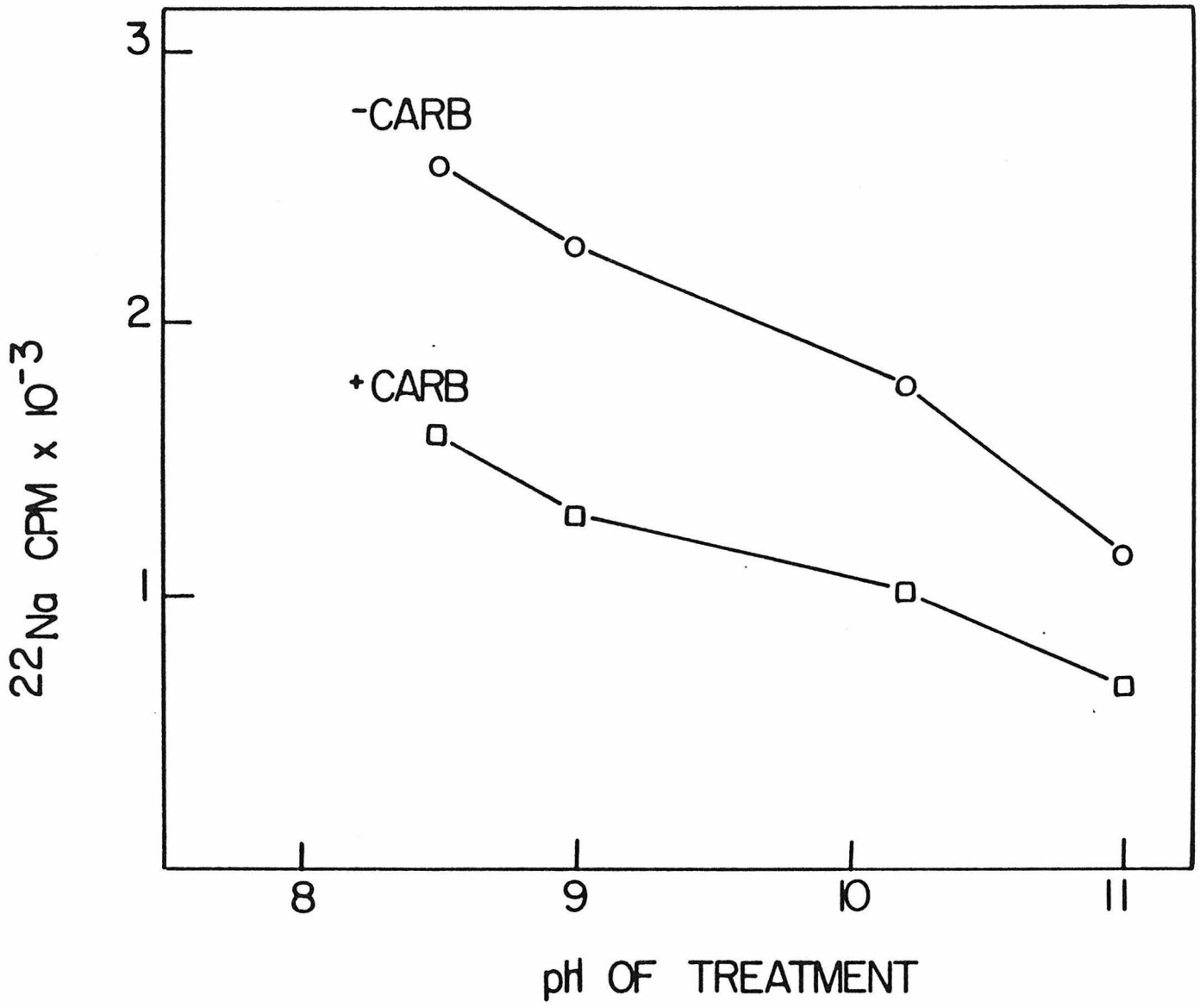
3
2
1
-CARB
+CARB
^{22}Na CPM x 10^{-3}
8
9
10
11
pH OF TREATMENT

FIGURE 9. Carb Induced $^{22}Na^{+}$ Efflux from Membrane Vesicles Treated at pH 11. (A) Isotonic dilution into buffer (10 mM Tris-Cl, pH 7.4) containing 100 μM (□) or 0 μM (0) Carb. (B) Effect of α-BuTx on Carb-induced $^{22}Na^{+}$ efflux. Membranes were incubated with a 1.5 fold excess of α-BuTx at $0^{o}C$ for 30 minutes before isotonic dilution into buffer containing 100 μM (□) or 0 μM (0) Carb. (C) Effect of agonist induced desensitization on Carb induced $^{22}Na^{+}$ efflux. Membranes were preincubated with 100 μM Carb at $0^{o}C$ for 30 minutes before a 20-fold isotonic dilution into buffer containing 100 μM (■) or 0 μM (●) Carb. Control experiments with membranes not preincubated with Carb are also indicated (dilution into buffer containing 100 μM (□) or 0 μM (0) Carb).

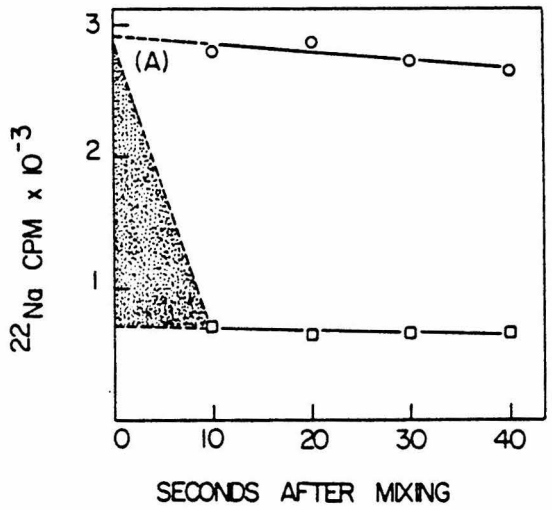
(A)
^{22}Na CPM x 10^{-3}
3
2
1
0
10
20
30
40
SECONDS AFTER MIXING

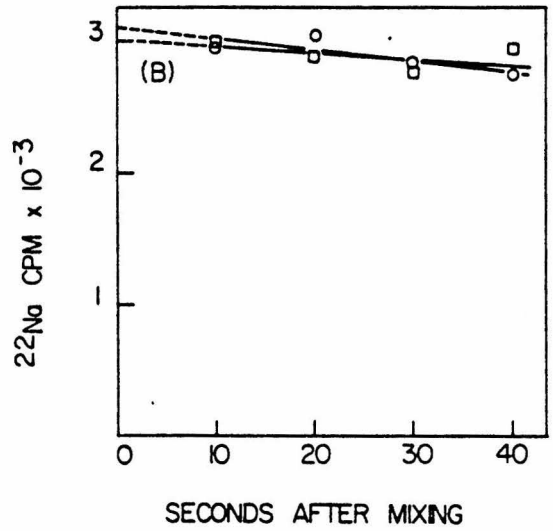
(B)
^{22}Na CPM x 10^{-3}
3
2
1
0
10
20
30
40
SECONDS AFTER MIXING

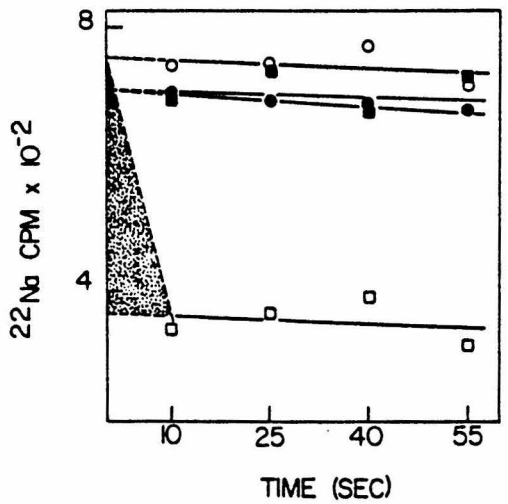
^{22}Na CPM x 10^{-2}
8
4
10
25
40
55
TIME (SEC)

FIGURE 10. H_{12}-HTX Inhibition of $^{22}Na^{+}$ Efflux from pH 11-treated Membrane Vesicles. Membranes were incubated with various concentrations of H_{12}-HTX on ice for 30 minutes before isotonic dilution into buffers containing 100 μM Carb and the same H_{12}-HTX concentrations as the incubation medium. The percent blockage of ^{22}Na efflux was plotted against the logarithm of the concentration of added H_{12}-HTX. The response was determined from the average of 4 data points from the Millipore flux assay.

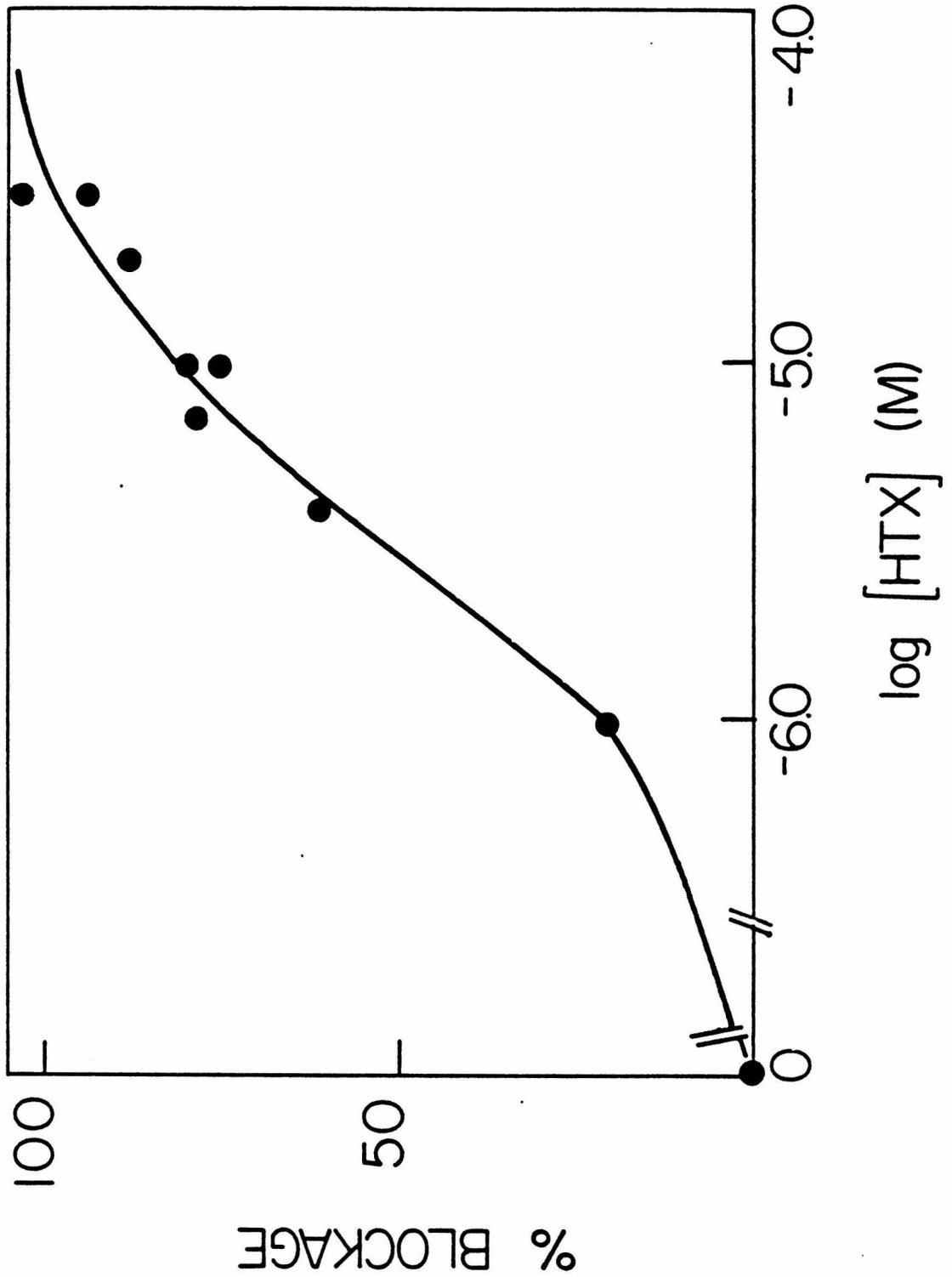
% BLOCKAGE
100
50
0
-4.0
-5.0
-6.0
log [HTX] (M)

concentration required for 50% of the effect is ∿2 μM.

Figure 11 shows the Carb-induced 'dose-response' curves for ^{22}Na efflux from both pH 11 treated and untreated membranes. In both cases a similar dependence of the flux amplitude on the Carb concentration was observed. The midpoint of these curves corresponds to a Carb concentration approximately 10 times larger than that observed for the crude membranes (see Fig. 4). This difference may be due to the differing salt concentration in the assay systems. Crude membranes were assayed in 0.4 M NaCl while the pH 7.4 and 11 treated membranes were assayed in 10 mM Tris-Cl. Agonist binding to AcChR-enriched membranes is inhibited by NaCl with an inhibition constant of 38 mM (Miller et al, 1979). The observed midpoint shift of the Carb-induced response can be adequately explained by this inhibition of agonist binding.

Thus the removal of a substantial fraction of the polypeptide component of 43,000 and 90,000 daltons does not alter the qualitative aspect of the agonist-induced $^{22}Na^{+}$ efflux process in the membranes. Such studies, however, do not by any means provide a definitive answer for the functional role of these polypeptides because the kinetics of the efflux process (which are a quantitative measure of receptor function) are too fast to be measured by filtration; only the amplitude of $^{22}Na^{+}$ release after all flux processes have terminated can be measured. Since each activated channel is capable of translocating a great number of cations, the presence of only a very small number of active AcChR on the vesicle surface may give rise to a full flux amplitude. The number

FIGURE 11. Plot of Carb 'dose response' of ^{22}Na efflux from pH 7.4 (A) and pH 11 treated membrane vesicles (B). Membranes were diluted into isotonic buffer containing various concentrations of Carb. The response, determined from the average of the 4 times points from the Millipore assay, was plotted against the concentration of added Carb in the solution.

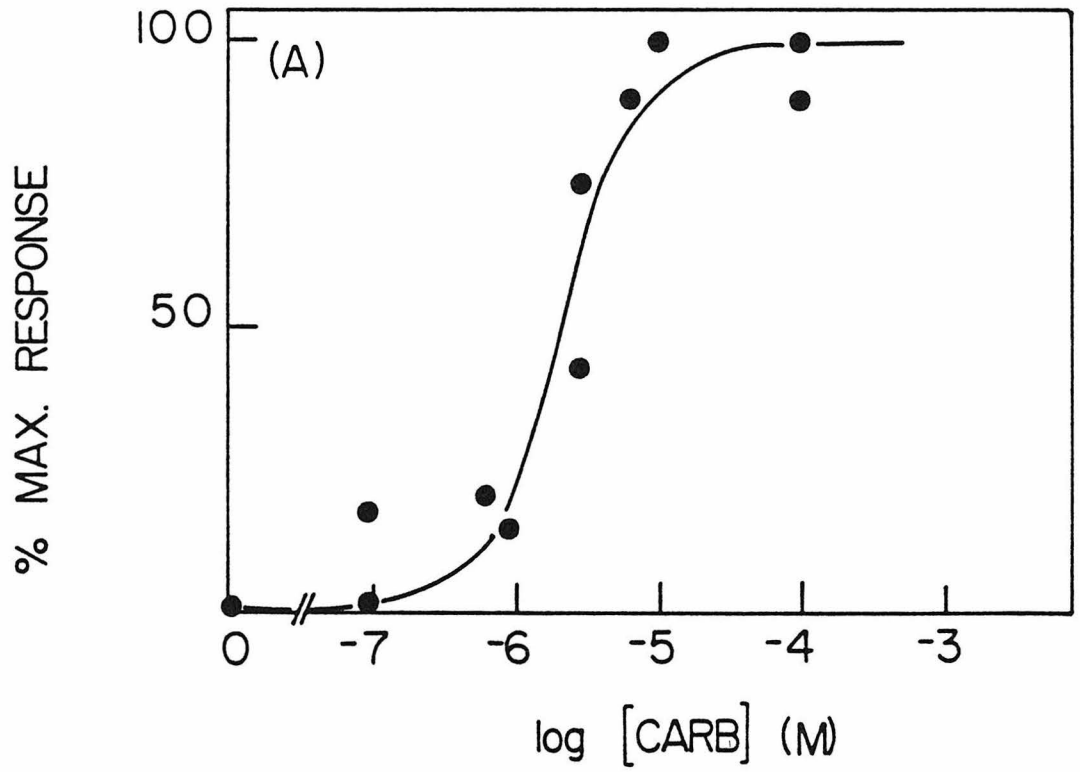
100
(A)
50
% MAX. RESPONSE
0
-7
-6
-5
-4
-3
log [CARB] (M)

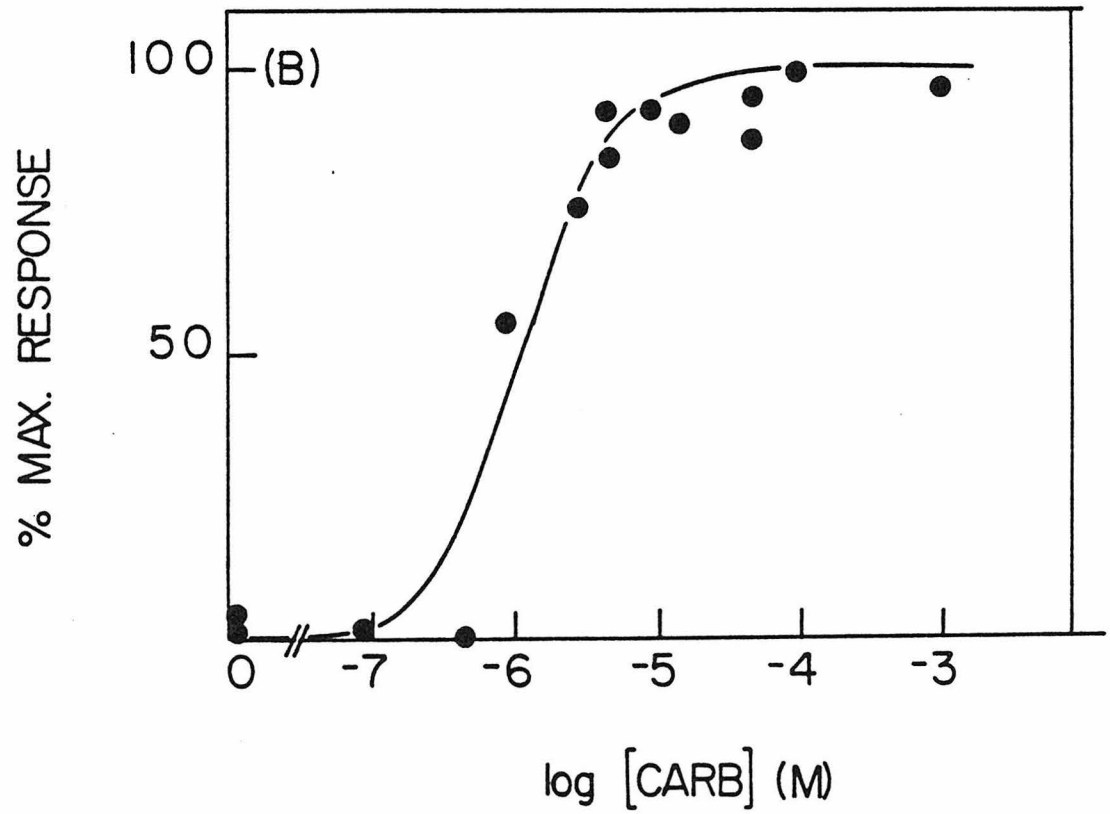
100
(B)
50
% MAX. RESPONSE
0
-7
-6
-5
-4
-3
log [CARB] (M)

of AcChR-associated channels on each vesicle may be far in excess over that required to completely empty the vesicle-entrapped $^{22}Na^{+}$. Therefore the apparently unaltered flux response in base-extracted membranes may simply be produced by a residual small fraction of 'active' polypeptides that remain after base extraction. For an unequivocal determination of the polypeptide components essential for the receptor mediated ion translocation, we have therefore carried out a more quantitative analysis of the flux response and employed a method of partial inactivation to quantitatively assess the receptor function.

Quantitative Assessment of Receptor Function by $^{22}Na^{+}$ Efflux from Partially Inactivated AcChR Vesicles

I. Theoretical Prediction of Ion Flux from AcChR Vesicles

Consider the case of a homogeneous population of AcChR vesicles equilibrated with carrier ions and with a radioactive tracer. Tracer efflux is initiated by dilution of the suspension into a large excess of isotonic buffer containing an agonist which increases the permeability to both tracer and carrier cations. The resulting ion efflux should be limited by ion transit through the open channel rather than diffusion to the pore mouth (Langer, 1976). In this case of pore-limited efflux the open channel should at all times be saturated with a combination of carrier and tracer. Tracer ion flux will be nearly unidirectional while carrier influx and efflux approximately cancel. If k is the maximal ion transport rate per open channel, and N and N_c are the number of tracer

and carrier ions, respectively, present inside a single vesicle, then the number of tracer ions transported per unit time per channel is $k\ N/(N+N_c) \approx k\ N/N_c$. The number of open channels per vesicle is $\alpha(t)\rho S$ where $\alpha(t)$ is the fraction of channels open at time t, ρ is the surface density of channels and S is the surface area. The tracer efflux rate per vesicle is thus

$$-\frac{dN}{dt} = \alpha(t)\rho Sk\,\frac{N}{N_c} \qquad (1)$$

Assuming that tracer efflux is slowed by a first order channel inactivation process with a rate constant k_i (see Discussion)

$$\alpha(t) = \alpha_0 e^{-k_i t} \qquad (2)$$

Combining Eqns. (1) and (2) and defining $k' = kS\alpha_0/N_c$

$$-\frac{dN}{dt} = k'\rho N e^{-k_i t}$$

Integrating from $t = 0$ to ∞

$$\ell n(N_\infty/N_0) = -(k'\rho/k_i)$$

Defining the flux response, R, as the fraction of tracer ions released by $t = \infty$ we have

$$R = 1 - (N_\infty/N_0) = 1 - e^{-\rho k'/k_i} \qquad (3)$$

This derivation resembles the analysis of Bernhardt and Neumann (1978) except that the involvement of carrier ions in the tracer efflux has been explicitly considered.

Effect of Partial Inactivation by α-BuTx

The effect that removal of an essential AcChR component would have on ion flux can be simulated by partially inactivating the AcChR with α-BuTx. Incubation of AcChR vesicles with α-BuTx will decrease the effective surface density of channels. The relationship between the fraction of toxin sites occupied and the inactivation of the channels will depend on the specific model (see Appendix) assumed for the α-BuTx, agonist and channel interactions. The most probable model is presented below.

T. californica AcChR is a 13.7S dimer (Raftery et al, 1972) probably with four α-BuTx sites and two high affinity agonist sites at equilibrium (Moody et al, 1973; Hamilton et al, 1977; Chang and Bock, 1977). Each dimer is considered to be a fluxing unit since HTX, which appears to interact with AcChR channels, binds with a stoichiometry of one per four α-BuTx sites (Elliott and Raftery, 1979). Affinity labeling studies indicate that two α-BuTx sites, one on each monomer, are competitive with agonists while two α-BuTx sites are independent (Damle and Karlin, 1978). Since α-BuTx binds to a single class of non-interacting sites (Quast et al, 1978), non-saturating levels of α-BuTx will be statistically distributed among the four sites associated with each channel. Electrophysiological studies indicate that two agonist molecules must bind per channel to efficiently induce the transition to the conducting form (Adams, 1975; Sheridan and Lester, 1977; Dionne et al, 1978). If 'Y' is the fraction of α-BuTx sites occupied then the fraction

of channels which remain capable of being activated by agonist can be shown to be $(1-y)^2$. The effective surface density of channels is thus

$$\rho = \rho_0(1-y)^2 \qquad (4)$$

The relationship between ion flux (Eqn. (3)) and toxin occupancy, assuming k' and k_i are not affected by partial toxin binding, thus becomes

$$R = 1-\exp(-A(1-y)^2) \quad \text{where} \quad A = \rho_0 k'/k_i \qquad (5)$$

II. Observed Cation Efflux from AcChR Membrane Preparations

In the absence of Carb, there was a $^{22}Na^+$ leakage from AcChR-enriched membrane preparations which exhibited two exponential time constants (Fig. 12, (●)). Dilution into Carb-containing buffer produced an additional rapid release of $^{22}Na^+$ (Fig. 12, (○)) within 10 sec as described earlier, followed by the two leakage components. The fast leakage component was not affected by Carb and therefore it is unlikely to be associated with functional AcChR. Vesicles which contain functional AcChR leak $^{22}Na^+$ slowly. The Carb response was determined by the final level of $^{22}Na^+$ retained at the end of the activator-induced efflux (N_∞ in Eqn. (3)). This was measured 10 min after dilution to (i) ensure that agonist-induced activation and inactivation was over and to (ii) allow complete discharge of the fast leakage component. The contribution of the slow leakage component was less than 2% during the

FIGURE 12. $^{22}Na^{+}$ Efflux from AcChR-Enriched T. californica Membrane Preparations. Vesicles equilibrated with $^{22}NaCl$ were isotonically diluted 20-fold into 0 μM (●) or 100 μM (○) Carb. Vesicle-entrapped $^{22}Na^{+}$ was determined at the indicated times after dilution. The curves can be described (——) by two single-exponential leakage components: $ae^{-.00624t} + be^{-.00001t}$ (a = 2390, b = 4260 (●) and a = 2150, b = 2450 (○)).

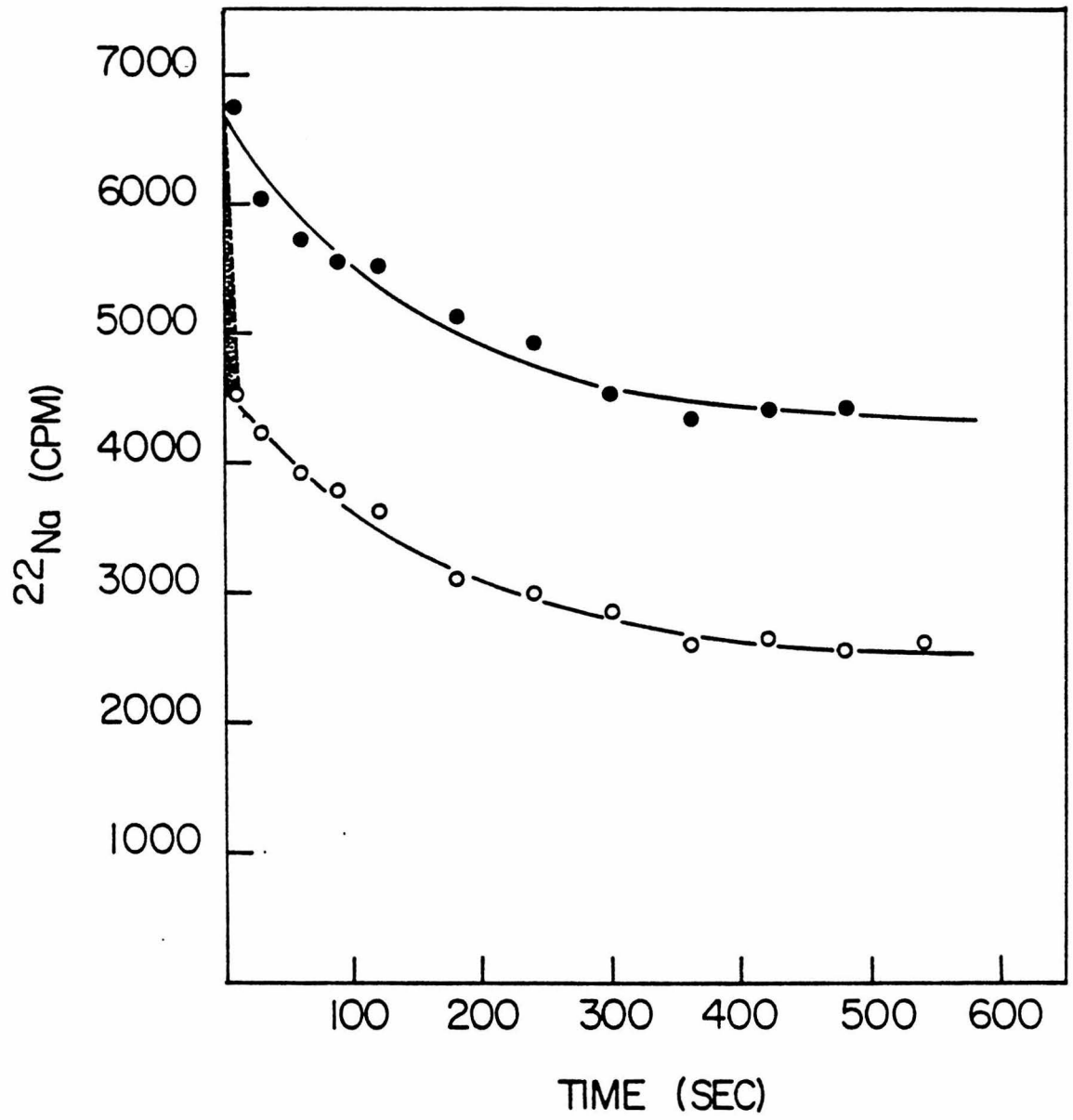
7000
6000
5000
4000
3000
2000
1000
^{22}Na (CPM)
100
200
300
400
500
600
TIME (SEC)

10 min incubation, and can be ignored. A similar method was used by Hess et al (1977) for studies on eel electroplaques except that addition of agonist was delayed until after the dilution incubation.

Effect of Partial Inactivation on the Observed Cation Efflux

We can determine the effect that removal of an essential AcChR component would have on ion flux by employing α-BuTx to partially inactivate the AcChR. It is essential that partial inactivation occurs through a random distribution of α-BuTx binding over all vesicles. Since α-BuTx binding is an irreversible process on the time scale of these experiments, the reaction was carried out under conditions which allowed complete mixing before significant binding occurred ($\leq$ 4% bound within the $\sim$3 sec required for mixing (Fig. 13). Membrane preparations from T. californica contain a single class of non-interacting α-BuTx sites (Quast et al, 1978). In the preparation used here a semilog plot of α-BuTx binding was linear up to more than 90% of the reaction (Fig. 14). Thus, the bound toxin will be homogeneously distributed over all AcChR vesicles.

$^{22}Na^{+}$ efflux experiments performed on partially toxin blocked membranes yielded response curves of the type illustrated in Fig. 15. Three response curves (no effectors, 100 μM Carb and gramicidin) were determined for each of the toxin blocked samples. Since the various toxin treated samples were washed separately before flux measurements the Carb response was normalized to the total amount of vesicle en-

FIGURE 13. Rate of [^{125}I]-α-BuTx Binding to Membranes under Conditions for Homogeneous Partial Inactivation of AcChR. Membranes were diluted to 1.15 μM in 400 mM NaCl-1mM EDTA-10mM Naphosphate, pH 7.4 and rapidly mixed with an equal volume of [^{125}I]-α-BuTx in the same buffer at t=0 to block 80% of the available sites. Formation of toxin-receptor complex was followed as described (Blanchard et al, 1979). C_t and C_∞ are the amount of complex formed at time t and ∞ respectively. C_b is the background level determined at t = 0. Under the conditions used (low toxin, receptor concentrations and high salt reaction medium) the reaction rate is sufficiently slow to allow homogeneous inactivation of the available receptor sites.

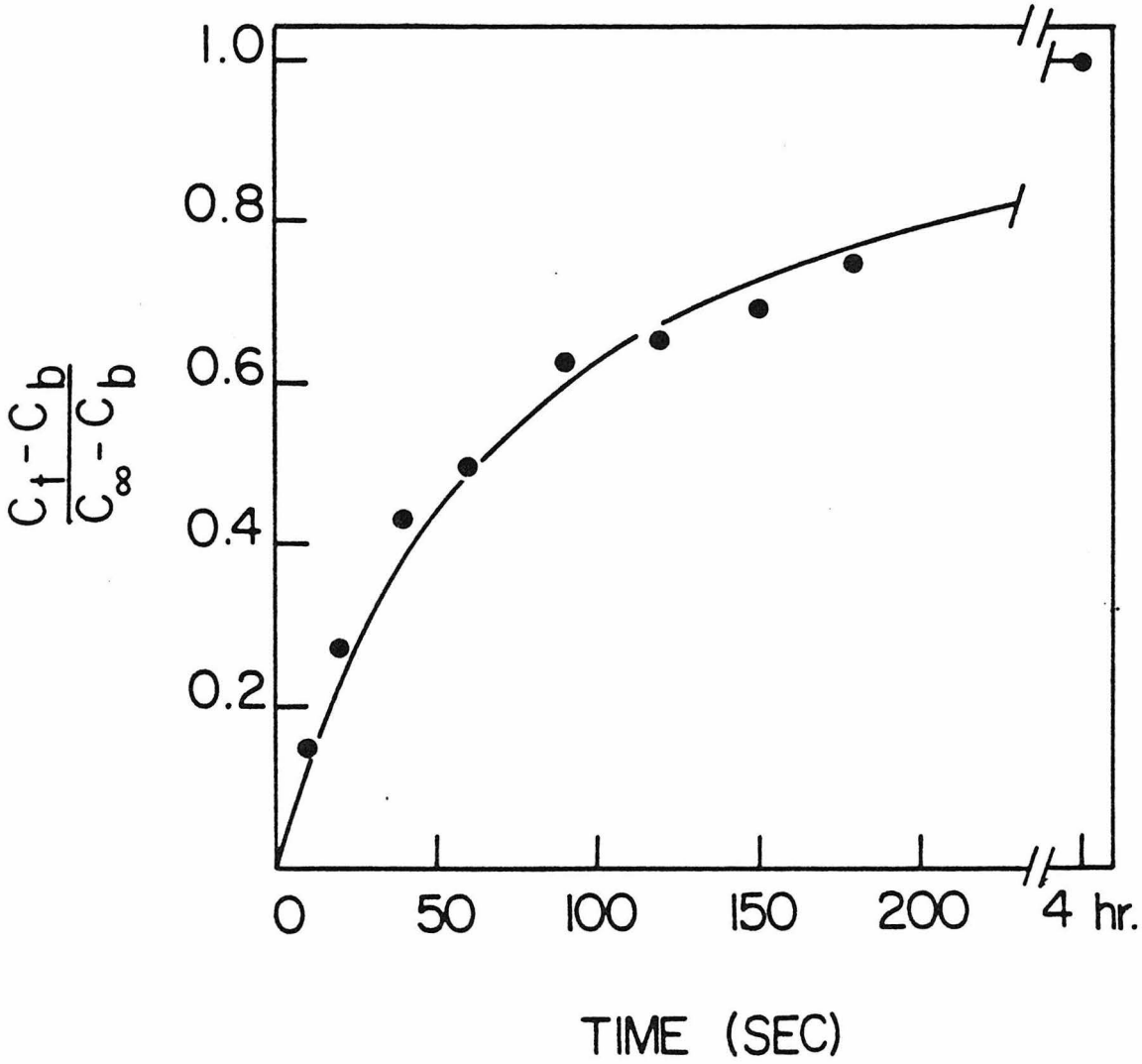
1.0
0.8
0.6
0.4
0.2
$\frac{C_t - C_b}{C_\infty - C_b}$
0
50
100
150
200
4 hr.
TIME (SEC)

FIGURE 14. Pseudo First Order Reaction of ^{125}I -α-BuTx with Membrane-bound AcChR. AcChR-enriched membranes (0.5 μM in α-BuTx sites) in 400 mM NaCl-1 mM EDTA-10mM Naphosphate, pH 7.4 were allowed to react with a large excess of [^{125}I]-α-BuTx (5 μM). A semilog plot of the formation of toxin-receptor complex vs reaction time is linear up to at least 92% completion of the reaction. Definitions of C_t, C_∞ and C_b are the same as in the legend to Figure 13.

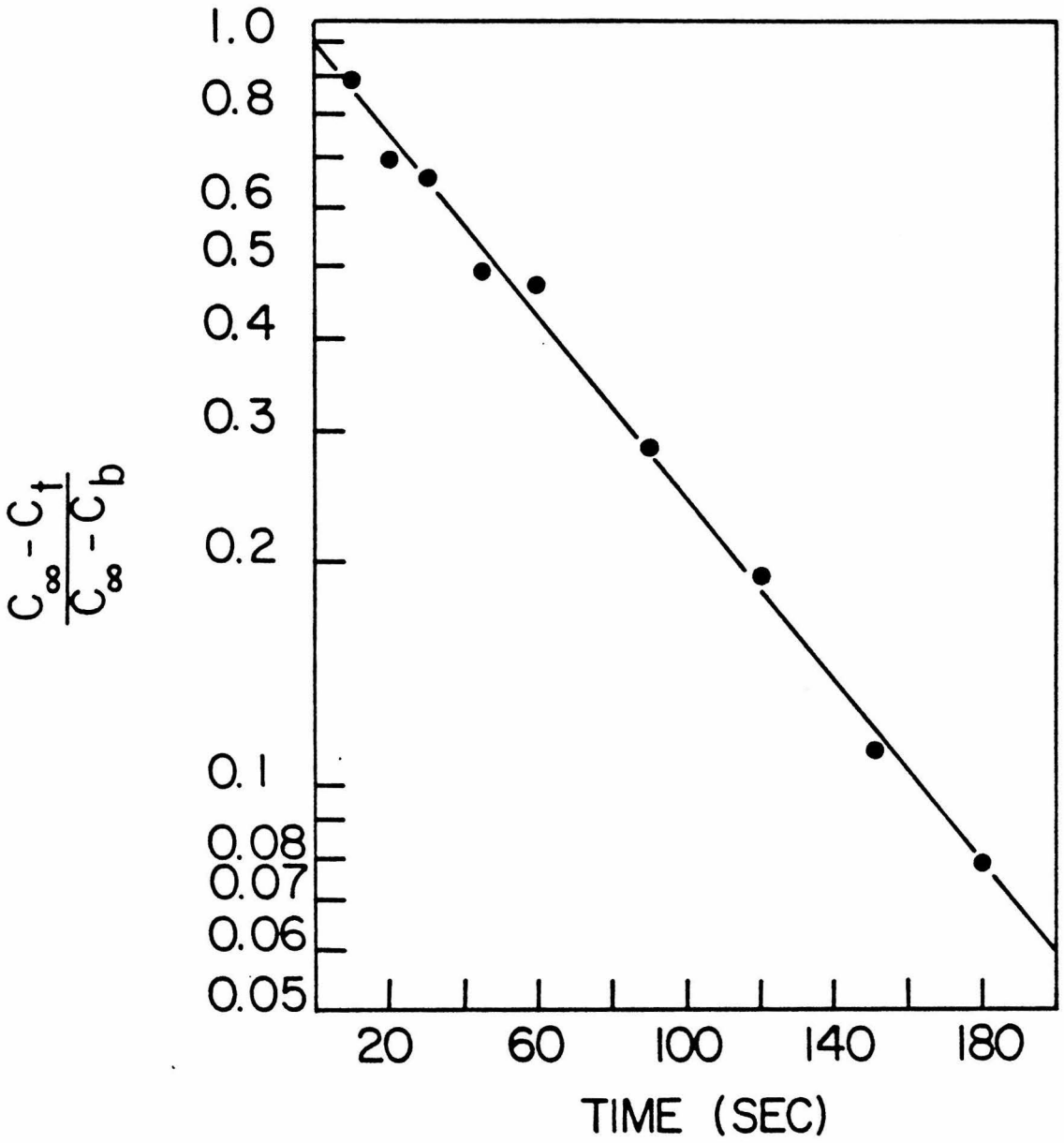
1.0
0.8
0.6
0.5
0.4
0.3
0.2
0.1
0.08
0.07
0.06
0.05
20
60
100
140
180
TIME (SEC)
$\frac{C_s - C_t}{C_s - C_b}$

FIGURE 15. $^{22}Na^{+}$ Efflux from AcChR-Membrane Preparations Partially Inactivated by α-BuTx. Membranes treated with various amounts of α-BuTx were loaded with $^{22}Na^{+}$ as described in experimental section. Flux assays were started 10 min after isotonic dilution into buffers containing 0 μM Carb (●), 100 μM Carb (○) or 5 μg/ml gramicidin (□). For a given sample, a flux amplitude was determined from the ratio of $^{22}Na^{+}$ released by Carb to that released by gramicidin.

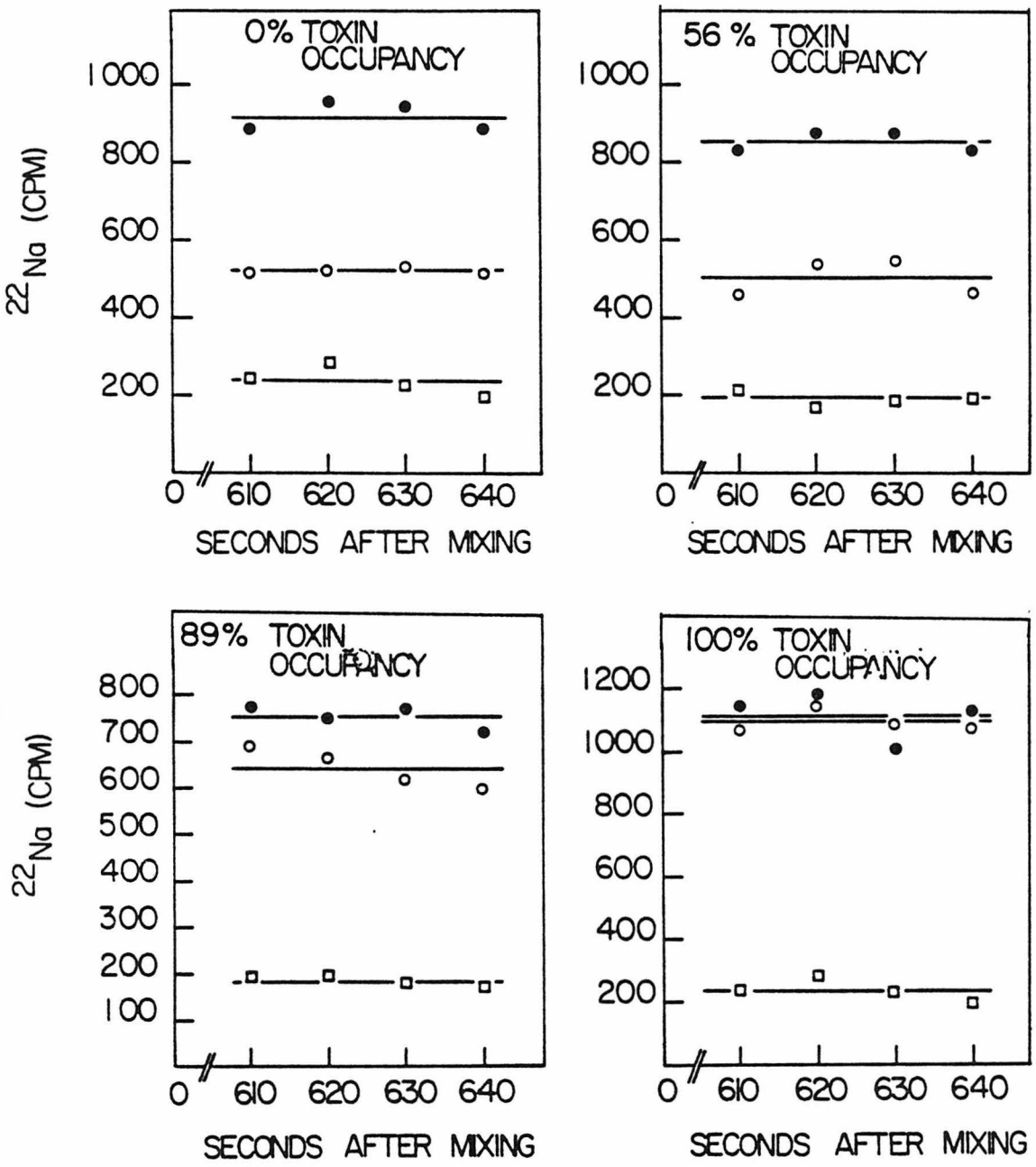
0% TOXIN OCCUPANCY
56 % TOXIN OCCUPANCY
89% TOXIN OCCUPANCY
100% TOXIN OCCUPANCY
^{22}Na (CPM)
SECONDS AFTER MIXING
0
610
620
630
640
200
400
600
800
1000
1200
100
300
500
700

trapped $^{22}Na^{+}$, which is the amount released by gramicidin. The difference between the response to Carb and that to gramicidin at 0% toxin occupancy is most likely due to vesicles which do not contain functional AcChR.

The Carb-induced $^{22}Na^{+}$ efflux responses of several AcChR membrane preparations (Fig. 16 (□)) were plotted as a function of the degree of toxin occupancy. Since the fraction of vesicles devoid of functional AcChR may vary from preparation to preparation, the flux responses of the various toxin blocked samples were normalized to the maximal response of that preparation. The plateau region of the curve indicates the presence of excess receptors over those necessary to completely empty the entrapped $^{22}Na^{+}$. As the fraction of occupied toxin sites increased to over 70%, the remaining receptors were no longer sufficient to empty the entrapped $^{22}Na^{+}$ before they were inactivated, resulting in a decreased flux response. The theoretical predictions of Eqn. (5) fit the data well with A = 37 (Fig. 16, (——)).

These results allow us to predict the effect that partial removal of an essential AcChR component would have on the flux response. For instance, removal of 98% of an essential AcChR component (one per channel) would result in a 98% reduction of the effective surface density of channels and hence of the "A" value in Eqn. (5). Substituting A=0.74 in Eqn. (5), we obtain the predicted flux dependence (Fig. 16 (---)). The predicted line shape deviates drastically from that for native membranes and drops off at much lower levels of toxin occupancy because

FIGURE 16. Effect of Partial Inactivation on the Carb-Induced $^{22}Na^+$-Efflux. The flux amplitudes, as determined in Fig.15, were expressed in percent maximum response for base treated (■) or untreated (□) membranes and plotted as a function of the fraction of α-BuTx sites occupied. The data were fitted by a non-linear least squares program to the normalized form of Eqn. (5) ($R = (1-\exp(-A(1-y)^2))/(1-\exp(-A))$) yielding an A value of 37.4 (——). The flux response predicted for a preparation in which 98% of the channels have been inactivated (Eqn. (5), A = 0.02x37.4 = 0.74) is shown as (---). The top legend represents the fraction of channel blocked at a given toxin occupancy (Eqn. (4)) for the model considered in the text. The flux amplitude at 0% toxin occupancy was normally 80-90% of the total entrapped $^{22}Na^+$ for base-extracted membranes and 40-60% for untreated membranes.

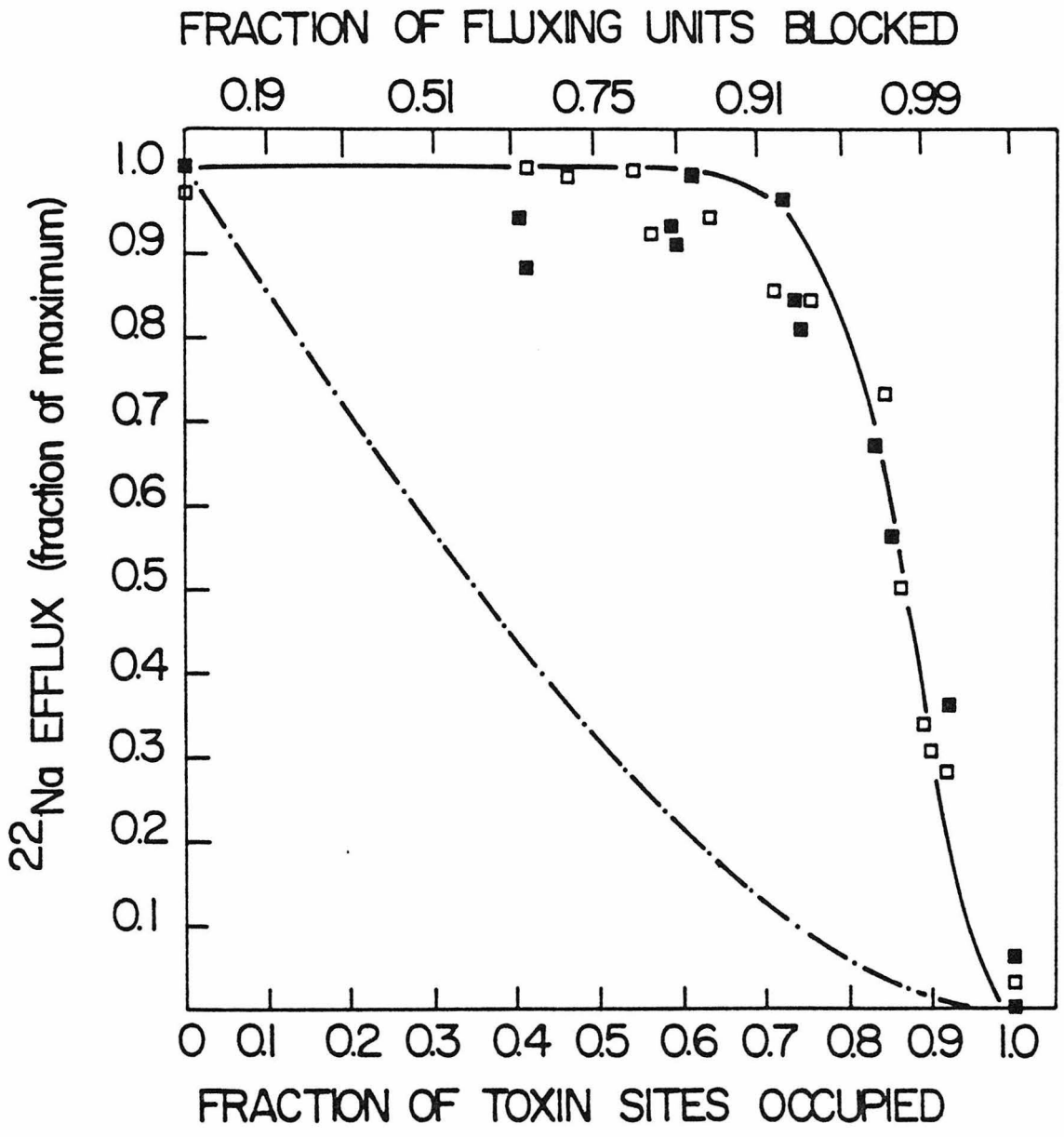
FRACTION OF FLUXING UNITS BLOCKED
0.19
0.51
0.75
0.91
0.99
1.0
0.9
0.8
0.7
0.6
0.5
0.4
0.3
0.2
0.1
^{22}Na EFFLUX (fraction of maximum)
0
0.1
0.2
0.3
0.4
0.5
0.6
0.7
0.8
0.9
1.0
FRACTION OF TOXIN SITES OCCUPIED

the number of excess receptors is greatly reduced. In addition, such a preparation should also exhibit a decreased flux amplitude at zero toxin occupancy. Since the relationship between the degree of toxin occupancy and channel inactivation is not linear (Eqn. (4)), the flux response of a toxin-free preparation in which 98% of the channels have been inactivated should be equivalent to that of an 86% toxin blocked membrane (Fig. 16). Such a preparation should never release more than 50% of the entrapped $^{22}Na^{+}$ (Fig. 16).

Neither of the results predicted above (line shape nor amplitude) were observed with the base extracted membranes from which over 98% of the 43,000 M_r, 90,000 M_r and other polypeptides were removed (Fig. 17). An almost superimposable dependence of the flux response on the degree of toxin occupancy was observed for the untreated (□) and the base extracted (■) membranes (Fig. 16). Furthermore, we frequently observed release of over 85% of the entrapped $^{22}Na^{+}$ of the base-extracted membrane vesicles. Therefore, the 43,000 M_r, 90,000 M_r and the many other polypeptides which were removed in excess of 90% during the base treatment are not essential for receptor-mediated ion translocation.

FIGURE 17. Densitometer scans of Coomassie Brilliant Blue-stained sodium dodecyl sulfate polyacrylamide gels of membranes before (---) and after (——) base extraction.

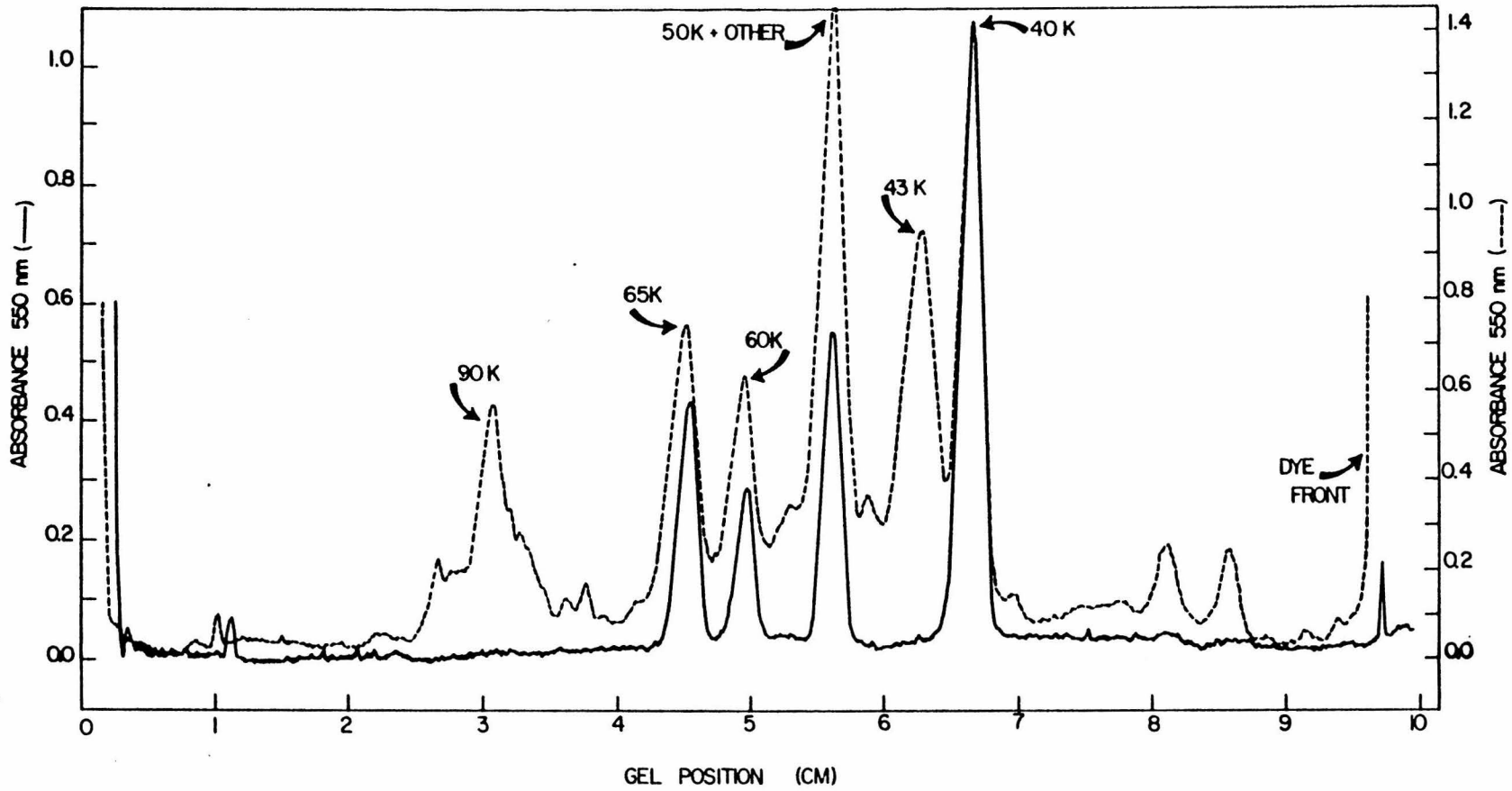
50K + OTHER
40 K
43 K
65K
60K
90 K
DYE FRONT
ABSORBANCE 550 nm (——)
ABSORBANCE 550 nm (- - - -)
GEL POSITION (CM)
0.0
0.2
0.4
0.6
0.8
1.0
1.2
1.4
0
1
2
3
4
5
6
7
8
9
10

DISCUSSION

We observed a rapid cation efflux from Torpedo californica electroplaques membrane vesicles in which the flux was complete before the first time point was taken at 10 seconds. This rapid flux signal represents a considerable increase in vesicle flux rates over those previously reported (minute range) for AcChR vesicles (Kasai and Changeux, 1971a; Hess et al, 1976; Andreasen and McNamee, 1977; Schiebler and Hucho, 1977). The observed amplitude changes are related to the in vivo postsynaptic permeability control since they exhibit the appropriate pharmacological specificities. The rapidity of the efflux process lends further credence to the notion that the observed effects are truly related to the physiological response which in vivo occurs on a time scale of milliseconds.

In a recent study of ^{22}Na efflux from Electrophorus electricus membrane vesicles Hess et al (1978) observed a rapid response to the agonist Carb. This response was found to be dependent, however, on the presence of potassium chloride inside and sodium chloride outside of the membrane vesicles. For the fast response described here we do not find this to be the case.

At low ligand concentrations a slow flux component visible on the time scale of seconds might be expected. This was not observed. Instead changes in the final amplitude of the flux signal were observed at low agonist concentrations. This indicates that desensitization may have

occurred before the decreased flux rate could empty the vesicle of its contents. The results obtained after preincubation with Carb (Figure 3B) support the notion that inactivation of flux occurred as a result of interaction with the ligand. Taken together, the data of Lee et al (1977), Quast et al (1978) and the results presented in Figure 3B support the idea that ligand-induced inactivation of response and increased ligand affinity may both represent manifestations of desensitization.

The slow sampling of the filtration technique severely limits kinetic measurements of the rapid flux processes. The flux signal, measured as a time-integrated amplitude of $^{22}Na^{+}$ release, is not linearly proportional to the number of active AcChR-associated channels and cannot be used directly as a quantitative measure of receptor function. Partial inactivation of AcChR by α-BuTx, on the other hand, provides a method to assess the size of the active receptor population in a given preparation without directly measuring the ion flux rate. By analyzing the flux amplitudes in a series of increasingly inactivated AcChR vesicles, the receptor function in two preparations can be quantitatively compared.

The flux signals produced by the base-extracted membranes and untreated membranes have been examined by this method. The relationship between toxin occupancy and channel inactivation depends on the specific model assumed for the Carb, toxin and channel interactions. In Results we have assumed a probable model based on current knowledge and five additional models are presented in the Appendix. All six models lead

to the same conclusion: removal of a large fraction of an essential AcChR component would drastically alter the vesicle flux-toxin occupancy response curve. Base extraction removes over 98% of the 43,000 M_r, 90,000 M_r and certain other popypeptides without altering the curve shape. Thus, these polypeptides do not appear to be essential for AcChR mediated ion translocation. In addition, five of the six models require that no more than 50% of the entrapped $^{22}Na^+$ would be released by agonist following 98% inactivation of channels. Base treated, toxin-free membranes depleted to >98% of nonreceptor peptides release over 85% of the entrapped $^{22}Na^+$, in support of our interpretation.

As discussed earlier, incomplete emptying of vesicle-entrapped $^{22}Na^+$ is indicative of the presence of a time-dependent channel inactivation process which terminates the flux. We have assumed a single exponential inactivation process which is consistent with any model in which a single overall rate constant dominates, such as the two state model of Katz and Thesleff (1957). In our analysis of the flux response this inactivation rate constant was assumed to be unaffected by base extraction. As demonstrated previously (Neubig et al, 1979; Elliott et al, 1980), base treatment does not alter the desensitization rate significantly. We have also assumed that fluxing vesicles are approximately homogeneous in size. In negative staining electron micrographs both base treated and untreated membranes show a relatively homogeneous field of large AcChR vesicles (Strader and Raftery, unpublished).

The presence of a plateau region in the vesicle flux-toxin occupancy response curve (Fig. 16) indicates the presence of excess AcChR over that necessary to release all entrapped $^{22}Na^{+}$. Taking a probable toxin-Carb-channel model as presented in Results, a drop-off in the flux response occurs after approximately 95% (see Fig. 16, top legend) of the channels have been inactivated. Thus, 95% of the channels remain silent in current ion flux assays. Obviously, any interpretation of vesicle flux experiments measured by amplitudes must be approached cautiously due to this population of excess AcChR channels. In recent work by Neubig et al (1979) removal of approximately 85% of the 43,000 M_r polypeptide by base extraction was shown to have no effect on the flux response. Assuming their Torpedo vesicles resemble our preparation, we would predict that this extraction would have no effect on flux amplitudes (see Fig. 16) even if the 43,000 M_r polypeptide were an essential AcChR component. Such flux amplitude studies yield only qualitative information, as noted by Neubig et al (1979).

At this time, the size of the excess AcChR channel population is still uncertain. In the alternative models presented in the Appendix, "A" values ranging from 3 to 2000 were obtained which lead to predictions of excess AcChR channel populations of less than 25% to over 99.9% of the total. Future verification of a single model will permit an exact determination of the excess AcChR channel population.

APPENDIX

The Relation of Ion Flux Amplitude to the Extent of Partial Inactivation by α-BuTx

We consider that the AcChR is a dimer with two α-BuTx sites (α and β) per monomer. Agonists bind to half the number of α-BuTx sites, presumably one to each monomer. The relationship between channel blockage and toxin site occupation depends on (i) the competition between Carb and toxin binding and (ii) whether one or two agonists are required to activate a channel.

Three possible models similar to those described by Damle and Karlin (1978) were considered for the Carb-toxin interaction. In these models each monomer is considered an independent unit for Carb and toxin binding.

MODEL I: Carb binds only to one of the two monomer sites, say site α. Binding of toxin to this site (α) inhibits Carb binding but binding of toxin to the other monomer site (β) has no effect on Carb binding.

MODEL II: Carb can bind to either of the two monomer sites (α or β) and binding to one site strongly inhibits further Carb binding to the same monomer by negative cooperativity. The occupation of both monomer sites (α and β) by toxin is required to inhibit Carb binding to the monomer.

MODEL III: Carb can bind to either site (α or β) of the monomer. When either (α or β) or both (α and β) of the sites are occupied by toxin, Carb can no longer bind to the monomer.

These models combined with the assumption that one or two agonists bound per dimer are necessary to activate a channel yielded the six cases considered in Table I. The fraction of potentially active channels (ρ/ρ_0) after partial inactivation is presented in Table I for these six cases. All six cases fit the experimental data reasonably well (Fig. 18), yielding "A" values ranging from 0.85 to 2000 (see Table I). Case 4 can be eliminated because the fitted "A" value predicts that no more than 57% of the entrapped $^{22}Na^+$ can be released at 0% toxin occupancy which is inconsistent with the observed flux (see Fig. 16).

For the remaining five cases, 98% inactivation of channels would reduce the "A" value by 98% and lead to theoretical predictions of a vesicle flux-toxin occupancy curve which deviates strongly from the observed response of base extracted membranes. Thus, the same conclusion is reached regardless of the case assumed. Base extraction, which substantially removes polypeptides of 43,000 M_r and 90,000 M_r does not affect AcChR-mediated ion flux.

Note that if the number of ligand sites is the same as that of α-BuTx at two per monomer, similar equations can be derived and the same conclusions will hold.

TABLE I

CARB-TOXIN-CHANNEL INTERACTION MODELS

The fraction of potentially active channels (ρ/ρ_o) remaining after partial toxin blockage was determined for each of the six cases as a function of y, the fraction of toxin sites occupied. This expression was substituted in Eqn. (3) and a least squares fit to the experimental data yielded the "A" values presented *. For each model we considered the case where two Carb molecules per dimer are needed to open the channel (RL_2 fluxes) and the case where either one or two Carb molecules can fully activate the channel (RL and RL_2 flux).

CASE	MODEL	$\rho(y)/\rho_o$	$A = \rho_o k'/k_i$
CASE 1	MODEL I - RL_2 FLUXES	$(1-y)^2$	37.4
CASE 2	MODEL I - RL, RL_2 FLUX	$1-y^2$	3.0
CASE 3	MODEL II - RL_2 FLUXES	$(1-y^2)^2$	10.9
CASE 4	MODEL II - RL, RL_2 FLUX	$1-y^4$	0.85
CASE 5	MODEL III - RL_2 FLUXES	$(1-y)^4$	1947.0
CASE 6	MODEL III - RL, RL_2 FLUX	$2(1-y)^2 -(1-y)^4$	18.9

* It is assumed that α stays fairly constant under the experimental conditions and only the ρ dependence on y was considered.

FIGURE 18. Analysis of the Flux Response in Partially Toxin-Inactivated AcChR Vesicles by the Various Carb-Toxin-Channel Interaction Models. The data in Fig. 16 were fitted to the various models for Carb-toxin-channel interactions described in Table I. (A) (——) Case 3, (---) Case 1, (-·-) Case 2, (B) (——) Case 6, (---) Case 5, (—·—) Case 4. Most of the models fit the data reasonably well and cannot be distinguished by the present data.

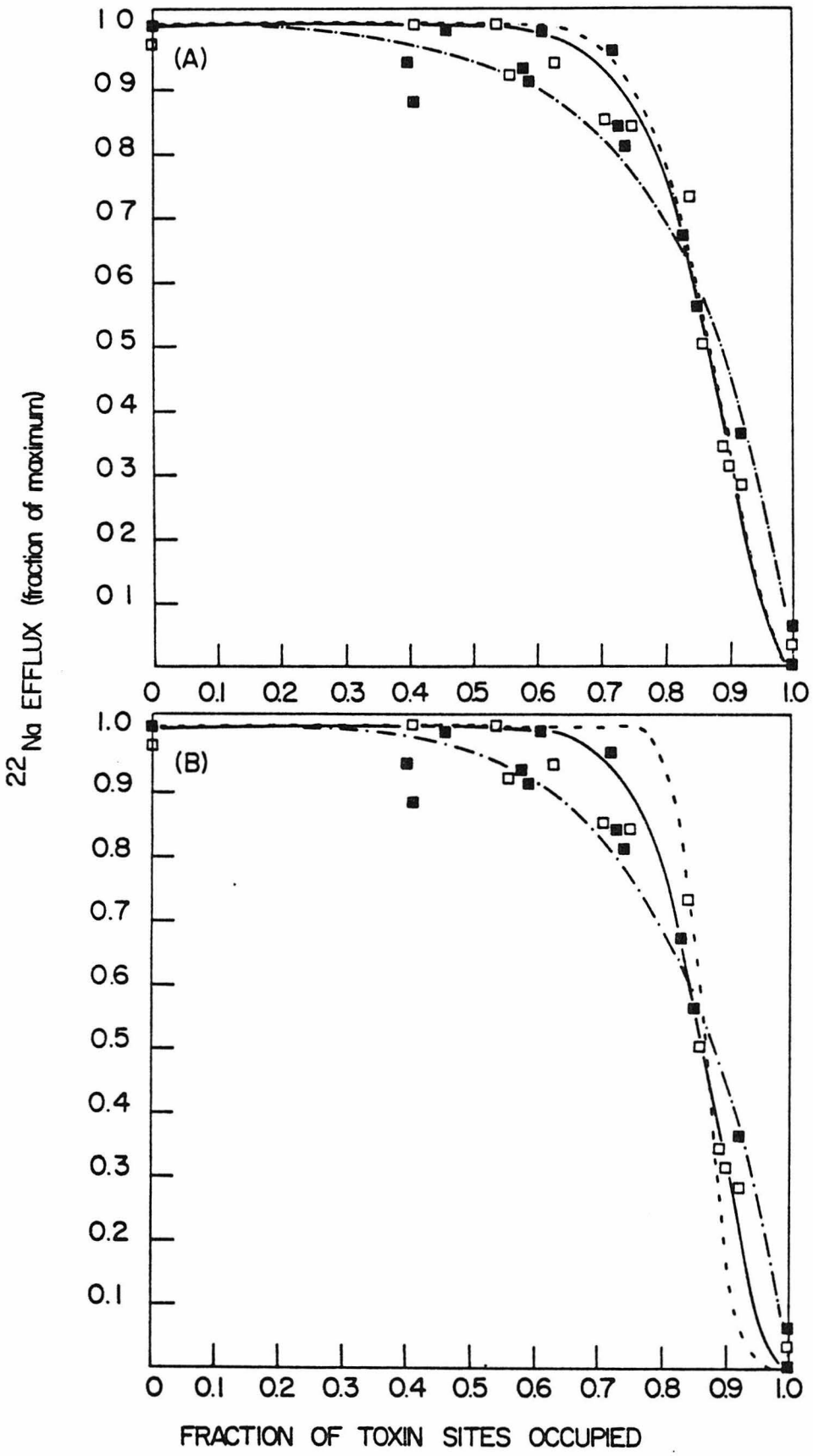
(A)
(B)
^{22}Na EFFLUX (fraction of maximum)
FRACTION OF TOXIN SITES OCCUPIED
0
0.1
0.2
0.3
0.4
0.5
0.6
0.7
0.8
0.9
1.0

REFERENCES

1. P. R. Adams (1975) Pflügers Arch. 360, 145.
2. T. J. Andreasen and M. G. McNamee (1977) Biochem. Biophys. Res. Commun. 79, 958.
3. J. Bernhardt and E. Neumann (1978) Proc. Natl. Acad. Sci. 75, 3756.
4. S. G. Blanchard and M. A. Raftery (1979) Proc. Natl. Acad. Sci. 76, 81.
5. H. W. Chang and E. Bock (1977) Biochemistry 16, 4513.
6. V. N. Damle and A. Karlin (1978), Biochemistry 17, 2039.
7. V. E. Dionne, J. H. Steinback, and C. F. Stevens (1978), J. Physiol. 281, 421.
8. J. Elliott and M. A. Raftery (1979) Biochemistry 18, 1868.
9. J. Elliott, S. M. J. Dunn, S. Blanchard, and M. A. Raftery (1979), Proc. Natl. Acad. Sci. 76, 2576.
10. J. Elliott, S. Blanchard, W. C.-S. Wu, J. Miller, C. Strader, P. Hartig, H.-P. H. Moore, J. Racs, and M. A. Raftery (1979) Biochem. J. 185, 667.
11. S. L. Hamilton, M. McLaughlin and A. Karlin (1977) Biochem. Biophys. Res. Commun. 79, 692.
12. G. P. Hess, J. P. Andrews, and G. E. Struve (1976), Biochem. Biophys. Res. Commun. 69, 830.

13. G. P. Hess and J. P. Andrew (1977) Proc. Natl. Acad. Sci. 74, 482.

14. G. P. Hess, S. Lipkowitz, and G. E. Struve (1978), Proc. Natl. Acad. Sci. 75, 1703.

15. M. Kasai and J.-P. Changeux (1971a), J. Mem. Biol. 6, 1.

16. M. Kasai and J.-P. Changeux (1971b), J. Mem. Biol. 6, 58.

17. B. Katz and S. Thesleff (1957), J. Physiol. 138, 63.

18. P. Lauger (1976), Biochimica et Biophysica Acta 455, 493.

19. T. Lee, V. Witzemann, M. Schimerlik, and M. A. Raftery (1977), Arch. Biochem. Biophys. 183, 57.

20. O. H. Lowry, N. J. Rosenbrough, A. Farr, and R. J. Randall (1951), J. Biol. Chem. 193, 265.

21. J. Miller, V. Witzemann, U. Quast, and M. A. Raftery (1979), Proc. Natl. Acad. Sci. 76, 3580.

22. T. Moody, J. Schmidt, and M. A. Raftery (1973) Biochem. Biophys. Res. Commun. 53, 761.

23. R. R. Neubig, E. K. Krodel, N. D. Boyd, and J. B. Cohen (1979), Proc. Natl. Acad. Sci. 76, 690.

24. U. Quast, M. Schimerlik, T. Lee, V. Witzemann, S. Blanchard, and M. A. Raftery (1978) Biochemistry 17, 2405.

25. M. A. Raftery, J. Schmidt, and D. G. Clark (1972), Arch. Biochem. Biophys. 152, 882.

26. M. A. Raftery, R. L. Vandlen, K. L. Reed, and T. Lee, Symp. on Quant. Biol. XL, Cold Spring Harbor Laboratory, Cold Spring

Harbor 193 (1976).

27. W. Schiebler, L. Lauffer and F. Hucho (1977), FEBS Letters 81, 39.

28. J. Schmidt and M. A. Raftery (1973), Anal. Biochem. 12, 349.

29. R. E. Sheridan and H. A. Lester (1977), J. Gen. Physiol. 70, 187.

30. A. Sobel, T. Heidmann, J. Hofler, and J.-P. Changeux (1978), Proc. Natl. Acad. Sci. 75, 510.

31. T. L. Steck and J. Yu (1973), J. Supramolecular Struct. 1, 220.

32. V. Witzemann and M. A. Raftery (1978) Biochem. Biophys. Res. Commun. 81, 1025.

CHAPTER FOUR

Rapid Cation Translocation in *Torpedo* Membrane Vesicles: II. Spectroscopic Studies on a Time Scale of Physiological Relevance

INTRODUCTION

It is evident from the discussion in Chapter 3 that biochemical studies of the structure and function of the excitable membranes require methods to measure biological activities *in vitro*. The conventional $^{22}Na^{+}$ flux measurements (Kasai and Changeux, 1971; Chapter 3) have been widely used for such purposes and have provided useful information on the functionality of biochemical preparations of AcChR. In the initial study by Kasai and Changeux (1971) a large discrepancy between the *in vivo* response time and that measured *in vitro* was revealed by this method; the efflux process in the *Electrophorus* membrane preparations occurs on a time scale of minutes, and is at least 10^5 slower than the physiological response which occurs over 1-2 milliseconds. This finding is important since it raises the possibility that the biochemical preparations may be functionally damaged during the isolation procedure and may have an altered structure compared to that of the native AcChR.

Recently advances in preparation techniques have been made and membrane vesicles which exhibit a flux response to agonists faster than 10 sec have been obtained (Chapter 3). Using membrane preparations derived from *Electrophorus*, Hess *et al* (1978) observed a rapid efflux component, induced by Carb, which is present only when the ion compositions on either side of the vesicle membrane are asymmetric. The kinetics of these rapid ion flux processes were, however, too fast to be resolved by the filtration technique and thus could not

be compared with the response in vivo. Furthermore, the lack of kinetic data prevents a detailed analysis of the mechanism for receptor function and complicates the quantitation of AcChR activity in the membrane preparations (see Chapter 3).

In the studies described here we have therefore developed a spectroscopic method to study AcChR-mediated ion translocation on the time scale achievable by stopped-flow spectroscopy. The spectroscopic method involves rapid mixing in a stopped-flow spectrometer of a fluorescence quencher, thallium (I) (the cation to be transported), with AcChR membrane vesicles entrapping a fluorophore. The Tl^+ ion possesses two distinctive properties which make it ideal for our purposes. First it is of similar ionic radius to K^+ and can be used as a substitute for K^+ ions in many membrane systems (Mullins and Moore, 1960; Landowre, 1975). For instance, it is actively transported in red blood cells (Behring and Hammond, 1964), and it is permeable through the excitable Na and K channels of nerve membranes (Hille, 1972, 1973). More recently it has been shown that Tl^+ effectively permeates AcChR-associated channels of the neuromuscular junctions (B. Hille, personal communication). Secondly, Tl^+ is a strong fluorescence quencher, presumably due to the heavy atom effect (Kasha, 1952; Parker, 1968). By placing a fluorophore on one side and Tl^+ on the other side of the membrane, ion transport through AcChR-associated channels can be studied by fluorescence quenching as Tl^+ moves across the membrane in response to an agonist to reach the fluorophore. The flux can be

initiated by rapid mixing of the AcChR vesicle with a cholinergic agonist and monitored in a commercially available stopped-flow spectrometer.

This method allows quantitative study of AcChR-mediated cation transport *in vitro* on the physiologically relevant time scale of a few milliseconds. It furthermore allows us to conclude that the AcChR protein complex of four homologous polypeptides (Raftery *et al*, 1980) constitutes the physiological receptor in its entirety and that this receptor has been isolated as a biochemical preparation with its physiological functionality intact.

EXPERIMENTAL

AcChR Membrane Preparations

AcChR-enriched membrane vesicles were purified from homogenates of Torpedo californica electroplaques by sucrose-density gradient centrifugation in a reorienting rotor as described in Chapter 2. Unless otherwise specified, these membranes were routinely subjected to alkaline-extraction to yield highly purified AcChR membrane preparations (Neubig et al, 1979; Elliott et al, 1979; Chapter 3). The purified membranes were suspended in 10 mM Na Hepes, pH 7.4 at 20-40 μM α-BuTx sites.

Loading of Fluorophore Within the Vesicles by Freeze-thaw Cycles

Membrane vesicles were loaded with the fluorescent probe, 8-amino-1,3,6-naphthalenetrisulfonate (ANTS, Chem. Services) by the freeze-thaw method (Chapter 2) as follows. 1 ml of 25 mM ANTS (Na salt) in 10 mM Na Hepes, pH 7.4 was mixed with 0.5 ml of membrane vesicles at $4^{o}C$ and the tube containing the mixture was quickly immersed in a liquid nitrogen bath for 3-5 minutes. The frozen mixture was allowed to thaw gradually in a stirred ice-water bath over a period of 1/2 to 1 hour. The above freeze-thaw cycle was repeated twice more on the same mixture. External ANTS molecules were then separated from the loaded vesicles by passing the mixture through a Sephadex G-25 gel filtration column (1.7x24 cm, coarse resin) equilibrated with 35 mM $NaNO_3$ mM Na Hepes, pH 7.4 at room

temperature. Membrane vesicles eluted in the void volume and were collected and used without further dilution (1.2 - 1.9 μM α-BuTx sites).

Measurement of Ion Flux by Fluorescence

Fast kinetic measurements of Tl^+ flux through the vesicle membrane were obtained using a Durrum Stopped-flow Photometer, Model D-110, set up in fluorescence mode and operating with a 75-W Xenon lamp for excitation at 370 nm. Ion flux was initiated by rapid mixing (machine dead time ~2.5 ms) of a suspension of ANTS-vesicles with an equal volume of 35 mM $TlNO_3$-10 mM Na Hepes, pH 7.4 containing a nicotinic agonist and/or antagonist at 25 ± 1°C. Fluorescence emission was monitored using a Corning C.S. 3-72 filter (50% transmission at 455 nm). The apparatus was connected to a Tektronix 5103N storage oscilloscope for visual monitoring of the data, and to a Biomation Model 805 Transient Recorder and a Digital Equipment Corporation Minc Computer for data storage and analysis as described elsewhere (Dunn et al, 1980).

Fluorescence spectra were recorded on a Perkin-Elmer MPF-4 Fluorescence Spectrometer. H_{10}-HTX was a generous gift of Richard Cherpeck and Dr. D. Evans.

RESULTS

Choice of Fluorophore and Quenching by Thallium (I)

We use a highly hydrophilic fluorophore, 8-amino-1,3,6-naphthalene-trisulfonate (ANTS, Scheme 1) as the fluorescent probe for spectroscopic study of Tl^+ permeation. Figs. 1A and 1B show the excitation and emission spectra of ANTS. Since the ion flux signal is generated by Tl^+ quenching of free fluorophore molecules present on one side of the vesicle membrane, it is important to minimize both the membrane permeability of the fluorophore and its insertion into the bilayer. Unlike most fluorophores, the highly charged ANTS offers two advantages. First it is impermeable to the vesicle membrane (data shown below) and secondly it does not bind or insert into the membrane bilayer significantly as judged by the following experiments. No spectral shift or intensity changes in ANTS fluorescence was observed upon addition of membrane vesicles; alterations of the dielectric constant of the medium is generally accompanied by spectral changes. Furthermore, incubation of ANTS with membrane vesicles and subsequent removal of membranes by centrifugation did not reduce the fluorescence intensity of the solution; indicating that very few, if any, of the fluorophore molecules had bound to the membranes.

ANTS exhibited broad excitation and emission spectra, with maxima at 370 nm and 515 nm, respectively (Figs. 1A, 1B). The fluorescence was effectively quenched by addition of Tl^+ (Fig. 2A). The quenching

SCHEME 1. Molecular Structure of 8-amino-1,3,6-naphthalenetrisulfonate (ANTS)

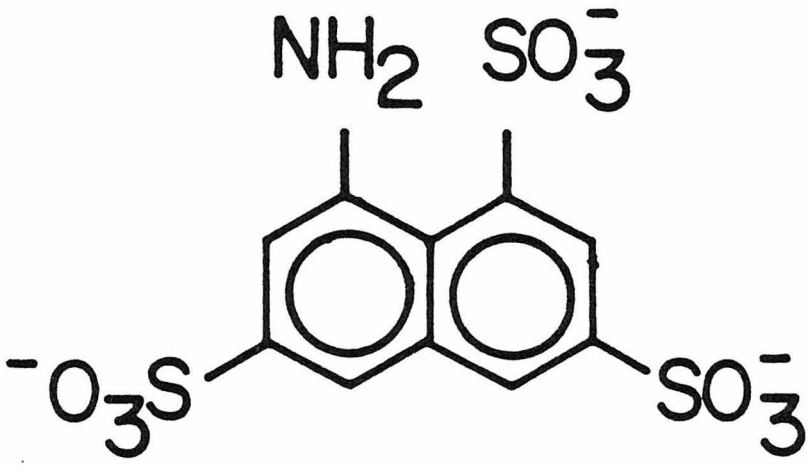

ANTS

FIGURE 1. (A) Excitation and (B) Emission Spectra of ANTS.

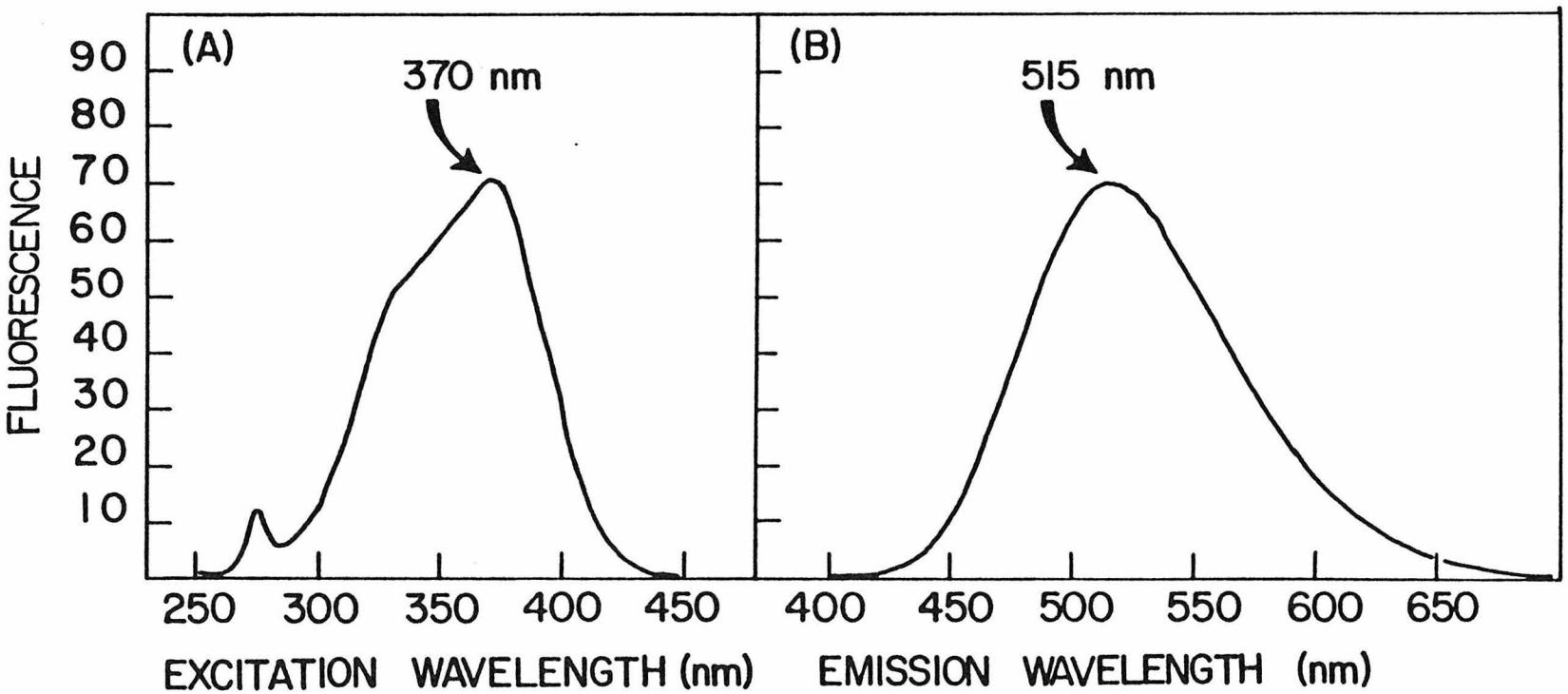
(A)
370 nm
(B)
515 nm
FLUORESCENCE
90
80
70
60
50
40
30
20
10
250 300 350 400 450
EXCITATION WAVELENGTH (nm)
400 450 500 550 600 650
EMISSION WAVELENGTH (nm)

FIGURE 2. Quenching of ANTS Fluorescence by Tl^+. (A) The fluorescence of 165 μM ANTS in the presence of increasing concentrations of $TlNO_3$ was measured at excitation = 370 nm and emission = 515 nm. The ionic strength of the solutions was kept at a constant value by replacing $TlNO_3$ with $NaNO_3$ (total concentration = 35 mM), and the solutions were buffered at pH 7.4 with 10 mM Hepes. (B) A Stern-Volmer plot of the data in (A). F^o and F are the fluorescence intensities in the absence and presence of Tl^+, respectively. The solid line indicates a least squares fit of the data to a straight line, with a slope of 96 M^{-1} and a correlation coefficient of 0.998.

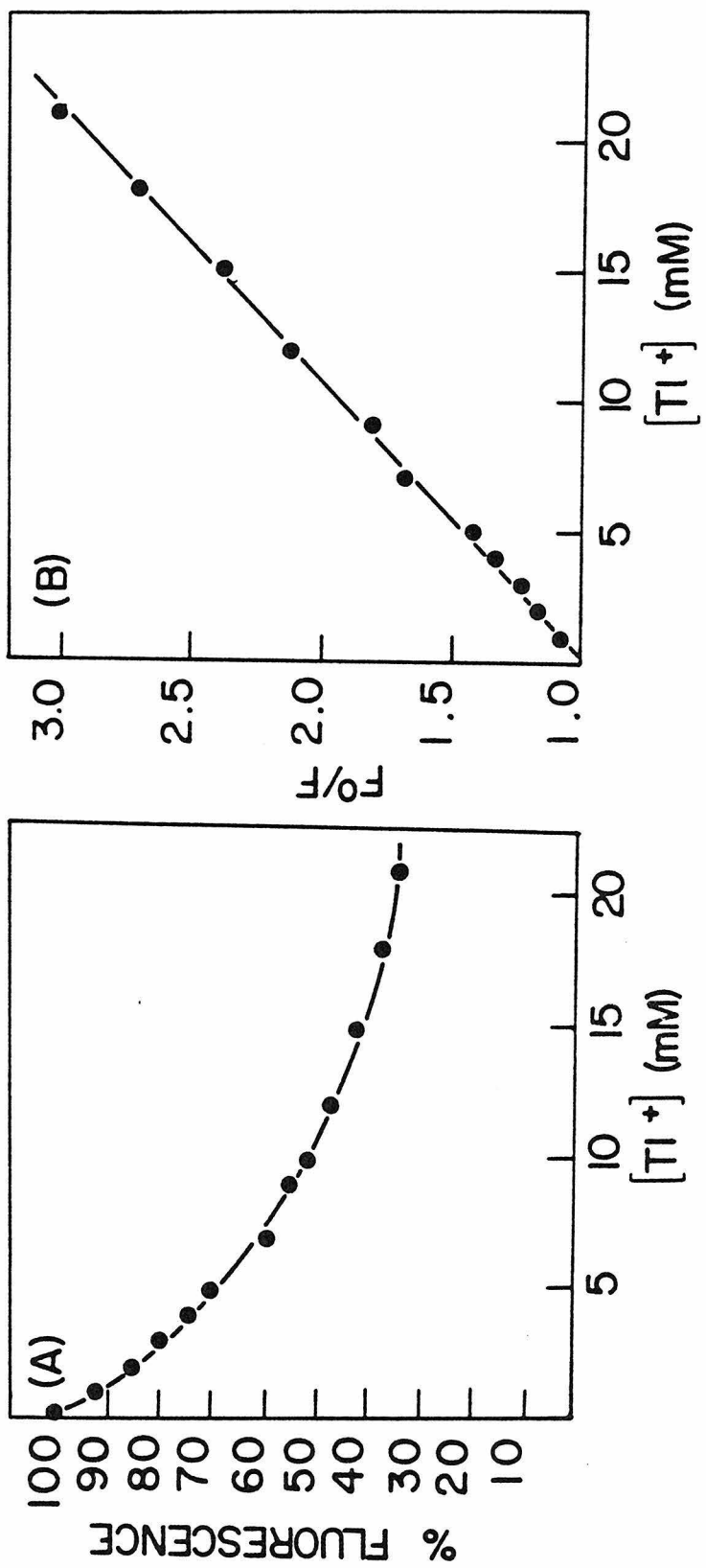
(A)
% FLUORESCENCE
100
90
80
70
60
50
40
30
20
10
5
10
15
20
[Tl+] (mM)
(B)
Fo/F
3.0
2.5
2.0
1.5
1.0
5
10
15
20
[Tl+] (mM)

of ANTS fluorescence by Tl^+ followed the Stern-Volmer relation as indicated by the linearity between F^o/F and $[Tl^+]$ (Fig. 2B). From the slope of the line a Stern-Volmer constant of 96 M^{-1} was calculated.

The observed fluorescence quenching effect is not dependent on the anionic characteristic of ANTS. A neutral fluorophore, the mercaptoethanol derivative of N-(1-Pyrenyl)-maleimide, is also efficiently quenched by Tl^+ (Stern-Volmer constant $\simeq$100 M^{-1}).

Loading of Fluorophore within the Vesicles

Due to its low membrane permeability, ANTS could not be loaded into the AcChR membrane vesicles by simple incubation. As described in Experimental, loading was achieved by performing "freeze-thaw" cycles on membrane vesicles premixed with ANTS.

Separation of Exterior Fluorophores from the Loaded Vesicles

Since the interior volume of the membrane vesicles at concentrations appropriate for spectroscopic studies is only 1/5000 that of the bulk solution (data not shown), the exterior fluorophore molecules must be carefully removed to reduce background fluorescence. This was achieved by passing the thawed ANTS-vesicle mixture through a Sephadex G-25 column as described in Experimental. This procedure removed in excess of 99.9% of the exterior ANTS molecules (as monitored by fluorescence) from the loaded AcChR-vesicles. The resulting AcChR-membrane vesicles are referred to as ANTS-vesicles. These vesicles

exhibited fluorescence at 515 nm, indicating that ANTS was entrapped within them. Control vesicles incubated with ANTS without freeze-thaw cycles followed by gel filtration did not exhibit significant fluorescence, indicating that ANTS was membrane impermeable.

Kinetics of Thallium (I) Leak Across Vesicle Membranes Measured by Fluorescence Decay

When ANTS-vesicles were rapidly mixed with $TlNO_3$-Hepes buffer in a stopped-flow instrument, a slow fluorescence decay with a half time of about 10 sec was observed (Fig. 3A). Presumably, this represented quenching of the fluorescence by slow Tl^+ leakage through the resting membrane into the vesicle interior. This interpretation was supported by the following observations. (a) No fluorescence change was observed when $NaNO_3$-Hepes buffer or KNO_3-Hepes buffer was mixed with ANTS-vesicles (Fig. 3B). The kinetic signal was therefore Tl^+ specific. (b) The slow kinetics of fluorescence decay were absent when vesicles with ANTS present only on the outside of the membranes were mixed with $TlNO_3$-Hepes buffer. Instead, the fluorescence dropped instantaneously (within the mixing time of the instrument) to the equilibrium quenched level. Similarly, the slow kinetic signal was abolished by disruption of the ANTS-vesicle membranes by Triton, Phospholipase, sonication or osmotic shock. Therefore, the slow kinetic signal observed when Tl^+ solutions were mixed with ANTS-vesicles was related to leakage processes across the intact membrane bilayer.

FIGURE 3. Rate of Tl^+ Leakage Through the Vesicle Membrane in the Absence of Agonist. (A) Membrane vesicles loaded with ANTS (Syringe 1) were mixed with 35 mM $TlNO_3$-10 mM Na Hepes, pH 7.4 (Syringe 2) in a stopped-flow instrument and the fluorescence was monitored. (B) Control experiment with $TlNO_3$ replaced by $NaNO_3$ (Syringe 2: 35 mM $NaNO_3$-10 mM Na Hepes, pH 7.4).

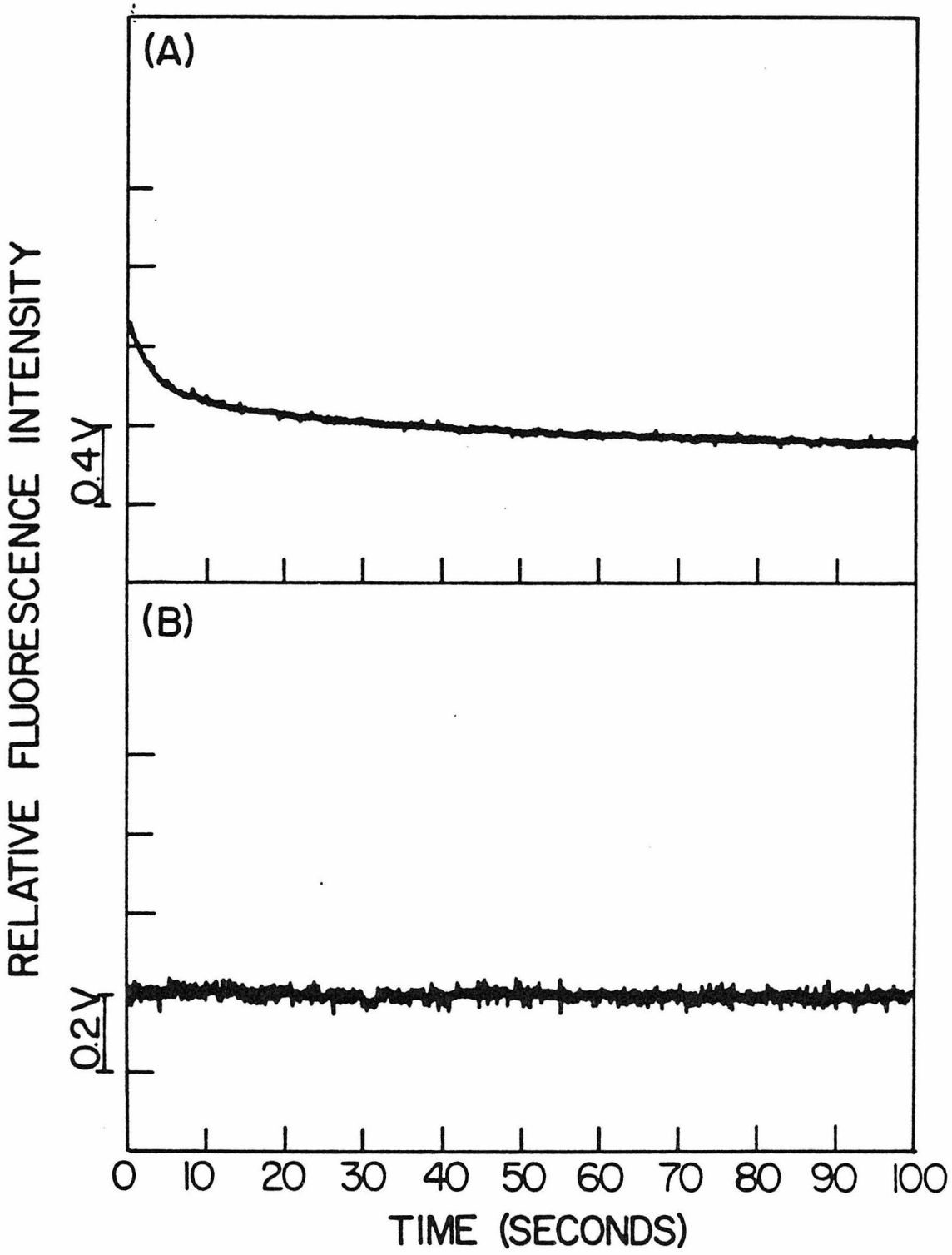
(A)
(B)
RELATIVE FLUORESCENCE INTENSITY
0.4V
0.2V
0
10
20
30
40
50
60
70
80
90
100
TIME (SECONDS)

Kinetics of Thallium (I) Influx in the Presence of Cholinergic Agonists

Addition of carbamylcholine to $TlNO_3$-Hepes buffer greatly enhanced the rate of fluorescence decay when the latter was mixed with ANTS-vesicles. The data in Fig. 4 (A1 & B1, lower traces) demonstrate the effect produced by 100 μM Carb. The fluorescence decayed rapidly with a half time of about 30 ms compared with the control (Fig. 4, A1 & B1, top traces). The slow leakage of Tl^+ through the resting membranes as described in the preceding paragraph ($t_{1/2} \sim 10$ sec) was thus negligibly small on this fast time scale. Acetylcholine also markedly increased the rate of fluorescence decay. Activation of AcChR-associated channels by nicotinic agonists therefore increased the permeability of the vesicle membrane to Tl^+ and the kinetics of ion transport could be measured by quenching of the ANTS fluorescence as Tl^+ entered the vesicular interior.

Pharmacological Effects on Thallium Influx Kinetics

In the presence of 1 mM d-Tc, the fast fluorescence decay produced by 100 μM Carb was completely inhibited (Fig. 4, B2). The antagonist by itself did not produce any detectable fluorescence change (Fig. 4, A2). The enhancement in the rate of fluorescence decay was therefore agonist-specific and could be abolished by an antagonist. HTX, an ion conductance perturbing agent (Albuquerque et al, 1973; Elliott et al, 1977) abolished the Carb-induced signal when present at a concentration of 10 μM (Fig. 4, B3). As shown in Fig. 4 (A3), the toxin had no effect on the fluorescence in the absence of Carb. Pre-

FIGURE 4. Kinetics of Agonist-Induced Tl^+ Influx Through the AcChR-Membrane Vesicles and its Blockage by Cholinergic Antagonists and by Desensitization. (A-1): Membrane vesicles entrapping ANTS (Syringe 1) were rapidly mixed with $TlNO_3$-buffer containing (lower trace) or lacking (top trace) 200 μM Carb (Syringe 2) and the fluorescence was recorded. Final concentration of Carb was 100 μM.
(B-1): Same as in (A-1) with a different membrane preparation. Solid lines indicate least-squares fits of the data to Equation (1) (see Appendix), yielding k_{app} = 20 and 17 s^{-1} for (A-1)and (B-1) respectively.
(A-2 & B-2) Effect of d-Tc: Syringe 1 contained ANTS-vesicles Syringe 2 contained 2 mM d-Tc in $TlNO_3$-buffer (A-2) or 2 mM d-Tc plus 200 μM Carb in $TlNO_3$ buffer (B-2).
(A-3 & B-3): Effect of HTX: Syringe 1 contained ANTS-vesicles preincubated with 10 μM HTX for 5 min. Syringe 2 contained 10 μM HTX in $TlNO_3$-buffer (A-3) or 10 μM HTX plus 200 μM Carb in $TlNO_3$-buffer (B-3).
(A-4 & B-4): Effect of α-BuTx: Syringe 1 contained ANTS-vesicles preincubated with excess α-BuTx. Syringe 2 contained $TlNO_3$-buffer (A-4) or 200 μM Carb in $TlNO_3$-buffer (B-4).
(A-5 & B-5): Effect of Desensitization: Syringe 1 contained ANTS-vesicles preincubated with 100 μM Carb for 30 min. Syringe 2 contained $TlNO_3$-buffer (A-5) or 100 μM Carb in $TlNO_3$-buffer (B-5).

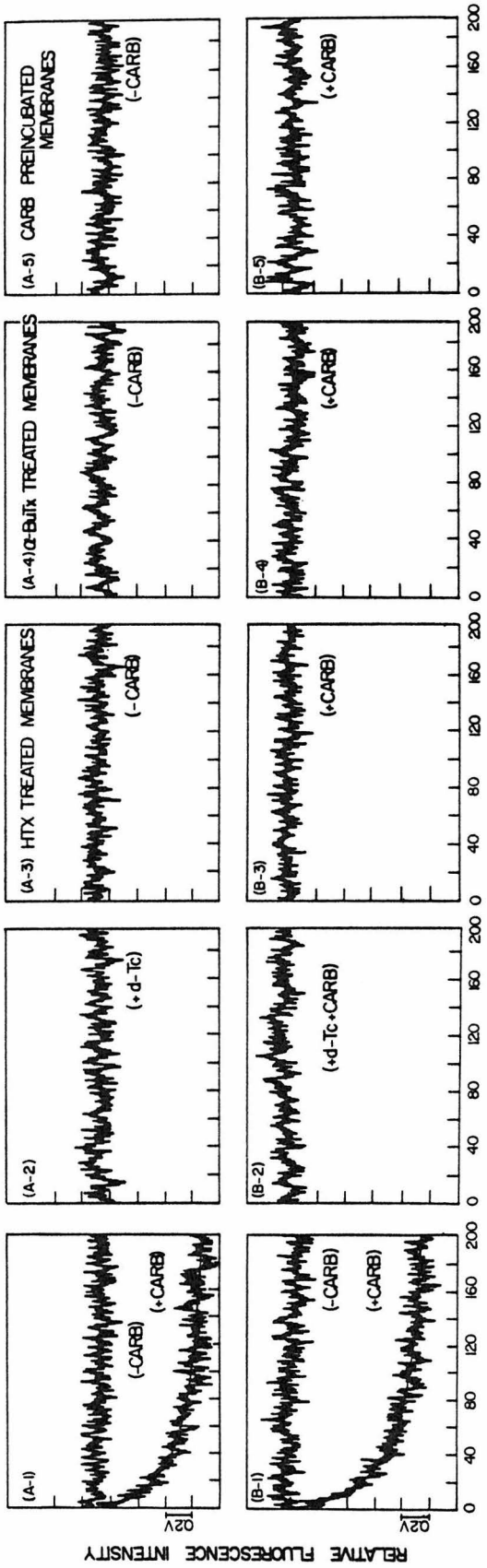
(A-1)
(-CARB)
(+CARB)
(A-2)
(+d-Tc)
(A-3) HTX TREATED MEMBRANES
(-CARB)
(A-4) α-BuTx TREATED MEMBRANES
(-CARB)
(A-5) CARB PREINCUBATED MEMBRANES
(-CARB)
(B-1)
(-CARB)
(+CARB)
(B-2)
(+d-Tc+CARB)
(B-3)
(+CARB)
(B-4)
(+CARB)
(B-5)
(+CARB)
0.2V
0 40 80 120 160 200
TIME (MILLISECONDS)
RELATIVE FLUORESCENCE INTENSITY

incubation of the AcChR vesicles with excess α-BuTx, the most effective inhibitor of cholinergic ligand binding, also blocked the effect produced by Carb (Fig. 4, B4). Again, the toxin alone had no effect on the fluorescence (Fig. 4, A4). ANTS-vesicles preincubated with 100 μM Carb at room temperature for 30 min did not exhibit any fast fluorescence decay when mixed with $TlNO_3$-Hepes buffer containing either 100 μM or 0 μM Carb (Fig. 4, A5 & B5). Activation of the permeability change was thus inhibited as a result of receptor desensitization.

These pharmacological tests support the notion that the fluorescence signal produced by cholinergic agonists indeed represented ion flux through AcChR-activated ion channels. The fluorescence quenching technique therefore enabled us to measure ion transport kinetics on the time scale of a few milliseconds to seconds. The use of this method to solve two fundamental problems related to AcChR function is presented below.

Rate of Thallium (I) Influx as a Measure of Functional AcChR Components

In general, the rate of ion flux through the vesicle membranes is proportional to the number of activated channels present on the vesicle membrane surface as analyzed in Chapter 3. The rate of fluorescence decay produced by cholinergic agonists therefore serves as a measure of the active AcChR population. The effect of a given treatment or modification on the function of the AcChR can be examined by comparing the rates of agonist specific Tl^+ induced fluorescence decay

under the same conditions for a preparation before and after the modification. One such example is illustrated in Fig. 5 where the flux kinetics of an AcChR preparation before and after alkaline extraction (Neubig et al, 1979; Elliott et al, 1979) to remove at least 98% of the M_r 43,000 and M_r 90,000 polypeptides (Chapter 3) were compared. The vesicles after alkaline extraction contained only the four AcChR polypeptide subunits (Moore et al, 1979). The apparent rates (see legend to Fig. 5) measured under the same conditions, were within a factor of 2 of each other. This result thus independently substantiates the notion (Chapter 3) that the M_r 43,000 and M_r 90,000 polypeptides or any polypeptides other than the four receptor subunits of M_r 40, 50, 60 and 65×10^3 daltons are not essential for AcChR-mediated ion translocation. In accord with the previous observations using $^{22}Na^+$ flux measurements (Chapter 3), the flux amplitude of the untreated preparation was much smaller than that of the treated membranes, indicating the former contained a larger population of contaminating vesicles lacking AcChR.

Ion Transport Rate Mediated by a Single AcChR Molecule

An important question concerning biochemical studies of the AcChR is whether the preparations of AcChR isolated in vitro, which have been subjected to relatively harsh isolation procedures represent functionally intact, unimpaired receptor. This question can be

FIGURE 5. Comparison of Tl^+ Influx Produced by 100 μM Carb for (A) Untreated AcChR Membranes and (B) Alkaline-extracted Membranes. An AcChR-enriched membrane preparation was divided in two halves. One was subjected to alkaline-extraction and the other was treated in parallel but keeping the pH at 7.4. Both were loaded with ANTS as described in Experimental and eluted from the gel filtration column with 70 mM $NaNO_3$-1 mM Na Hepes, pH 7.4. Stopped-flow measurements were carried out with Syringe 1 filled with ANTS loaded vesicles and Syringe 2 with 70 mM $TlNO_3$-1 mM Na Hepes, pH 7.4 (top trace) or the same solution containing 200 μM Carb (lower trace). Least squares fits of the data to Equation (1) gave k_{app} = 8 and 5 s^{-1} for the untreated and treated vesicles respectively. Observed rates differ by a factor of 2-3 compared with those observed in Figure 4 due to use of buffers of differing ionic composition.

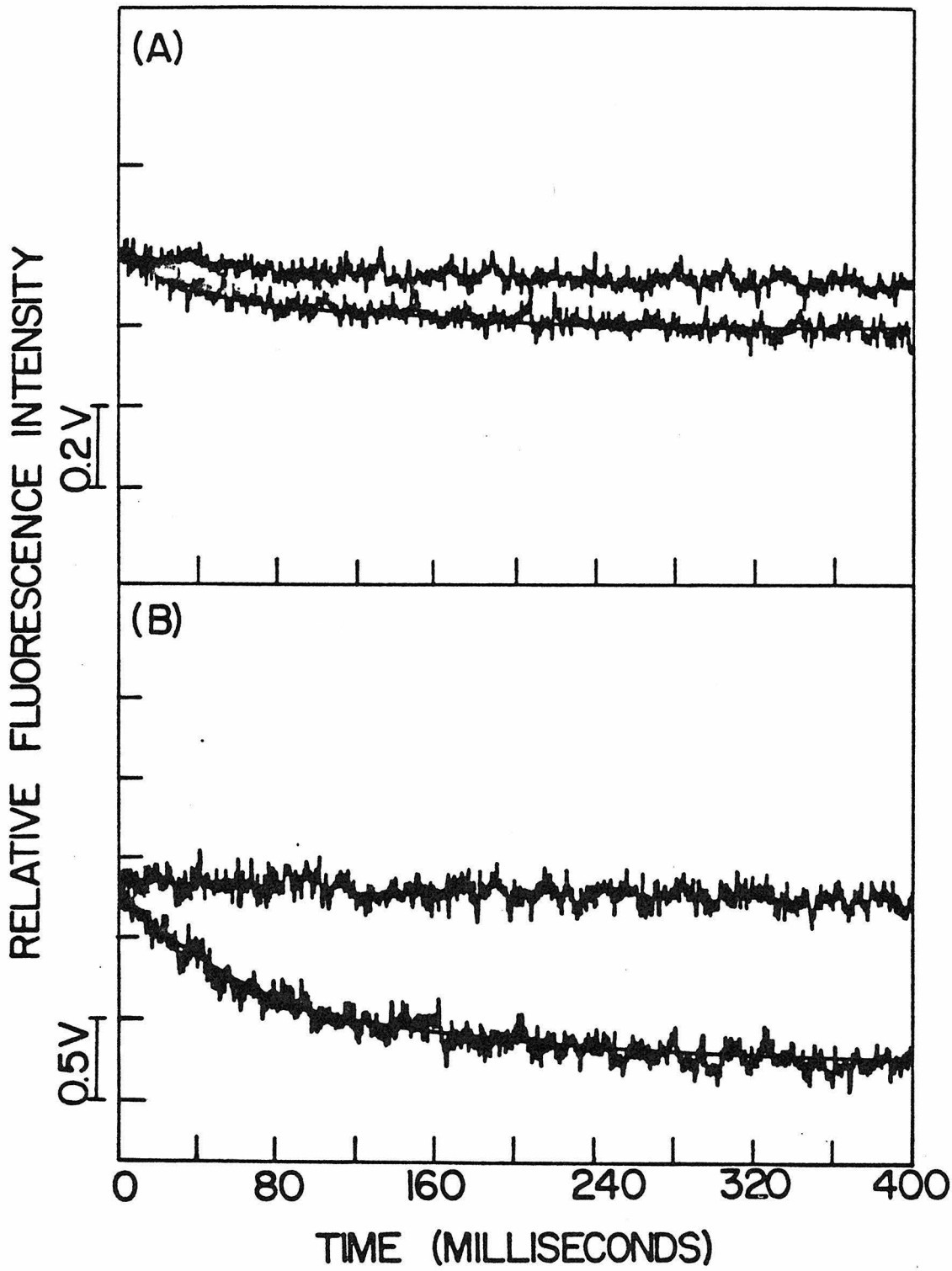
(A)
(B)
RELATIVE FLUORESCENCE INTENSITY
0.2V
0.5V
0
80
160
240
320
400
TIME (MILLISECONDS)

approached by determination of the number of ions transported per second through each activated channel, and comparison to the known single channel conductance measured in vivo. In the absence of detailed mechanisms for channel activation and inactivation, this number could be estimated by measuring the full flux rate at high Carb concentrations, and dividing it by the total number of AcChR molecules present in each vesicle. The number calculated in this manner will represent the lower limit of the actual transport number, since an extreme situation was assumed in which all the channels present were considered to be open at saturating Carb concentrations throughout the time course of the flux experiments.

Fig. 6A illustrates the signals produced by increasing concentrations of Carb; the rate of fluorescence decay increased sharply when the concentration of Carb was raised from 0-500 μM, indicating that higher degrees of activation were obtained.

The rate of fluorescence decay at Carb concentrations higher than 500 μM was too fast to be measured by the stopped-flow instrument. In order to estimate the full flux rate at high Carb concentration, titration with Carb in the high concentration range was carried out in the presence of 1-2 μM HTX to partially inactivate the channels in each vesicle and thereby reduce the flux rate. It was found in different experiments that addition of 1-2 μM HTX slowed the flux rate by a factor of 4-6 at 100 μM Carb without appreciably affecting the amplitude. For each preparation this factor was determined and used em-

FIGURE 6. Dependence of the Observed Flux Rate on the Concentration of Carb. (A) Kinetics of Tl^+ influx produced by 0 μM, 50 μM, 100 μM and 500 μM Carb (top to bottom). Solid lines indicate computer-fitted curves to Equation (1).

(B & C): Plot of the apparent flux rate constant as a function of the concentration of Carb. Data were obtained from three different preparations. The kinetic traces were fitted to Equation (1) and k_{app} was determined. The rate constants at concentrations of Carb higher than 500 μM were obtained by carrying out the flux experiments in the presence of 1-2 μM HTX, and normalizing the values by a factor predetermined at 100 μM Carb for the given preparation to give those in the absence of HTX. The normalization procedure assumed a constant % of blockage of the flux rate at all agonist concentrations by a given concentration of HTX. The data were fitted to binding isotherms assuming either one (B) or two (C) Carb molecules were associated with each activated channel ($k_{app} = k_{max}/(1+(K_D/[L])$ for (B) and $k_{app}=k_{max}/(1+(K_D/[L]))^2$ for (C), yielding $k_{max} \simeq 1500$ and $K_D \simeq 5$ mM for (B) and $k_{max} \simeq 1100$ and $K_D \simeq 1$ mM for (C).

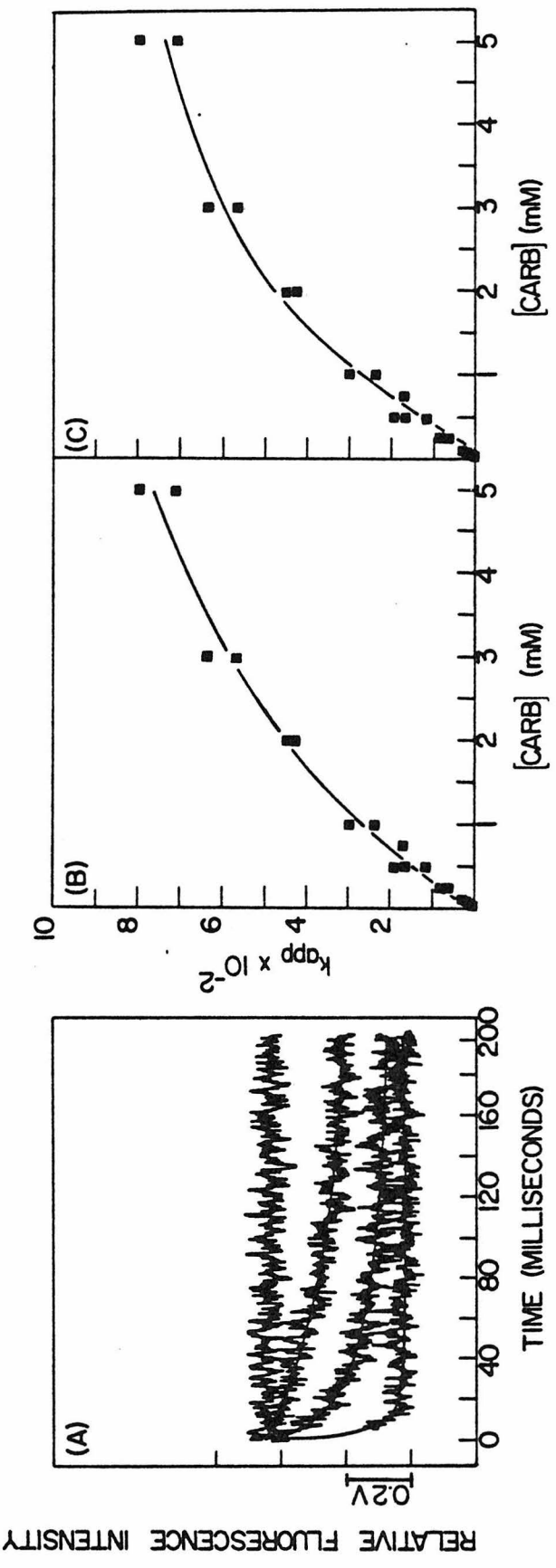
(A)
0.2V
0
40
80
120
160
200
TIME (MILLISECONDS)
RELATIVE FLUORESCENCE INTENSITY
(B)
(C)
$k_{app} \times 10^{-2}$
10
8
6
4
2
1
2
3
4
5
[CARB] (mM)
[CARB] (mM)

pirically to normalize the flux rates measured in the presence of HTX at higher Carb concentrations. Fig. 6B shows the flux rates measured at different Carb concentrations after such normalization. The rate began to level off at a few millimolar Carb. At the maximal rate (1500 sec^{-1}) extrapolated from these data, a transport number of minimally 10^6 ions per second per activated channel was calculated (see Appendix). This number is within an order of magnitude of that reported for AcChR-activated channels in intact cells ($\simeq 10^7$ per sec, Katz and Miledi, 1972; Anderson and Stevens, 1973; Lester, 1977). The AcChR complex in the isolated preparations therefore closely resembles that in intact cells, and a large fraction of the AcChR is apparently functional in our purified membranes.

The dependence of the flux rate on Carb concentration was fitted to a simple model which assumed either one or two agonists for channel activation, (Fig. 6B & 6C and legends). Both models fit equally well and cannot be differentiated based on the current data. Future experiments should allow detailed analysis of the mechanism involving channel activation and inactivation.

DISCUSSION

For quantitative analysis of ion transport processes across vesicle membranes *in vitro* it is highly desirable to have the high information content of a continuously recording method such as an optical signal, especially to facilitate computer aided analysis of the data and ultimately for dissection of reasonable mechanisms. Spectroscopic approaches for such studies, however, encounter the difficulty of small signals since the interference of light-scattering by vesicles greatly limits the concentration of vesicles at which measurements can be made. The interior volume of vesicles at concentrations sufficiently low to allow optical measurements is several orders of magnitude smaller than that of the bulk solution. We have overcome such problems by employing a sensitive detection method of fluorescence quenching by Tl^+, and by loading the optical probe within the vesicles and measuring ion influx. Other potential methods for such studies which failed to give detectable signals include the use of a Ca^{2+} metallochromic indicator, antipyriazo III, (Scarpa *et al*, 1978) and membrane-potential sensitive dyes such as merocyanine 540. The former suffers from the drawback of membrane aggregation in high concentrations of Ca^{2+} and the limited solubility of the dye. The latter yields fast optical changes on the order of 10^{-4} - 10^{-3} (Waggoner, 1976), which is too small to be detected by the stopped-flow instrument. The fluorescence quenching technique described in this chapter, on the other hand, successfully

generates agonist-specific signals as large as 1.0 V (Figure 4-1) and provides a useful method for in vitro studies of cation translocation on a time scale considerably faster than has been achieved previously.

The observed kinetic signals were not due to changes in fluorescence of the probe molecules in response to transmembrane potentials (similar to the action of some membrane potential sensitive dyes) since no change in the ANTS fluorescence was observed when Tl^+ outside the vesicles was replaced by K^+. Neither were the signals caused by changes in the quantum yield of the ANTS fluorescence as a result of agonist induced conformational changes of AcChR; no Carb-specific fluorescence decay was observed in the absence of Tl^+. Furthermore, the signals were sensitive to reagents such as Triton or phospholipases which perturbed the membrane permeability. The fluorescence changes therefore directly measure ion transport through the membrane barrier; the observed Carb effect being agonist-specific as attested to by the expected pharmacology.

The first use of this method has been to show that polypeptide components other than those of 40,000, 50,000, 60,000 and 65,000 daltons are not essential for AcChR-mediated cation translocation. Direct comparison of the ion flux kinetics from an untreated AcChR preparation and one lacking the polypeptides of 43,000 and 90,000 daltons following alkaline extraction showed striking similarities between the two preparations (Fig. 5). These polypeptides were thus not es-

sential for the AcChR-mediated ion translocation, a result consistent with the findings described in Chapter 4 by analyzing $^{22}Na^{+}$ flux amplitudes in partially toxin-inactivated membrane vesicles.

It has always been a major question whether the biochemically purified AcChR preparations retain their functional integrity. The slow ion flux first reported by Kasai and Changeux (1971) suggested that loss of functional elements during the isolation procedures was not unlikely. Although better preparative methods have since been used and preparations which exhibited ion flux on a faster time scale obtained (Chapter 3) until now the functional integrity of receptor preparations could not be unequivocally determined due to the absence of available techniques to measure ion flux kinetics on fast time scales. The method described here enables such determination and allows measurement of ion transport capability of the isolated AcChR to be made on the time scale of a few milliseconds. From the kinetics of such ion flux measurements, it is estimated that at least 10^6 ions were transported through each AcChR molecule per second in our purified preparations (see Appendix). This number is without doubt a minimal estimate since channel activation and inactivation processes have been neglected in the calculations and all the channels were assumed to be open at all times at saturating concentrations of agonist. Since the channel opening probabilities when agonists are bound are often less than 1 (Dionne et al, 1978), this implies that the actual transport number should be higher than calculated. This result and the differences in membrane potential and ion composition may therefore adequately account for the difference

between the estimated transport number and that reported for the intact AcChR *in vivo* ($\sim 10^7$ per sec, Katz and Miledi, 1972; Anderson and Stevens, 1973; Lester, 1977). Our purified AcChR preparations, which are predominantly in the 13S dimeric form (Witzemann and Raftery, 1978), thus closely resemble the native molecules in intact cells and very little, if any, damage to functional integrity occurred during the isolation processes.

Recently the $^{22}Na^+$ filtration method has been extended by Hess *et al* (1979) to the subsecond range with the fastest samples corresponding to 25 msec time points. The method involves tedious washing of individual samples for each time point and its accuracy relies on efficient quenching of the efflux processes by antagonists and is complicated by the leakage processes in the quenched reaction mixture before filtration. Furthermore, the reported flux rates for the *Electrophorus* vesicles are much slower than those determined in the present studies using *Torpedo* membrane vesicles (half time $\sim$160 ms at 1 mM Carb as compared to 2.5 ms determined here, see Fig. 6). Whether this discrepancy is due only to differences in the AcChR densities in the two species or in the functional integrity of the two preparations awaits further clarification.

The observed dependence of the flux rate on the concentration of agonists showed that the flux rate did not saturate at concentrations expected for binding of agonists to the low-affinity site of the AcChR (Quast *et al*, 1978). Instead, the rate begin to level off only

at very high concentrations of Carb (mM range). This implies that a scheme more complicated than the simple occupancy mechanism may be involved in channel activation. Similar high Carb concentration dependence of the flux rate has recently been reported (Cash et al, 1980). Future quantitative analysis of the flux kinetics coupled with fluorescence studies of AcChR-associated conformational changes (Quast et al, 1979; Dunn et al, 1980) should reveal a detailed mechanism for activation and inactivation of the AcChR associated channels. In addition since Tl^+ can be substituted for K^+ in many biological systems, the Tl^+ quenching technique presented here can be applied to study ion transport through other excitable membranes in vitro.

APPENDIX

Calculation of Ion Transport Rate Mediated by a Single Receptor Site from the Kinetic Data of Tl^+ Influx

Quantitative analysis of the kinetic signal produced by activation of the AcChR can be achieved by combining the rate law of Tl^+ influx and the Stern-Volmer relation for fluorescence quenching. Under conditions in which the number of activated channels is constant during the flux process, the kinetics of Tl^+ influx can be described by a first-order process: $T(t) = T_\infty(1-e^{-kt})$ where T is the concentration of Tl^+ inside the vesicles at time t, and k is the apparent rate constant of Tl^+ flux which is a complex function of channel conductance, vesicle size, surface density of channels, ion composition and the agonist concentration (Chapter 3). The fluorescence of ANTS at a given internal Tl^+ concentration, T, is given by the Stern-Volmer relation $F^o/F = 1 + KT$ (see Fig. 2) where K is the Stern-Volmer constant. Substituting T into the above expression, one obtains the fluorescence intensity as a function of time $F = F^o/(1+KT_\infty(1-e^{-kt}))$.(1)

By fitting the kinetic traces to this equation, apparent rate constants for Tl^+ flux were determined (see Fig. 4). The minimal number of ions transported through each activated channel was estimated as follows. For each vesicle, the rate of unidirectional flux of Tl^+ is the concentration of Tl^+, 'C', multiplied by the apparent flux rate constant, 'k'. Under the experimental conditions used, 'C' is 17 mM

(concentration of Tl^+ outside the vesicles) and 'k' is ∿1500 from the empirically fitted flux rate (Fig. 6). The rate of entry of Tl^+ is therefore ∿26 M/sec. Taking into consideration the interior volume of the vesicles (with an average diameter of 6000 Å (Elliott et al, 1980), this is $\sim 10^{-16}$L/vesicle), this means that $26 \times 10^{-16} \times 6.02 \times 10^{23}$ or $\sim 2 \times 10^9$ Tl^+ ions entered each vesicle per second when the surface AcChRs were activated. The number of AcChR oligomers per vesicle calculated from the reported density ($\sim 10^4/\mu m^2$, Nickel and Potter, 1973; Pepper et al, 1974) and the surface area of vesicles 6000 Å in diameter is $\sim 10^4$. The number of Tl^+ ions transported per second through each activated AcChR channel is therefore minimally (see Discussion) 2×10^5. Since other permeant ionic species were present (the total concentration of Na^+ and Tl^+ on both sides of the bilayer was 104 mM), the transport number for Tl^+ should be corrected to give the total transport number for bidirectional flux of all ionic species. Assuming Na^+ and Tl^+ have similar permeabilities, this means at least 10^6 ions were transported through each activated channel per second.

REFERENCES

1. E. X. Albuquerque, E. A. Barnard, T. M. Chiu, A. J. Lapa, J. O. Dolly, S.-E. Jansson, J. Daly, and B. Witkop (1973), Proc. Natl. Acad. Sci. 70, 949.
2. C. R. Anderson and C. F. Stevens (1973), J. Physiol. 235, 655.
3. D. J. Cash and G. P. Hess (1980), Proc. Natl. Acad. Sci. 77, 842.
4. V. E. Dionne, J. H. Steinbach, and C. F. Stevens (1978), J. Physiol. 281, 421.
5. S. M. J. Dunn, S. G. Blanchard, and M. A. Raftery (1980) Biochemistry, submitted.
6. J. Elliott and M. A. Raftery (1977), Biochem. Biophys. Res. Commun. 77, 1347.
7. J. E. Elliott, S. M. J. Dunn, S. G. Blanchard, and M. A. Raftery (1979), Proc. Natl. Acad. Sci. 76, 2576.
8. J. Elliott, S. Blanchard, W.C.-S. Wu, J. Miller, C. Strader, P. Hartig, H.-P. H. Moore, J. Racs, and M. S. Raftery (1980) Biochemical Journal, in press.
9. P. J. Gehring and P. B. Hammond (1964), J. Pharma. Exp. Ther. 145, 215.
10. G. P. Hess, S. Lipkowitz, and G. E. Struve (1978) Proc. Natl. Acad. Sci. 75, 1703.
11. G. P. Hess, D. J. Cash, and H. Aoshima (1979) Nature 282, 329.
12. B. Hille (1972), J. Gen. Physiol. 59, 637.

13. B. Hille (1973), J. Gen. Physiol. 61, 669.

14. M. Kasai and J.-P. Changeux (1971), J. Membrane Biol. 6, 1.

15. M. Kasha (1952), J. Chem. Phys. 20, 71.

16. B. Katz and R. Miledi (1972), J. Physiol. 224, 665.

17. D. Landowre (1975), J. Physiol. 752, 79.

18. H. A. Lester (1977), Scientific American, Feb., 106.

19. H.-P. H. Moore, P. R. Hartig, and M. A. Raftery (1979), Proc. Natl. Acad. Sci. 76, 6265.

20. L. J. Mullins and R. D. Moore (1960), J. Gen. Physiol. 3, 759.

21. R. R. Neubig, E. K. Krodel, N. D. Boyd, and J. B. Cohen (1979), Proc. Natl. Acad. Sci. 76, 690.

22. E. Nickel and L. T. Potter (1973), Brain Research 57, 508.

23. C. A. Parker (1968), Photoluminescence of Solutions, Elsevier Publishing Company, Amsterdam.

24. K. Pepper, F. Dreyer, C. Sandri, K. Akert, and H. Moor (1974), Cell and Tissue Res. 149, 432.

25. U. Quast, M. Schimerlik, T. Lee, V. Witzemann, S. Blanchard, and M. A. Raftery (1978), Biochemistry 17, 2405.

26. U. Quast, M. Schimerlik, and M. A. Raftery (1979), Biochemistry 18, 1891.

27. M. A. Raftery, M. W. Hunkapiller, C. D. Strader, and L. E. Hood, (1980) Science, submitted.

28. A. Scarpa, F. J. Brinley, and G. Dubyak (1978), Biochemistry 17, 1378; A. Waggoner (1976), J. Membrane Biol. 27, 317.

29. V. Witzemann and M. A. Raftery (1978), Biochem. Biophys. Res. Commun. 81, 1025.

CHAPTER FIVE

Effects of Sulfhydryl and Disulfide Reagents on the Affinity States of Membrane-Bound Acetylcholine Receptor from Torpedo californica.

INTRODUCTION

In addition to its well characterized depolarizing effects in response to cholinergic agonists, the AcChR exhibits the phenomenon of desensitization *in vivo*. Prolonged application of the agonists AcCh, Carb or succinylcholine to frog sartorius end plates resulted in decreased effectiveness of these agonists. The AcChR was considered to change from an "effective" (low ligand affinity) to a refractory (high affinity) state in the presence of ligand (Katz and Thesleff, 1957). After complete removal of agonist, a slow recovery of the original activity was observed. Rang and Ritter (1970a,b) found that preincubation with certain agonists caused an increase in AcChR affinity for antagonists. Subsequent *in vitro* studies with AcChR-enriched membrane preparations have shown that preincubation with agonists induced a high affinity form of the AcChR (Weber *et al*, 1975; Weiland *et al*, 1976, 1977; Lee *et al*, 1977; Quast *et al*, 1978). Preincubation of AcChR with Carb also abolishes the characteristic agonist-induced $^{22}Na^+$ and Tl^+ flux in membrane vesicle preparations (Chapters 3,4). The desensitization process observed *in vivo* is thus reproduced *in vitro* and both inactivation of the flux response and the ligand-induced affinity changes may represent manifestations of receptor desensitization. Interactions of AcChR with cholinergic ligands therefore trigger a series of functional events and interconvert the receptor to states of differing ligand affinities. The work presented in this chapter was initiated with the aim of exploiting

the chemical interactions involved in the desensitization process, and searching for methods to stabilize the receptor in states of differing affinities which may be useful for deducing molecular mechanisms for receptor function.

Nicotinic AcChRs are known to contain a reactive disulfide bond(s) in the vicinity of the cholinergic ligand binding site(s) (Karlin and Bartels, 1966; Lindstrom et al, 1973; Ben-Haim et al, 1973). Electrophysiological studies have shown that reduction of this bond(s) inhibits the depolarizing effect of cholinergic agonists while 5,5'-dithio-bis(2-nitrobenzoic acid) (DTNB) completely restores the membrane sensitivity to AcCh. The reduced receptor could be alkylated by N-ethyl maleimide (NEM) and could then no longer be reoxidized. Noise analysis has shown that a decreased single channel conductance is associated with DTT-reduced preparations (Ben-Haim et al, 1975).

The studies presented here describe the effects of chemical modification of sulfhydryl groups and disulfide bonds on the interconversion of affinity states of the AcChR induced by cholinergic ligands. Reagents directed against both free sulfhydryl groups and disulfide bonds were found to inhibit the Carb-induced affinity change of AcChR-enriched membrane fragments. In addition, reversion of high affinity AcChR to the low affinity state(s) was blocked by the reagent p-chloromercuribenzoate (PCMB). These results are discussed in terms of two possible simple models which involve both cysteine and cysine residues in interconversion of the affinity states of the AcChR.

EXPERIMENTAL

Membrane Preparations

Crude AcChR membrane preparations were prepared according to the procedures described in Chapter 2. Buffer used throughout the preparation was 10 mM sodium phosphate, pH 7.4, 400 mM NaCl, 1-5 mM EDTA and 0.02% NaN_3. Membranes were resuspended in Torpedo Ringers (250 mM NaCl, 5 mM KCl 4mM $CaCl_2$, 2mM $MgCl_2$, 5 mM TrisCl, pH 7.4) for [^{125}I]-α-BuTx binding studies.

Ligand-Induced Interconversion of Affinity States in Membrane-bound AcChR Monitored by [^{125}I]-α-BuTx Binding

All membrane fragment preparations were routinely assayed to determine whether they exhibited low or high affinity for Carb. The initial rate of [^{125}I]-α-BuTx binding was measured in the absence of agonist, and in the presence of 1 μM Carb, added either 30 min prior to, or at the same time as [^{125}I]-α-BuTx, under conditions in which the toxin was in large excess over the AcChR toxin binding sites (Fig. 1a). Membrane fragments were judged to be completely in the low affinity form when the initial toxin binding rate observed in the absence of Carb (Curve A) and when Carb and toxin were added simultaneously (Curve B) were equal. Determination of the rates of Carb-induced isomerization of the AcChR and recovery of the AcChR from high to low affinity state were carried out as described previously (Lee et al, 1977). Apparent K_d values of Carb for the AcChR were determined

by preincubating AcChR membrane suspensions with various concentrations of Carb and monitoring the initial rates of [^{125}I]-α-BuTx-AcChR complex formation by DEAE disc assay (Schmidt and Raftery, 1973). [^{125}I]-α-BuTx was prepared by a procedure (Blanchard et al, 1979) modified from that of Vogel et al (1972) as described in Chapter 1.

Chemical Modification of AcChR

For chemical modification, membrane suspensions of AcChR containing 1-2 μM α-BuTx sites in Hepes Ringers (250 mM NaCl, 5 mM KCl, 4 mM $CaCl_2$, 2 mM $MgCl_2$ 20 mM Hepes, pH 7.4, 0.02% NaN_3) were allowed to react with 1 mM DTT or PCMB (Sigma). The reaction vials were flushed with argon and allowed to stand at room temperature for one hour. Alkylation of reduced AcChR was accomplished by adding 3 mM iodoacetamide (Sigma) or iodoacetic acid (Matheson Coleman & Bell Co.) to the reduced membrane preparation, and the reaction was allowed to continue for another 2 hours at 4°C. The membrane fragments were then pelleted, washed, and resuspended in fresh Torpedo Ringers. Stock solutions of reagents were made in 200 mM Tris buffer, pH 8.5.

RESULTS

Effects of Sulfhydryl and Disulfide Reagents on the Conversion of Membrane-Bound AcChR from Low Affinity to High Affinity State(s) by Carb

A. Reduction by DTT

Membrane-bound AcChR from Torpedo californica underwent a reversible conformational change to a high affinity form upon incubation with the agonist Carb (Figure 1a) as described previously (Lee et al, 1977; Weiland et al, 1976, 1977; Quast et al, 1978). Addition of DTT to a membrane preparation enriched in AcChR abolished the induction of this affinity change by 1 μM Carb (Figure 1b). However, upon removal of excess reducing agent, by centrifugation or dialysis, the AcChR gradually recovered its ability to undergo the affinity change as illustrated in Figure 1c,d; immediately after removal of excess DTT, preincubation of the AcChR with 1 μM Carb for 30 min reduced the initial toxin binding rate to approximately 50% of that in the absence of Carb (Figure 1c, Curve C) and after these membrane fragments were stirred in the cold for two days, complete recovery of the phenomenon was approached (Figure 1d, Curve C). The recovery process was accelerated by the addition of DTNB to the reduced membrane preparations. Neither the toxin binding rate nor the number of toxin binding sites was affected by these treatments. The half-time for conversion from low to high affinity state(s) in the presence of 1 μM Carb was

FIGURE 1. Effect of DTT and Its Subsequent Removal on the Carb Induced AcChR Affinity Change. Curve A: (●) [^{125}I]-α-BuTx was added to a receptor membrane preparation (4-8x10^{-8} M in Torpedo Ringers) to a final concentration of 5x10^{-7} M at time zero and the formation of the receptor-toxin complex was followed by DEAE disc assay. Curve B: (Δ) Same as in Curve A, except that 1 μM Carb was added with toxin at time zero. Curve C: (×) Same as in Curve A, except that the AcChR was preincubated with 1 μM Carb for 30 min prior to toxin addition. (A) Unmodified AcChR. (B) DTT-treated membrane-bound AcChR, (C) Membrane preparation which was modified as in (B) and dialyzed against Torpedo Ringers for 16 hours to remove DTT, (D) Membrane preparation which was treated as (C) and stirred at 4^{o}C for two days after dialysis.

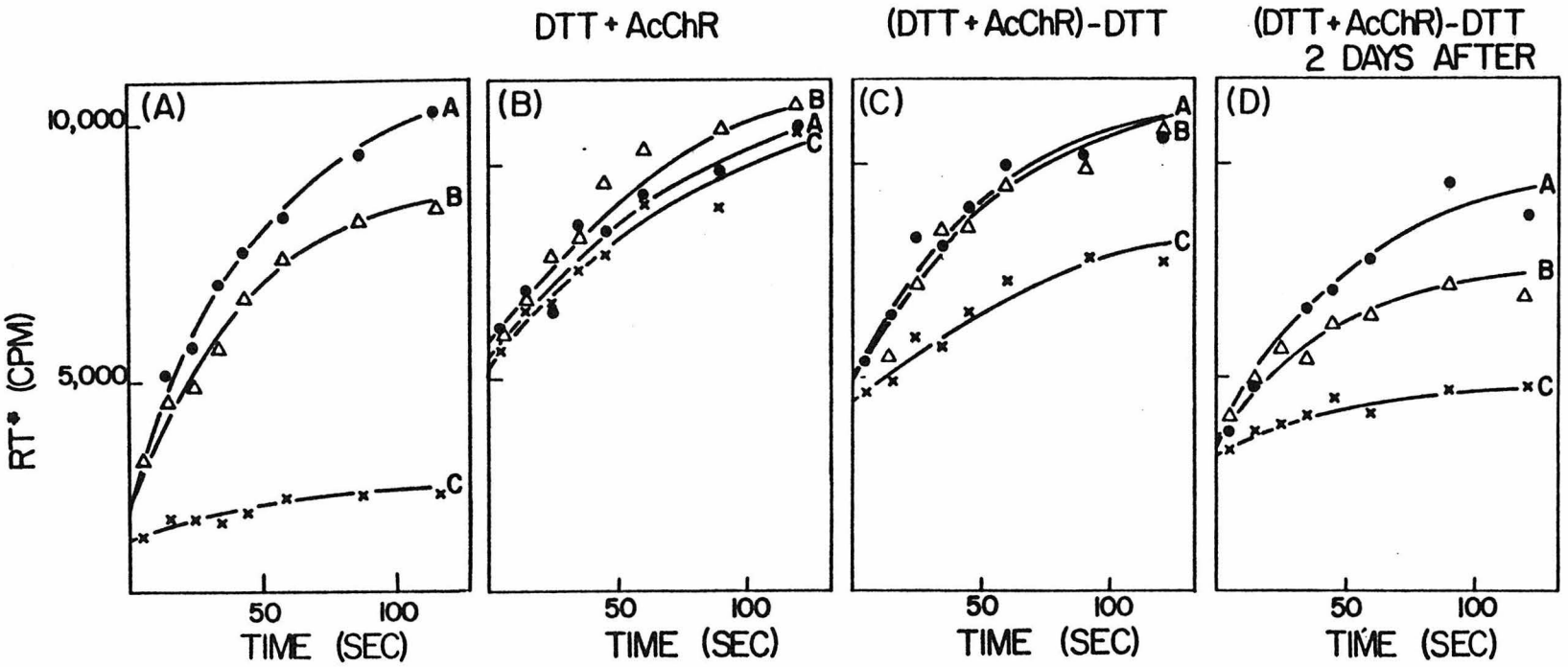
DTT + AcChR
(DTT + AcChR)-DTT
(DTT + AcChR)-DTT
2 DAYS AFTER
(A)
(B)
(C)
(D)
10,000
5,000
RT* (CPM)
A
B
C
50
100
TIME (SEC)

determined for these "recovered" membrane fragments, by the toxin binding technique, giving a value of $T_{1/2}$ = 80 sec. This value is in close agreement with that previously reported for unmodified membrane fragments (Lee et al, 1977).

B. Reduction and Alkylation

When a DTT-reduced membrane preparation was alkylated with iodoacetic acid or iodoacetamide, a blockage of the affinity state conversion induced by 1 μM Carb occurred (Figure 2) similar to that observed upon DTT treatment alone. However, in contrast to the results obtained with DTT alone, removal of excess reagents did not restore the ability of the AcChR to undergo the affinity change. Again, neither the toxin binding rate nor the number of toxin binding sites was substantially affected. A similar effect was observed by reduction and alkylation with NEM. Investigation of the affinity for Carb of a preparation which had been treated with DTT and iodoacetic acid revealed that a 50% reduction of the initial toxin binding rate was obtained at approximately 30 μM Carb. This value is clearly different from the equilibrium value of 50-120 nM obtained with untreated preparations (Quast et al, 1978) and is closer to the value of 30-50 μM obtained by the same authors for low-affinity membrane preparations. In control experiments it was found that NEM, iodoacetic acid or iodoacetamide alone (without prior reduction) at similar concentrations did not affect the affinity change induced by Carb.

FIGURE 2. Effect of Reduction and Alkylation on the Conversion of AcChR from Low to High Ligand Affinity by Carb. Membrane-bound AcChR was reduced by DTT and alkylated with iodoacetic acid or iodoacetamide. The membranes were washed to remove the excess reagent and assayed for capability of ligand induced affinity change by the method described in Fig. 1.

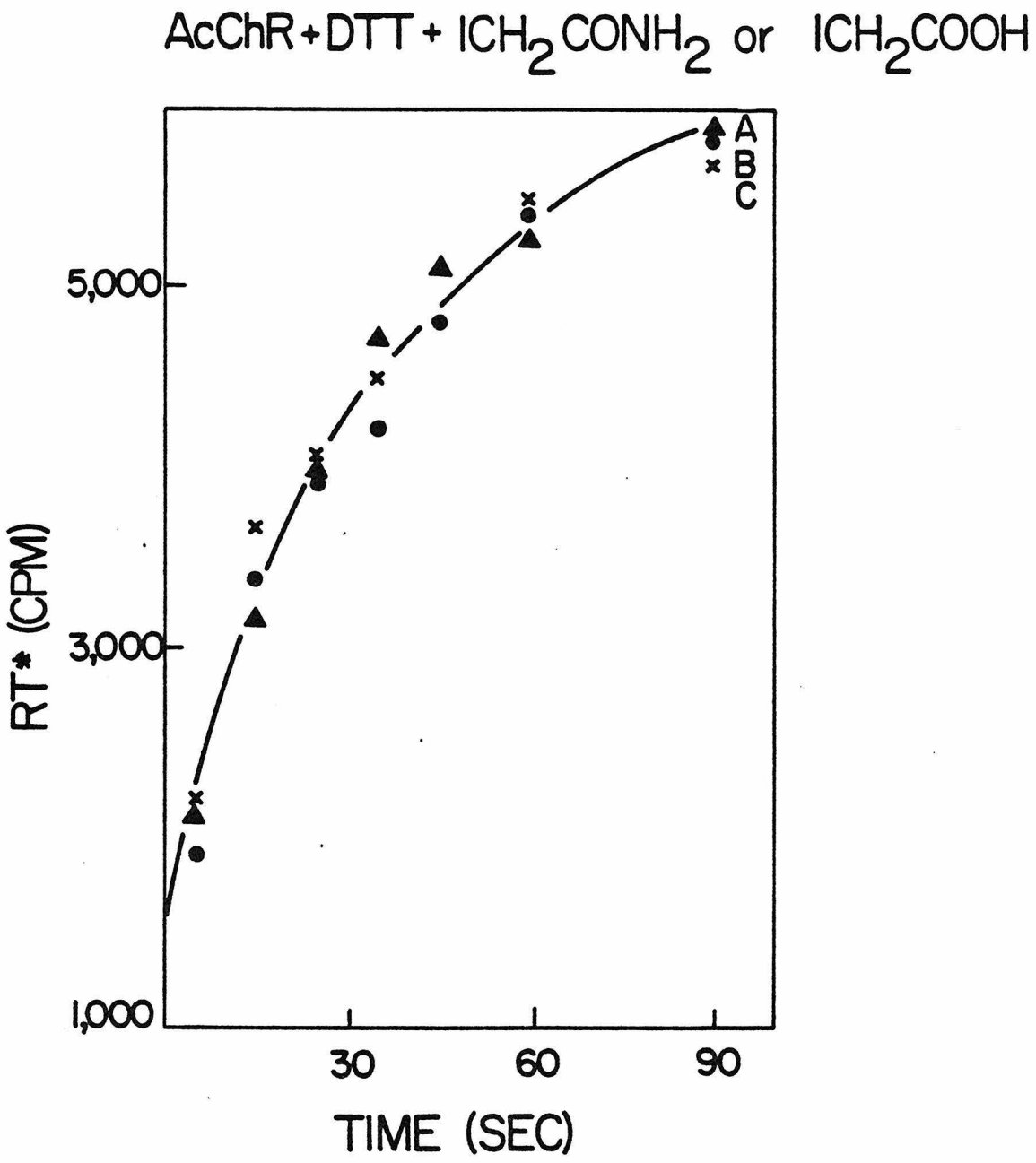
AcChR+DTT+ICH2CONH2 or ICH2COOH
A
B
C
5,000
3,000
1,000
RT* (CPM)
30
60
90
TIME (SEC)

C. PCMB

Treatment of membrane-bound AcChR with 1 mM PCMB (without DTT treatment) also prevented the change in affinity induced by 1 μM Carb (Figure 3). This treatment did not affect the toxin binding rate or the number of toxin sites significantly. Values of K_d obtained for Carb by the [^{125}I]-α-BuTx binding technique indicated that the AcChR was present in a form of low ligand affinity after PCMB modification (K_d = 30 μM, Figure 4).

Effect of PCMB on Recovery of AcChR-enriched Membrane Fragments to Low Affinity from Carb Induced High Ligand Affinity

Membrane-bound AcChR (1.4 μM in α-BuTx sites) was first converted to the high affinity state by incubation with 3 μM Carb. After 50 min at room temperature, the mixture was diluted forty-fold into Torpedo Ringers and the reversion of the AcChR to the low affinity form was followed by the toxin binding assay method. Figure 5B illustrates the results. At different times after dilution 1 μM Carb and 4 μg/ml α-BuTx were added simultaneously and the initial toxin binding rates were monitored by DEAE disc assay. As has been shown previously (Lee et al, 1977), recovery of low ligand affinity was essentially complete 10 min after dilution. However, if after 25 min of incubation with Carb, the AcChR was allowed to react with 1 mM PCMB for 25 min, the dilution experiment gave a completely different result (Figure 5A); there was essentially no reversion of the AcChR to the

FIGURE 3. Effect of PCMB on the Transition of AcChR from Low to High Affinity State. Membrane-bound AcChR was modified with 1 mM PCMB for 1 hour at room temperature. The membranes were washed and assayed for ligand induced affinity change as described in Figure 1.

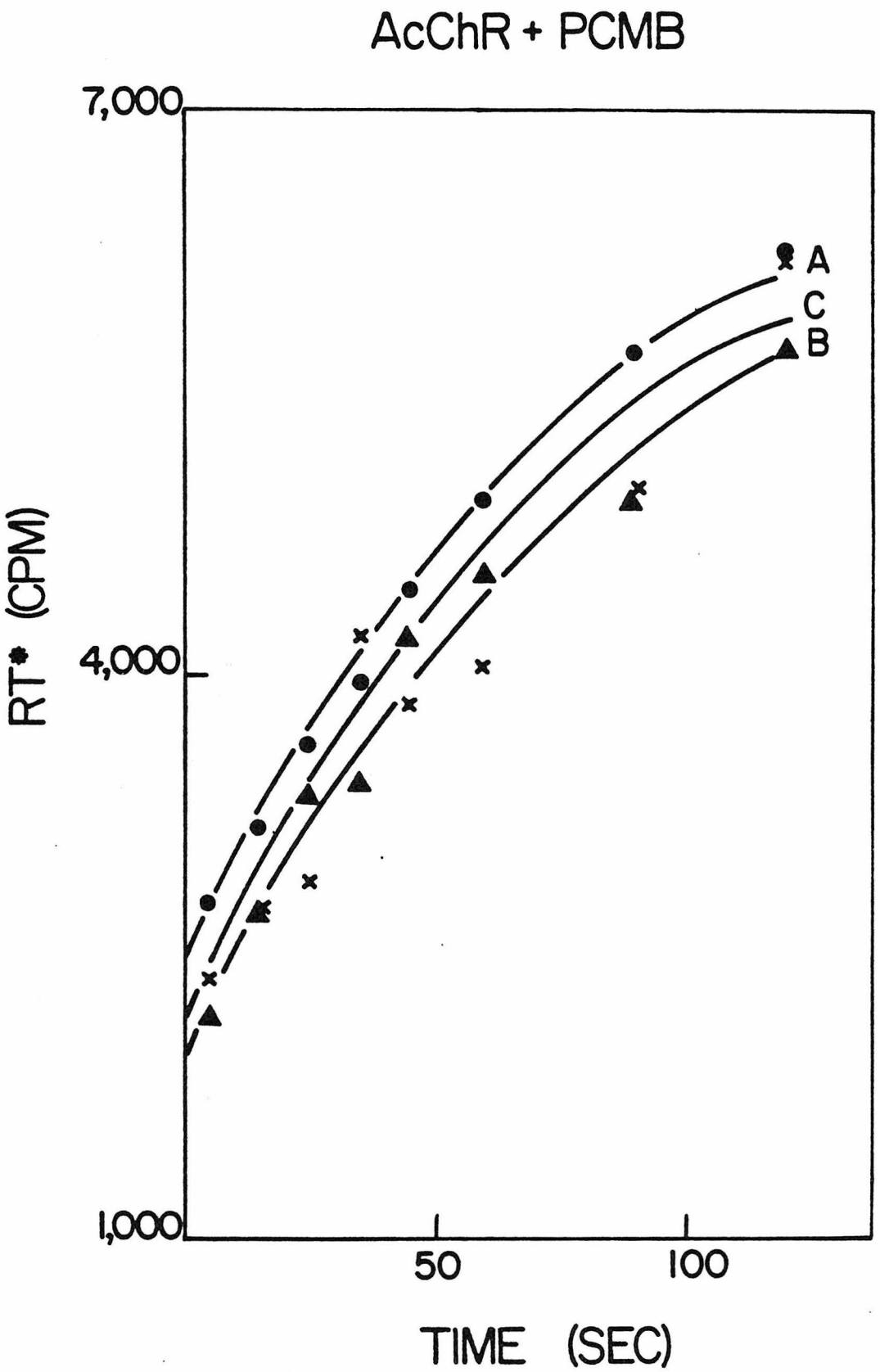
AcChR + PCMB
7,000
4,000
1,000
RT* (CPM)
A
C
B
50
100
TIME (SEC)

FIGURE 4. K_D of Carb for AcChR Modified with PCMB (as in Figure 3). 6-8x10^{-8}M PCMB treated AcChR was preincubated with various concentrations of Carb for at least 30 min. [^{125}I] α-BuTx was added to a concentration of 5x10^{-7} M and the initial rate of toxin receptor complex formation was followed by DEAE-disc assay. The data were fitted to the equation (Quast et al, 1978) $k_{obs} = \frac{kT_o}{1+[L]/K_{app}}$ where T_o is the total toxin concentration ($T_o >> [AcChR]$), k is the bimolecular rate constant for toxin binding to AcChR, [L] is the free Carb concentration and K_{app} the apparent dissociation constant for Carb. The predicted curve for K_D = 30 μM from the fit is indicated as a solid line.

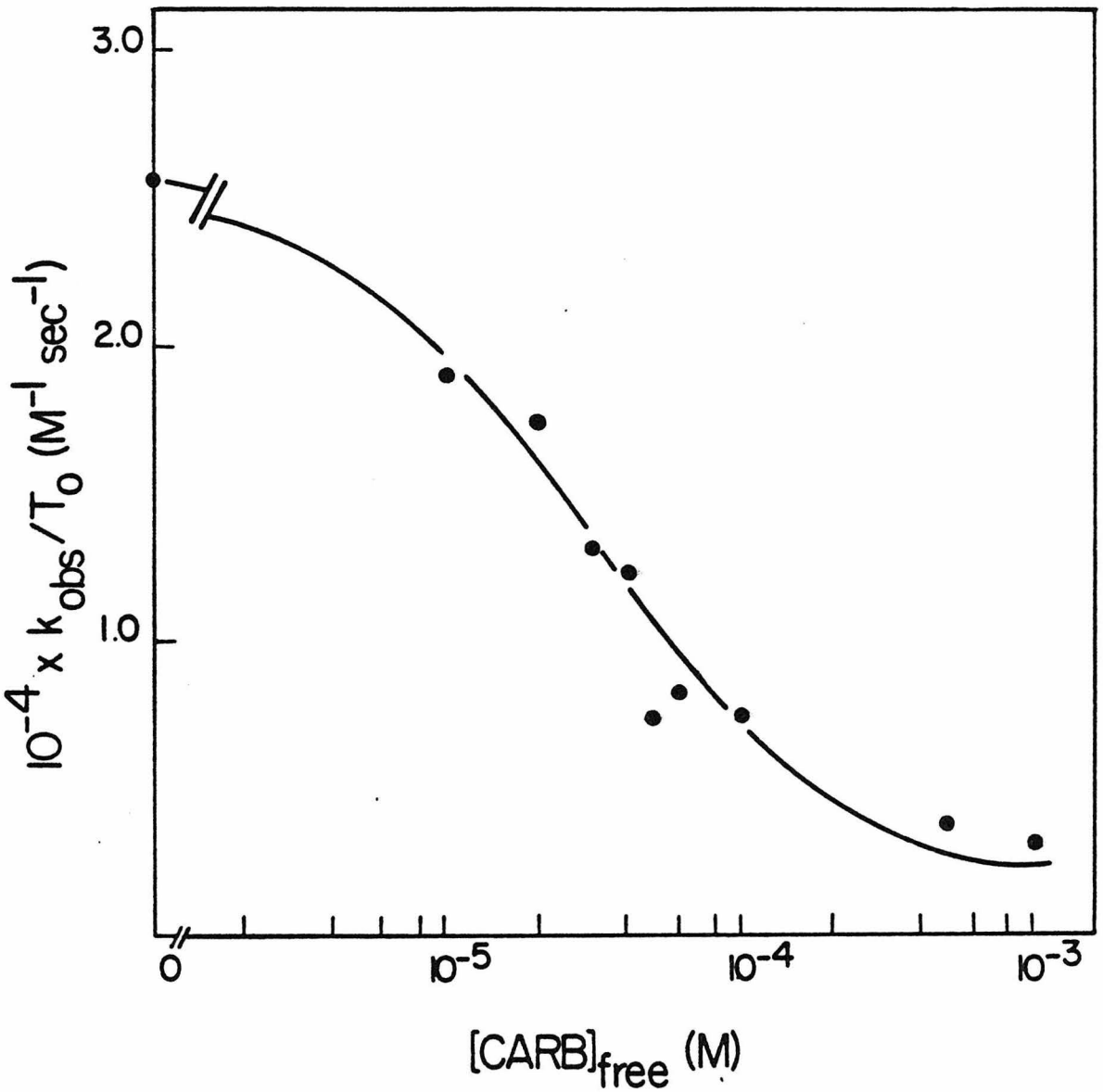
3.0
2.0
1.0
$10^{-4} \times k_{obs}/T_0$ (M^{-1} sec^{-1})
0
10^{-5}
10^{-4}
10^{-3}
$[CARB]_{free}$ (M)

FIGURE 5. Effect of PCMB on the Recovery of AcChR-containing Membrane Fragments to Low Affinity from Carb Induced High Ligand Affinity. AcChR-containing membranes (1.8×10^{-7} M in Torpedo Ringers) were incubated with 3 μM Carb for 20 min at room temperature. (A) 1 mM PCMB (in 200 mM Tris, pH 8.5) was added and the reaction was allowed to proceed for 20 min. The reaction was then diluted 40-fold into Torpedo Ringers; 0 min (●) and 10 min (▲) after dilution, ^{125}I α-BuTx (5×10^{-7} M) and Carb (1 μM) were added simultaneously and formation of the toxin-receptor complex was followed by disc assay. (▼) is identical to (▲), except that only toxin was added 10 min after dilution. (B) Control, same as in A except that PCMB was replaced by Tris buffer. Carb concentration after dilution was 75 nM.

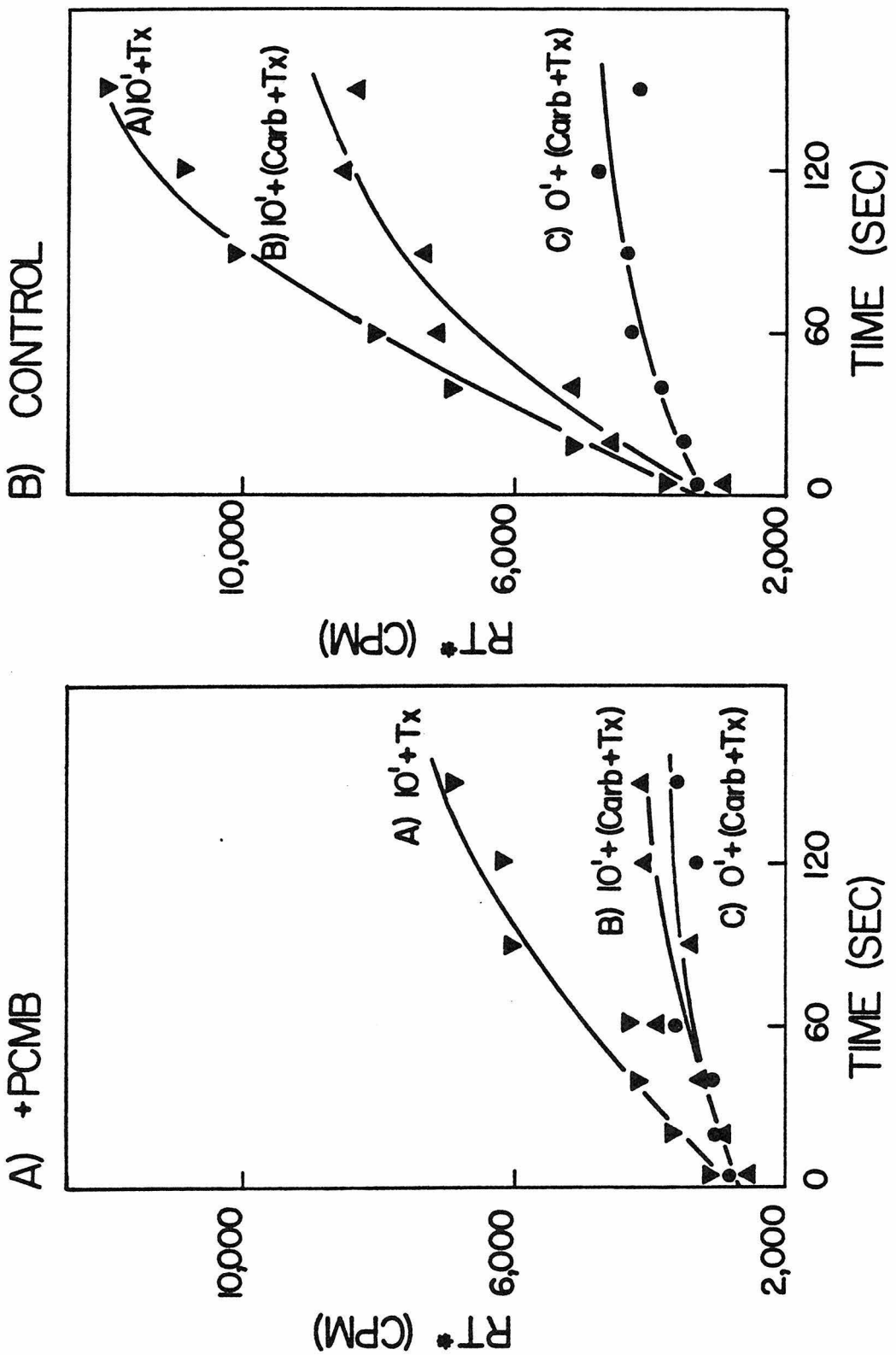
A) +PCMB
B) CONTROL
RT* (CPM)
10,000
6,000
2,000
0
60
120
TIME (SEC)
A) 10'+Tx
B) 10'+(Carb+Tx)
C) 0'+(Carb+Tx)

low affinity form, as shown by the nearly superimposable curves (Curves B and C in Figure 5A).

In another experiment, the PCMB modified membrane fragments described above were washed extensively to remove the added Carb (this amounted to 75 nM after forty-fold dilution from 3 μM used to convert to the high affinity state). The membrane preparation was then tested for its state of affinity for Carb (Figure 6). The PCMB-treated membrane fragments showed exclusively high affinity for Carb, whereas the control membrane fragments exhibited over 80% recovery of the low affinity form. Thus, PCMB treatment of the Carb-converted AcChR appeared to stabilize the receptor in a high affinity form(s).

The toxin binding time course of PCMB-treated AcChR 10 min after dilution (Figure 5A, curve A) was 30% of the control value. After complete removal of Carb, this rate (Figure 6A, Curve A) was measured to be 50-65% of the control value; the total number of α-BuTx sites, however, remained unaffected.

FIGURE 6. Effect of PCMB on the Recovery of AcChR-containing Membrane Fragments to Low Affinity from Carb Induced High Ligand Affinity. Membrane fragments, modified with PCMB as described in the legend to Figure 5, were washed extensively with Torpedo Ringers to remove Carb and then assayed by the method described in Figure 1 for the state of receptor affinity towards Carb. (A) PCMB-treated membrane fragments; (B) Control.

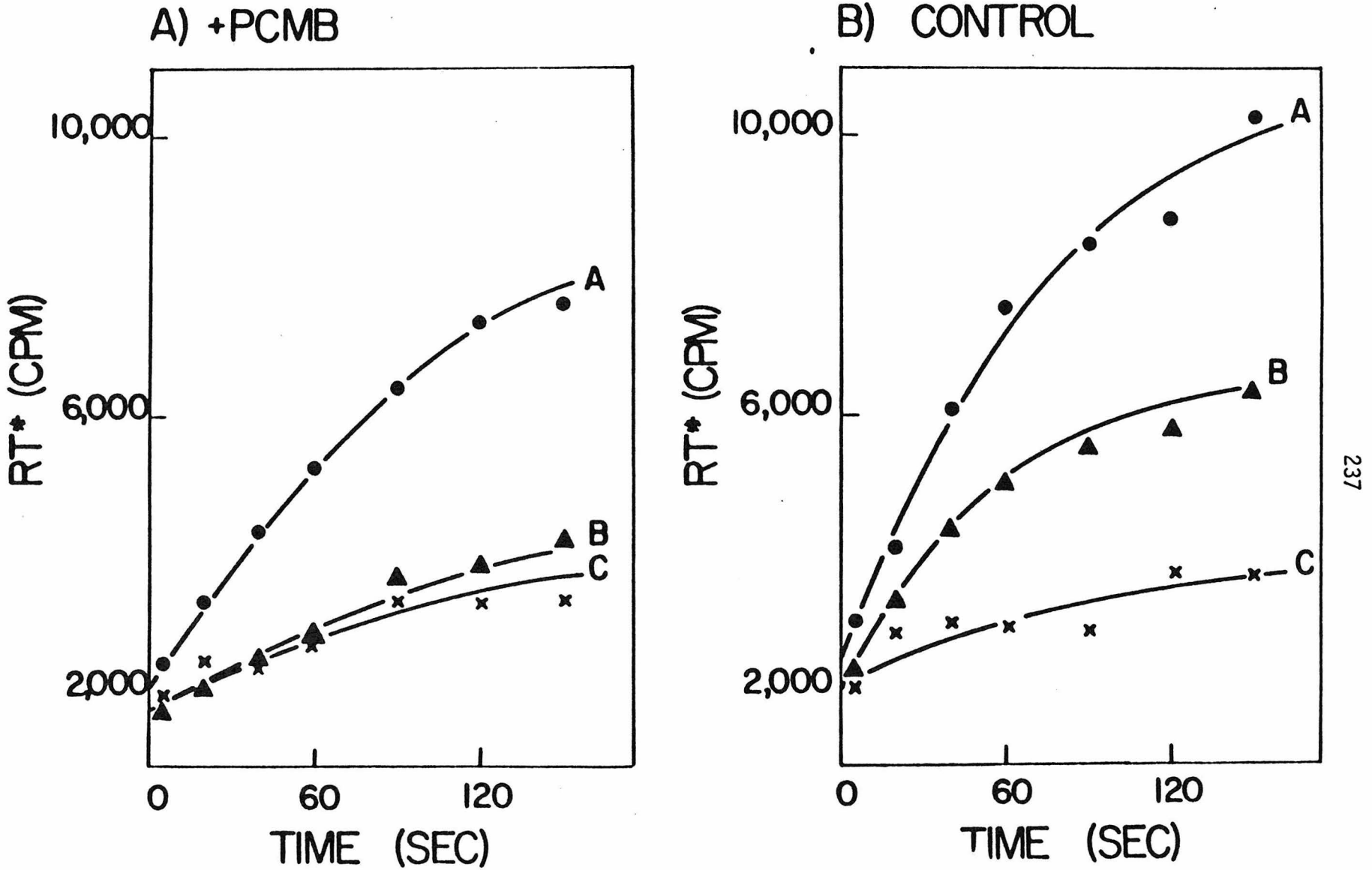
A) +PCMB
B) CONTROL
10,000
6,000
2,000
RT* (CPM)
0
60
120
TIME (SEC)
A
B
C

DISCUSSION

Several approaches have been tested in an attempt to stabilize the membrane-bound AcChR in the various conformational states for mechanistic studies of receptor function. Cross-linking reagents have been widely used for stabilizing the tertiary structure of water soluble proteins (Wold, 1967). Their use in the membrane-bound AcChR system, however, is limited by the finding that the reagents invariably inactivate AcCh or α-BuTx sites on the receptors when cross-linking is directed towards the water soluble phase of the membrane protein. The use of lipid-soluble bifunctional reagents (Smith and Brown, 1951), on the other hand, is complicated by the sensitivity of receptor function to low concentrations of organic solvent required to solubilize the reagents. Studies of the effects of chemical modifications on the affinity states of the AcChR provide an alternative method, which in addition allows one to examine the chemical basis for the desensitization process.

After reduction by DTT, the AcChR-enriched membrane preparation from Torpedo californica can no longer be converted from a low affinity form(s) to one(s) of higher affinity by 1 μM Carb. Removal of excess reducing reagents gradually restored the ability to undergo the conversion, presumably by allowing reoxidation of a DTT reduced -S-S-bond(s). This interpretation is consistent with the effect observed with DTNB, which facilitates the recovery process by reoxidizing

the reduced receptors. Alkylation of the reduced receptor with iodoacetamide or iodoacetic acid, however, irreversibly modified the reduced disulfide bridges and no recovery of interconversion of states of ligand affinity was observed after removal of excess reagents. Iodoacetamide and iodoacetic acid alone at similar concentrations did not have any significant effect on the Carb-induced conversion, suggesting that disulfide bond(s), rather than sulfhydryl groups, play an important role in the effects described above.

Treatment of the low affinity form of the AcChR with PCMB, unlike iodoacetic acid, NEM or iodoacetamide, also inhibits the conversion of AcChR to the high affinity state(s) by 1 μM Carb. The apparent Kd for Carb of both reduced, iodoacetate-alkylated membranes and PCMB-treated native membranes as determined by the inhibition of initial α-BuTx binding rate was approximately 30 μM, a value close to the low affinity state(s) of AcChR (Quast et al, 1978). These results are consistent with a model in which both sulfhydryl group(s) and disulfide bridge(s) are involved in the conversion of AcChR from low to high affinity state(s) by ligands; reduction-alkylation of the disulfide(s) or PCMB-treatment of the sulfhydryl(s) prevents conversion of the system to a state(s) of high ligand affinity and hence stabilizes the AcChR in a low affinity state(s). If such a model is indeed accurate, these reagents should in the future be useful for mechanistic studies utilizing receptors stabilized in the low-affinity conformation. It should also be of interest to determine

whether these treated membranes are capable of translocating cations, using the spectroscopic method described in Chapter 4. Future study is required to determine if the disulfide bonds responsible for the effects observed in this study are (1) the "reactive" disulfide(s) in the preparation (Karlin and Bartels, 1966; Ben-Haim et al, 1973) that resulted in altered electrophysiological responses following DTT treatment and that was labeled by the antagonist MBTA (Weill et al, 1974) or the agonist bromoacetylcholine (Chapter 1) or (2) those involved in AcChR dimer formation through the 65,000 - 67,000 dalton subunits (Suarez-Isla and Hucho, 1977; Chang and Bock, 1977; Hamilton et al, 1977; Witzemann and Raftery, 1978) or (3) still other disulfides.

The lack of effect of iodoacetic acid, NEM and iodoacetamide may be due to differing reactivities with freely accessible or less accessible sulfhydryl groups in the AcChR. This suggestion is based on the relative ease with which PCMB is known to form mercaptides relative to reacting with other amino acid side chains (Means and Feeney, 1971), but reaction with other residues cannot be totally excluded. In addition PCMB is known to react with buried sulfhydryl residues in proteins such as hemoglobin which are unreactive toward iodoacetic acid or iodoacetamide (Kilmartin and Wooton, 1970). Similar observations were reported by Karlin and Bartels (1966), who demonstrated that treatment of intact electro-

plaques with PCMB affected the AcCh-dependent excitability, whereas NEM had no effect.

PCMB modification of the AcChR enriched membranes which were first converted to the high affinity state by preincubation with Carb prevented reversion from this state(s) to the resting state of low ligand affinity when the Carb concentration was reduced. Such treatment caused a decreased α-BuTx binding time course as depicted in Figure 5A. This result would be expected if the AcChR were stabilized in a high affinity form(s), since the residual Carb concentration after dilution was still large (75 nM) compared to the K_d of Carb for the high affinity form (50 nM) (Quast et al, 1978). However, after complete removal of residual Carb, the toxin binding rate of the treated AcChR was not totally restored to the control value (Figure 6A). The precise reason for this observation remains unclear; it could, for example,be caused by steric effects of the added PMB residues resulting in a slowing of the kinetics of α-toxin binding.

At least two possible explanations exist for the effects of PCMB. First, PCMB may interact with the AcChR in such a way that it sterically blocks conformational transitions, thus stabilizing a low affinity form(s) when allowed to react with the resting state of the AcChR, and stabilizing a high affinity form(s) when allowed to react with this form following induction by Carb. Alternatively, the results could be explained in terms of a disulfide interchange model, depicted as follows:

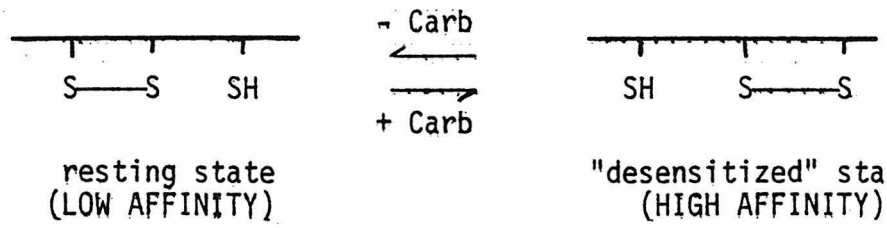

In this case, modification of the SH group of either state would prevent conversion to the other state. We favor this model since it is consistent with the results obtained with reduction and alkylation of AcChR described earlier in the Discussion. Further supporting evidence, however, is needed to establish the validity of this hypothetical model of the interconversion process.

These preliminary results thus indicate that free sulfhydryl groups and disulfide bonds are present in the AcChR-enriched membrane preparations and their modification interferes with interconversion of the affinity states of the AcChR. They therefore suggest possible chemical bases for the ligand-induced affinity change of membrane-bound AcChR.

REFERENCES

1. D. Ben-Haim, E. M. Landau, and I. Silman (1973) J. Physiol. 234, 305.
2. D. Ben-Haim, F. Dreyer, and K. Peper (1975) Pflugers Arch. 355, 19.
3. S. G. Blanchard, U. Quast, K. Reed, T. Lee, M. I. Schimerlik, R. Vandlen, T. Claudio, C. D. Strader, H.-P. Moore, and M. A. Raftery (1979) Biochemistry 18, 1875.
4. H. W. Chang and E. Bock (1977) Biochemistry 16, 4513.
5. S. L. Hamilton, M. McLaughlin, and A. Karlin (1977) Biochem. Biophys. Res. Commun. 79, 692.
6. A. Karlin and E. Bertels (1966) Biochem. Biophys. Act. 126, 525.
7. B. Katz and S. Thesleff (1957) J. Physiol. 138, 63.
8. J. V. Kilmartin and O. Wooton (1970) Nature (London) 228, 766.
9. T. Lee, V. Witzemann, M. Schimerlik, and M. A. Raftery (1977) Arch. Biochem. Biophys. 183, 57.
10. J. M. Lindstrom, S. J. Singer and E. S. Lennox (1973) J. Membrane Biol. 11, 271.
11. G. E. Means and R. E. Feeney (1971) Chemical Modification of Proteins, Holden-Day Inc., San Francisco.
12. U. Quast, M. Schimerlik, T. Lee, V. Witzemann, S. Blanchard, and M. A. Raftery (1978) Biochemistry 17, 2405.
13. H. P. Rang and J. M. Ritter (1970a) Mol. Pharmacol. 6, 357.
14. H. P. Rang and J. M. Ritter (1970b) Mol. Pharmacol. 6, 383.

15. J. Schmidt and M. A. Raftery (1973) Anal. Biochem. 52, 349.

16. P. A. S. Smith and B. B. Brown (1951) J. Am. Chem. Soc. 73, 2438.

17. B. A. Suarez-Isla and F. Hucho (1977) FEBS Letters 75, 65.

18. Z. Vogel, A. J. Sytkowski and M. A. Nirenberg (1972) Proc. Natl. Acad. Sci. USA 69, 3180.

19. M. Weber, T. David-Pfeuty and J. P. Changeux (1975) Proc. Natl. Acad. Sci. USA 72, 3443.

20. G. Weiland, B. Georgia, V. T. Wee, C. F. Chignell and P. Taylor (1976) Mol. Pharmacol. 12, 1091.

21. G. Weiland, B. Georgia, S. Cappi, C. F. Chignell, and P. Taylor (1977) J. Biol. Chem. 252, 7648.

22. C. L. Weill, M. G. McNamee, and A. Karlin (1974) Biochem. Biophys. Res. Commun. 61, 997.

23. V. Witzemann and M. A. Raftery (1978) Biochem. Biophys. Res. Commun. 81, 1025.

24. F. Wold (1967) Methods in Enzymology XI, 617.